Prof. Jerzy Ranachowski

THE OUTPUT OF THE FIFTY YEARS' SCIENTIFIC ACTIVITY OF PROF. DR. JERZY RANACHOWSKI

I. MALECKI

1. Introduction

Professor Jerzy Ranachowski began his research as an assistant at the Electrical Faculty of the Technical University in Wrocław under the guidance of Professor J. Skowroński.

After getting a degree in 1951, he started working at the Institute of Electrical Engineering of this University. At that time, this Institute introducing innovative technical solutions was one of the most important research institution in Poland. The international prestige of the Institute opened a chance to encounter the newest achievements of world-wide science. The research of J. Ranachowski at this Institute concerned two fields related closely to one another: the high-voltage techniques and the technology of ceramic materials. Just at the beginning of these works, he focused his attention on the application of ultrasounds to testing of ceramic materials and high-voltage electric devices. In 1956, he established a close co-operation with the Institute of Fundamental Technological Research of the Polish Academy of Sciences. His interest in the problems of acoustics was gradually increasing. In 1975, Prof. Ranachowski started to work at the latter Institute, where, besides managing a research team, he held several responsible positions; among other, deputy director of the Institute. He still continued his acoustic research as well as the study of ceramic materials and high-voltage insulating systems. Professor Ranachowski retired in 1996 but remained a creative scientist and manages a team of research and technical workers.

The scientific work and technical achievements of Prof. Ranachowski gained high recognition from the whole scientific community. This respect was expressed by appointing him full professor in 1987 as well as in the many rewards for his scientific and technical achievements. Furthermore, one should stress his considerable contribution to the development of acoustics in Poland as well as his engagement in the national and European co-operation in this research field. Professor Ranachowski is vice-president of the Committee on Acoustics of the Polish Academy of Sciences and an honorary member of the Polish Acoustical Society and has been its president since 1996. He has made a considerable contribution to the increasing co-operation of the latter society with the Federation of the Acoustical Societies of Europe (FASE) and later with the European Acoustics Association (EAA) that get through to FASE; at present, he is a member of

the EAA Council. His membership of the European Material Research Society (E-MRS) is important for the international co-operation.

The contribution of Prof. Ranachowski to the co-operation of the countries of Central and Eastern Europe in the field of acoustics and the research of ceramics should be stressed. Under his scientific and organisational leadership, varied scientific and technological conferences are held regularly in which participate specialists in acoustics and ceramics from Poland and the neighbouring countries, i.e Belorus and the Ukraine. Also, the membership of Prof. Ranachowski in the Polish Electricians Society should be mentioned; he has established the Polish Committee of Electrotechnological Materials of this society.

2. The research linking acoustics and materials technology

The research work of Prof. Ranachowski was always guided by problems arising from technological needs vital to Polish industry and power engineering. This is why his scientific achievements should be considered as a logically developing whole. The knowledge of the physicochemical properties of ceramic materials and the production of those materials nowdays is one of the crucial problems of materials technology. The achievements of Prof. Ranachowski, a brief account of which is given below, are of unique character. He belongs to the sparse scientists and technicians who are able to apply broadly the acoustic methods in materials technology. His fundamental assumption was that the indispensable condition of achieving improvement in the production of ceramic materials is the perfection of the measuring methods. Professor Ranachowski applied broadly the electric [4], magnetic [46] and microscopic methods and the X-ray analysis. He gradually became interested in the application of acoustic methods, first in the classic ones (measurements of the velocity and attenuation of ultrasound), later in the extension of those applications to surface waves (SAW) [40, 49] and to the photoacoustic spectroscopy (PAS) [24]. The most considerable achievements of Prof. Ranachowski in the last period concern the applications of the acoustic emission (AE) methods. Those works lead to new technical applications of the research results of Prof. Ranachowski. To them belong: the investigation of the mechanical properties of concrete and the application of acoustic methods to the detection of contaminations of gases and to the testing of industrial oils. The developing of acoustic methods for the study of static and dynamic processes for material engineering was an essential novelty.

The static investigations have concerned the structure and microstructure of ceramics, their mechanical, electrical and thermal properties and the dependence of those parameters on the composition of the materials and the production procedure. The dynamic investigations are aimed mainly at the time dependence of the cracking of the materials under mechanical, electrical and thermal stresses; this time dependence allows to determine "life-time" and the usefulness of ceramic materials. The measurement techniques used in those investigations are essentially different. While in the static investigations most information is provided by the microscopic and ultrasonic methods, the acoustic emission is most useful in dynamic investigations. However, static and dynamic investi-

gations supplement one another giving a complete picture of the technically important properties of the object under test.

3. The most important scientific achievements

One of the most momentous scientific achievements of Prof. Ranachowski was the comprehensive theoretical and experimental investigation of the structure of ceramic materials. The first stage of this work consisted in the improvement of the method of getting microscopic pictures of those structures and in the working out in atlas of electrotechnical porcelain [6]. Next, he worked on the electrical method of measuring the leakage and inverse currents and on the dielectric strength of ceramic materials [36]. The study of ceramic materials, and particularly of their porosity, by applying acoustic methods was scientifically and practically most fruitful [9, 11]. The starting point was the study of the investigation of the triple point of the phase equilibrium of porcelain-like materials [10]. An undoubted scientific success of Prof. Ranachowski was the finding of a correlation between the velocity of propagation of ultrasounds and their attenuation and the parameters characterising the degree and structure of the porosity of the ceramic materials of the K_2O-Al_2O_3-SiO_2 system; simultaneously, the influence of the degree of porosity on the mechanical [13] and dielectric strength of the material was determined [19]. A theoretical extension of Prof. Ranachowski's experimental work were studies on the distribution of electrical, mechanical and thermal stresses in heterogeneous materials, particularly in ceramics; this was connected with the discovery of the effect of the textural deffects on the internal stresses [5]. His work concerned also the application of the theory of complex cross-sections to porous materials with scattered enclosures [55]. His considerable achievements belong to the results of studies concerning the measurements of the critical value of the stress intensity coefficient K_{IC} [14, 54] that is a parameter adequately characterising the brittleness of ceramic materials.

The studies of Prof. Ranachowski have proved the particular usefulness of the acoustic emission method (AE) in the investigation of dynamic states. The improvement and extension of those methods has been his main task during the last years. The starting point was the monitoring of acoustic signals generated by microfractures developing in the ceramic material under the influence of a groving mechanical stress [23]; a corresponding theory has been developed [47]. It turned out that the analysis of the AE signals provides unique information about the initial stage of the structure distortions that cannot be detected by other methods. The studies of Prof. Ranachowski were aimed at the choice of appropriate descriptors of the acoustic emission signals that are essential for the effectiveness of the AE method [41, 48]. The fact that the force at which threshold AE signals appear is a linear function of the destructive force [23] paved the way for new applications of the acoustic method to the non-destructive testing of materials (NDT). Also, an important find for Prof. Ranachowski is that there exists a correlation between the activity of the AE and the variations of the conductivity and the magnetic effects in the ceramic material [32, 33]. However, two of his publications seem to be of greater importance.

The first one concerned the prediction of the "life-time" of ceramic elements, particularly of high-voltage insulators, based on the ratio between the exploitation stress and the destructive one [25]. Beside the conventional methods, Prof. Ranachowski has applied to this end the acoustic emission method. The theoretical calculations, confirmed by testing of insulators on lines of the highest voltage, were based on the Weibull's statistics.

The second publication concerned the evaluation of thermal shocks on the degradation and strength of ceramics used in electrical engineering. Professor Ranachowski studied both the effect of single strong thermal shocks (of the order of 400°C) [39] and that of periodic temperature oscillations that affect high-voltage lines [44]. In both cases, the dependence of the activity of the AE on the state of the object under test was proved. The finding that the extent of defects in the ceramic material influenced the consecutive maxima of the AE counting rate due to periodic variations of the thermo-mechanical stresses [34, 56] was of particular interest.

4. Contributions to the technological development and technical innovations

The scientific activity of Prof. Ranachowski was closely related to practical needs. It is therefore difficult to separate his scientific achievements from the technical ones. It is nevertheless worthwhile to mention which of his works have been fully used in practice, mainly in the technology of ceramic materials and in the control of electrical power systems. The practical importance of the atlas of porcelain structures has been mentioned previously. The studies of Prof. Ranachowski on the causes of breakdowns of insulator systems and the co-ordination of overload protection systems in 12 Polish power plants and substations had a broad range. These works concerned the co-ordination of insulations in high-voltage systems, connecting links, transformers and transmission lines. They have contributed significantly to the failure-free work of electrical power systems exploited in Poland.

High-voltage insulators were the object most extensively investigated by Prof. Ranachowski. His contribution to the improvement of the production of those insulators is unquestionable, but most importantly are his works for the industry of electro-ceramic materials concerning the control of the mechanical and electrical parameters of insulators. The latter works concerned also the influence of parameters of the production process and the composition of the raw material on those properties. Prof. Ranachowski worked out the fundaments of defectoscopic investigations of insulators for the detection of inner flaws and implemented those methods in the industry [1, 3, 4]. For electrical power engineering, the most important works were those concerning the determination of the degradation of insulators during their long-term work on high-voltage lines; this is important for the replacement of used up insulators. Those investigations are of great economic and social importance because of the enormous cost of renovation of high-voltage lines and the disastrous consequences of a possible breakdown. The application of the AE monitoring of the influence of periodical variable thermo-mechanical loads on the ageing of insulators was a significant progress in this field [33–35, 56]. The acoustic emission method worked out by Prof. Ranachowski was found to be particularly

useful in the study of the mechanism of ageing and the "life-time" of ceramic materials. Prof. Ranachowski worked out the methods of investigation of insulating materials and a device that also enables the investigation of insulators in the place of their work. This method received wide acceptance and recognition as it allows for the replacement of station postinsulators and long rod insulators that are of uncertain mechanical strength.

Recently, the estimated lifespan of long rod insulators by the method of acoustic emission depended on the choice of insulators and producers during the modernisation of the Polish 220 kV and 400 kV transmission lines. Despite the strong competition of many reputable firms worldwide the tender entrusted the production to the firm ZAPEL in Boguchwala. The crucial argument was the long life-time of their insulators (reaching 50 years); the latter was evaluated by Prof. Ranachowski.

Among the achievements in the production engineering of materials of desirable parameters, i.e. among the investigations in the field of materials technology, the study and going into production of the following materials should be mentioned:
- the materials for the production of insulators working at high temperatures,
- the silicate-zirconium materials for chambers of medium-voltage contactors,
- arc-resistant materials for high-voltage arc interruption chambers [8],
- steatite materials [16, 17] for electronic and electrical engineering,
- ceramics for electro-optics [27],
- cordierite materials for welding technology,
- polimeric materials of decreased electric resistance for fuel tanks.

The accomplishment of the above tasks were possible only on condition that the measurement techniques and devices were constantly improved. This concerned the comprehensive application of methods used in materials engineering, mainly, as mentioned above, the methods of structural analysis, acoustic techniques including ultrasound velocity and attenuation measurements as well as the AE methods. The application of the acoustic emission is a particularly momentous achievement of Prof. Ranachowski. Besides the innovative application of this method to the mentioned above investigation of materials, Prof. Ranachowski receives the credit for putting the AE method into practise as a tool for the testing of technical objects. This is the consequence of the many years' standing work of Prof. Ranachowski and of the team working under his leadership. The goals of their activities were:
- initiation of the production and the perfection of analyzers of acoustic emission. The DEMA analyzers, worked out under the leadership of Prof. Ranachowski, are currently in use in many scientific and industrial laboratories;
- popularising of the AE methods amid scientists and engineers. This aim was accomplished by papers in professional journals, collective monographs and conference materials;
- promotion of the scientific staff dealing with those problems that resulted in the initiation of Ph.D. dissertations and postdoctoral lecturing qualifications as well as in the endorsement of applications for academic titles for scientists dealing with the acoustic emission.

The most important publications of prof. J. Ranachowski
(in chronological order)

References

[1] J. RANACHOWSKI, J. WEHR, *Zastosowania defektoskopii ultradźwiękowej do prób ceramicznych izolatorów wysokonapięciowych*, Przegląd Elektrotechniczny, 10–11 (1955).

[2] J. RANACHOWSKI, J. WEHR, *O możliwościach strukturalnych badań materiałów elektroizolacyjnych metodami ultradźwiękowymi*, Przegląd Elektrotechniczny, 1 (1958).

[3] M. BOSEK, J. RANACHOWSKI, *Badania izolatorów długopniowych metodą ultradźwiekową. Nieniszczące metody badania materiałów*, Zeszyty Problemowe Nauki Polskiej, Ossolineum, **24**, 326 (1965).

[4] J. RANACHOWSKI, *Nieniszczące metody badań niektórych dielektryków stałych*, Aktualne Zagadnienia Techniki Wysokich Napięć, PWN, Warszawa 1965.

[5] J. RANACHOWSKI, T. ŁAŚ, *Effects of structure on electric properties of ceramics*, Ceramika, 10, Kraków 1968.

[6] J. RANACHOWSKI, V. HERMAŃSKI, *Album of structures of electrical porcelain*, Wydawnictwo Instytutu Elektrotechniki, Warszawa 1972.

[7] J. RANACHOWSKI, *Aktualny stan badań i zastosowań ceramiki wysokonapięciowej*, Mat. II Kongresu Nauki Polskiej, Wrocław 1972.

[8] J. RANACHOWSKI, *Ceramiczne tworzywa odporne na działanie łuku elektrycznego*, Ceramika, PWN, Kraków 1975.

[9] J. RANACHOWSKI, *Propagation of ultrasonic waves in porous ceramic*, Ultrasonics, 203–207 (1975).

[10] W. PESSEL, J. RANACHOWSKI, *Prace nad układem potrójnym równowagi faz dla porcelany*, Szkło i Ceramika, 2, 50–52 (1964).

[11] W. KREHER, J. RANACHOWSKI, F. REJMUND, *Ultrasonic waves in porous ceramics with non-spherical holes*, Ultrasonics, 3, 70–74 (1977).

[12] W. WŁOSIŃSKI, J. RANACHOWSKI, *Calculation of diffusion coefficients of manganese in Debacsol alumina*, [w:] Ceramics International, **3**, 3 (1977).

[13] J. RANACHOWSKI, F. REJMUND, *Zniszczenie mechaniczne tworzyw ceramicznych*, Szkło i Ceramika, **28**, 3 (1977).

[14] J. RANACHOWSKI, F. REJMUND, Z. ŚWIĘCKI, D. WALA, *Ocena wytrzymałości mechanicznej modyfikowanych tworzyw korundowych na podstawie pomiarów krytycznego współczynnika intensywności naprężeń*, Acta Ceramica, 5, 109–112 (1979).

[15] J. LEWANDOWSKI, J. RANACHOWSKI, F. REJMUND, W. KREHER, W. POMPE, *Mechanical strength estimation of brittle heterogeneous solids from ultrasonic measurements*, Conf. Proc. Ultrasonics Int. 79, 109–112, Graz, Austria 1979.

[16] M. CIEŚLA, J. RANACHOWSKI, *Properties of steatite body and the modification of its structure*, Science of Ceramics, 9, 45–50 (1979).

[17] Z. GUZEK, J. RANACHOWSKI, *Versuche zur Erhöhung der Mikrostruktur von Steatit*, Hermsdorfer Technische Mitteilungen (1980).

[18] J. RANACHOWSKI, Z. KRZEŚNIAK, J. RZESZOTARSKA, *Conductivity, photoconductivity and acoustic properties of halogen derivatives of poly (n-inylocarbazole)*, Intern. Symposium on Macromolecules, IUPAC, Florence 1980.

[19] J. RANACHOWSKI, *Wytrzymałość dielektryczna tworzyw ceramicznych, elektroceramika własności i badania*, vol. 1, PWN, Warszawa–Poznań 1981, 133–155.

[20] A. Juszkiewicz, J. Ranachowski, *Ultraschallunterschungen verschiedener physikalisch-chemischer processe in flussigkeiten*, Wissentschaftliche Zeitschrift der Technische Hochschule, Merseburg 1981.

[21] M. Cieśla, J. Ranachowski, Z. Święcki, *Application of acoustic emission for investigation of alumina*, Science of Ceramics, 11 (1981).

[22] Z. Jakubczyk, A. Opilski, Z. Krześniak, J. Ranachowski, J. Rzeszotarska, *Investigation of the relation acoustic field parameters and electric conductivity of selected polymers*, Acoustic Letters, **4**, 3, 49–50 (1980).

[23] J. Ranachowski, F. Rejmund, Z. Librant, *Applications of Acoustic Emission to investigate ceramic materials*, Acta Ceramica (1982).

[24] J. Motylewski, J. Ranachowski, *Photoacoustic spectroscopy as a method in biological investigations*, Archives of Acoustics, **9**, 1-2 (1984).

[25] J. Ranachowski et al, *Microstructure and subcritical crack growth in long rod high-voltage insulators*, [in:] Brittle Matrix Composites, A.M. Brandt, L.H. Marshall [Eds.], p. 205, 1985.

[26] J. Skubis, J. Ranachowski, B. Gronowski, *Detection, measurement and location of PD in power transformes using acoustic emission method*, Journal Acoustic Emission, **5**, 1, 25–30 (1986).

[27] J. Ranachowski, K. Smolińska, *Ceramics in electrooptical technology* [in:] Acoustooptics and Applications, A. Śliwiński [Ed.], World Scientific, Singapore 1989.

[28] L. Radziszewski, J. Ranachowski, *Schallemission in Verbundstoffen mit Kohlenstroffen der Wiss*, Berichte THZ 1273, 24, 93–95 (1990).

[29] L. Woźny, B. Mazurek, J. Ranachowski, *Acoustic emission accompanying the super-conducting transitions of* $YBa_2Cu_3O_2$, Physica B, **173**, 309 (1991).

[30] J. Ranachowski, M. Aleksiejuk, J. Raabe, *Technology and acoustical properties of the ceramic high-temperature superconductors*, Arch. Acoust., **16**, 3-4, 387–412 (1991).

[31] W. Opyto, J. Ranachowski, *Emisja polowa z rzeczywistych katod układów izolacyjnych próżniowych*, Elektryka, Politechnika Poznańska, 1992.

[32] J. Ranachowski et al., *Interrelation between acoustic emission and electrical conductivity*, Acoustic Letters, **16**, 7, 167 (1993).

[33] J. Ranachowski, Z. Ranachowski, F. Rejmund, H. Baumbach, *An investigation of the mechanical destruction processes using electric and acoustic measurement*, Ceramics 43, Polish Ceramic Bulletin, 5, 141–152 (1993).

[34] J. Ranachowski, I. Malecki, J. Rzeszotarska, *The comparative study of the appearance of acoustic emission (AE) signals*, Ultrasonics International 93 Conference Proceedings, Butterworth–Heinemann Ltd., 1993, 471–474.

[35] I. Malecki, J. Ranachowski, F. Rejmund, J. Rzeszotarska, *Acoustic emission generated by thermomechanical processes*, Acustica, **79**, 102–111 (1993).

[36] J. Ranachowski et al. *An investigations of the mechanical destruction processes using electric and acoustic measurements*, Ceramics 43, Polish Ceramic Bulletin, 5, 141–152 (1993).

[37] J. Ranachowski, F. Rejmund, J. Raabe, *Przewodność elektryczna i EA w procesie zniszczenia ceramiki*, Akustyka Molekularna i Kwantowa, **14**, 95–104 (1993).

[38] I. Malecki, J. Ranachowski, *Methods and applications of acoustic emission comparative analysis*, Arch. Acous., **18**, 3, 371–415 (1993).

[39] J. Ranachowski, F. Rejmund, *Acoustic emission in thermomechanical investigations of ceramics and cement materials*, Ceramic 45, Polish Ceramic Bulletin 7, 177–186 (1994).

[40] J. Ranachowski, E. Adamczyk, J. Rzeszotarska, A. Opilski, *Wykorzystanie akustycznych fal powierzchniowych do analizy gazów. Aparatura i doświadczenia*, Prace IPPT PAN, 12 (1994).

[41] I. MALECKI, J. RANACHOWSKI, Z. RANACHOWSKI, *The descriptors of acoustic emission signals and their correlation with other effects of mechanical load*, Mat. Conf. DAGA 94 – Dresden, Teil B, 829–832 (1994).

[42] J. RANACHOWSKI, F. REJMUND, *Emisja akustyczna w ceramice technicznej*, [w:] Emisja Akustyczna. Źródła, Metody, Zastosowania, I. MALECKI, J. RANACHOWSKI [Red.], Wyd. Biuro Pascal, Warszawa 1994.

[43] I. MALECKI, J. RANACHOWSKI, J. RZESZOTARSKA, *New application of acoustic emission method*, Proc. Conf. 11th FASE Symposium, Valencia 1994, 85–88.

[44] J. RANACHOWSKI, F. REJMUND, *Zastosowanie EA w badaniu własności materiałów i urządzeń*, XXIV Krajowa Konferencja Badań Nieniszczących, Poznań 1995, 281–300.

[45] M. URBAŃCZYK, A. OPILSKI, W. JAKUBIK, J. RANACHOWSKI, E. ADAMCZYK, J. RZESZOTARSKA, *Akustyczne metody monitorowania środowiska naturalnego*, Materiały XLIII Otwartego Seminarium z Akustyki, OSA'95, Warszawa–Białowieża 1995, 179–190.

[46] E. KANIA, J. RANACHOWSKI, A. JĘDRZEJEWSKI, *Aparatura i metody magnetyczne w badaniach nieniszczących*, XXIV Krajowa Konferencja Badań Nieniszczących, Poznań 1995, 95–98.

[47] I. MALECKI, J. RANACHOWSKI, *Zależność emisji akustycznej (AE) od nieliniowych procesów kruchego pękania*, Materiały XLII Otwartego Seminarium z Akustyki, OSA'95, Warszawa–Białowieża 1995.

[48] I. MALECKI, J. RANACHOWSKI, *The informatic contents of acoustic emission signals*, Proc. 15th International Congress on Acoustics, 1995, 523–526.

[49] Z. PĘSKI, J. RANACHOWSKI, *Surface waves and their applications with the use of ultrasonic wedge shaped probe*, Ultrasonics World Congress Proceedings, Part 1 or 2, Humboldt Universität, Berlin 1996, 467–470.

[50] J. RANACHOWSKI, F. REJMUND, *Zastosowanie EA w badaniu własności materiałów i urządzeń*, Procesy niszczenia i wytrzymałość kości, ceramiki i betonu, J. RANACHOWSKI, F. REJMUND [Red.], IPPT PAN, 43–73 (1996).

[51] J. RANACHOWSKI, F. REJMUND, *Zastosowanie EA w badaniu materiałow i urządzeń. Część 1*, Przegląd Mechaniczny, 3, 9–18 (1996).

[52] J. RANACHOWSKI, F. REJMUND, *Zastosowanie EA w badaniu materiałów i urządzeń. Część 2*, Przegląd Mechaniczny, 4, 25–28 (1996).

[53] J. RANACHOWSKI, A. SERDYUKOV, S. AHALUPAYEV, E. SHERSHNEV, *Forming dynamics of temperature stress fields in process of parallel termosplitting*, Prace IPPT, 10 (1996).

[54] A.M. LEKSOVSKIJ, J. RANACHOWSKI et al., *Mikrowgłębnikowe badania ceramiki z rejestracją emisji akustycznej*, [w:] Procesy niszczenia i wytrzymałości ceramiki, kości i betonu, Wyd IPPT PAN, Warszawa 1996, 105–128.

[55] I. MALECKI, J. RANACHOWSKI, *The acoustic cross-section method for evaluation of porous material parameters*, Bull.Pol.Acad. of Sciences, **44**, 1, 43–56 (1997).

[56] J. RANACHOWSKI, P. RANACHOWSKI. J. BERTRAND, *Emisja akustyczna w próbach termomechanicznych izolatorów liniowych*, Mat. Konf. Nowe kierunki technologii i badań materiałowych, Wyd. IPPT PAN, Warszawa 1999, 47–59.

ACOUSTIC EMISSION IN PZT CERAMIC IN POLING PROCESS

M. ALEKSIEJUK

Polish Academy of Sciences
Institute of Fundamental Technological Research
(00-049 Warszawa, Świętokrzyska 21, Poland)

Results of measurements of acoustic emission in PZT type ceramic in strong alternating electric field are presented. Measurements were performed with Sawyer–Tower experimental setup for poling of polarisation of these ceramic materials. Obtained signals of acoustic emission were submitted to spectrum analysis. To the interpretation of spectrum the statistical theory of noise with interactions between events was applied. Time interval parameters applied to the description of domain walls hops were found for the investigated ceramic materials.

1. Introduction

Acoustic emission method (AE) is widely applied in nondestructive testing of ferroelectric materials [1, 2]. AE was applied, among others, in studies of phase transitions [3, 4, 5] and of structure and domain dynamics [6–9]. Besides the cognitive value, the knowledge of behaviour of the domain structure in strong electric fields is important with regard to possibility of application of ferroelectric ceramics to construction of actuators, transformers, large power ultrasonic transducers etc. [9].

In this paper results of investigations of the poling process of industrial ferroelectic PZT ceramics are presented. In Sec. 2 an experimental setup is presented. In section 3 the results of AE measurements are described. In Sec. 4, analysis of the obtained experimental results and the use of statistical theory of noise to explanation of AE related to domain processes in ferroelectic materials is described.

2. Experimental setup

Acoustic emission measurements were performed in PZT ceramic materials (commercial symbols PP-1, PP-3, PP-6 and PP-9) produced in Cerad works in Warsaw. Basic properties of these materials are presented in Table 1. Measured samples had cylindrical shape (thickness $1-2$ mm, diameter 10 mm). On the back surfaces of samples, metallic electrodes were fixed. Measurements of hysteresis loops were performed using

Table 1. Properties of measured PZT samples.

Name of parameter	Dimension	PP-1	PP-3	PP-6	PP-9
density	g/cm^3	7.4	7.4	7.4	7.0
dielectric constant (E_{33}^T/E_0)	–	1700	550	850	450
quality factor (Q)	–	200	1000	600	650
piezoelectric constant (d_{31})	10^{-12} C/N	160	30	90	60
piezoelectric constant (d_{33})	10^{-12} C/N	400	60	210	450
electr.-mech. coupling factor (d_{33})	–	0.3	0.16	0.26	0.22
electr.-mech. coupling factor (d_{33})	–	0.7	0.4	0.6	0.50

Sawyer–Tower method. To make it possible to disseminate heat emerging as a result of dielectric losses in ceramics the measured samples were placed in a container with transformer oil. Samples were alternatively polarised with a sinusoidal voltage at 50 Hz and with controlled amplitude up to 3.5 kV. Acoustic emission signals were detected with a broadband AE transducers located in the container. Location of the transducers in the container made it possible to obtain stronger AE signals and reduced the level of external noise. In the head of each transducer a large rate preamplifier was mounted. By this way signals from transducers were fed directly to a Tektronix oscilloscope without an additional amplification. The obtained AE signals were recorded in the memory of the oscilloscope and then they were transmitted trough a GPIB interface to a PC computer. Experimental setup is presented in Fig. 1.
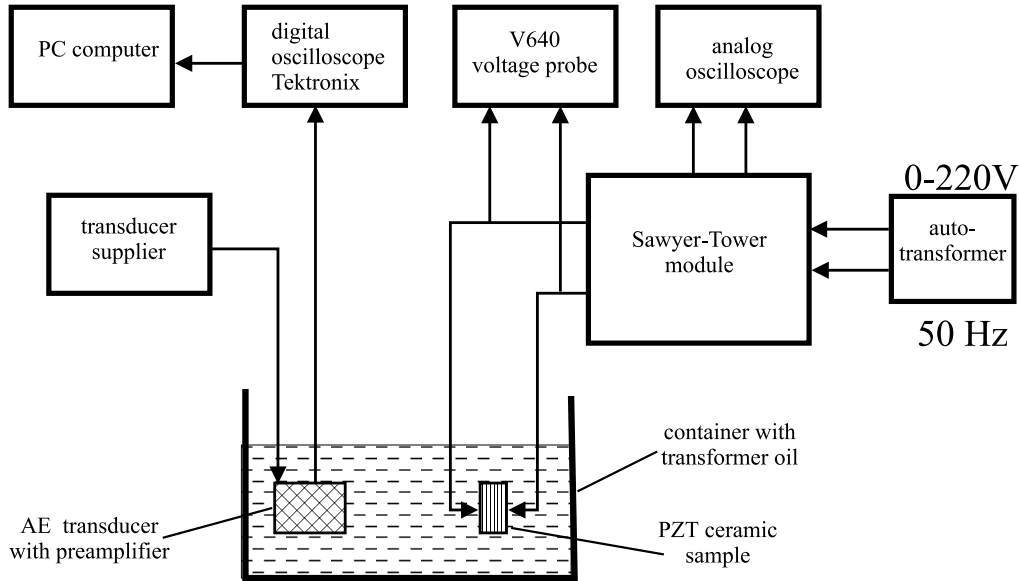
Fig. 1. Schematic diagram of experimental setup.

3. Experimental results

The AE signals repeated at 10 ms periods when the poling electric field reached its maximum. An example of a dielectric hysteresis loop for a measured sample is presented in Fig. 2. The presence of two AE signals in each cycle of change of the electric field testified that AE signals were caused by poling of material and not by creation of microcraks. The motion of domain walls caused by the electric field applied to the sample was the source of acoustic emission. In the literature there exist two different interpretations of this phenomena. In the majority of cases it is assumed that the main source of acoustic emission are the movements of the domain walls by 180° [9]. In publications of others authors it is supposed that the movements of the domain walls by 90° are the reason of the phenomenon of acoustic emission [10]. Figures 3–7 present the signals of acoustic emission for the following ceramic samples: PP-1, PP-3, PP-6, PP-9 (time scale −50 μs/cm). It can be seen that for a certain value of electric field a strong AE signal lasting for few milliseconds appears. A fast increase of amplitude of the AE signal after a certain level of poling voltage is exceeded is caused by group hops of domain walls, that is, by the
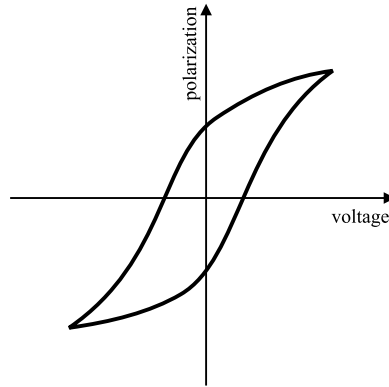
Fig. 2. Dielectric hysteresis loop of PZT ceramic (oscilloscope view).
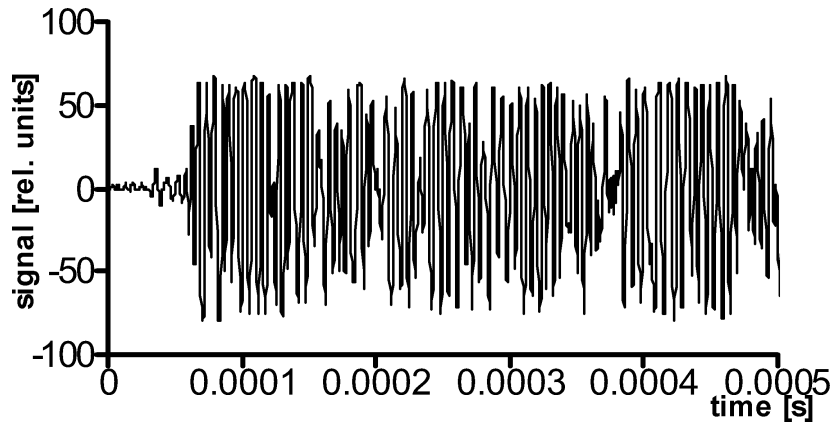
Fig. 3. AE signals of PZT ceramics (PP-1); poling voltage $U = 2.4$ kV.
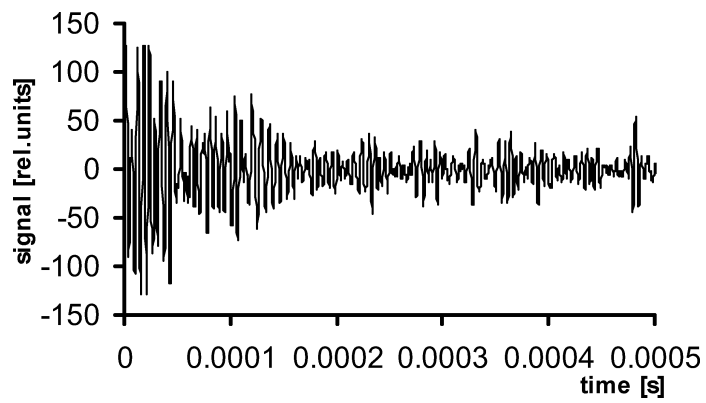
Fig. 4. AE signals of PZT ceramics (PP-3); poling voltage $U = 2.4\,\text{kV}$.
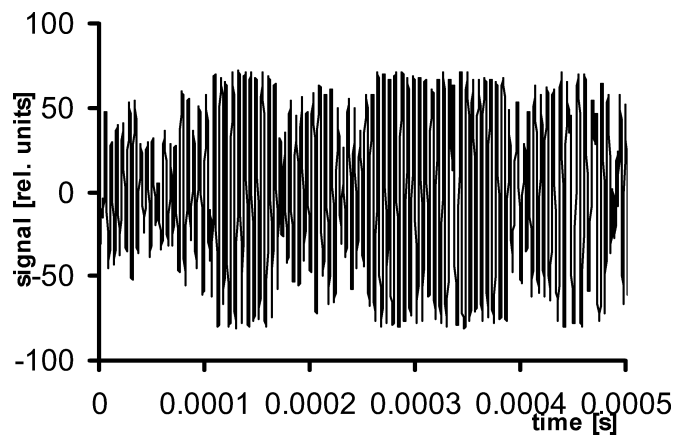
Fig. 5. AE signals of PZT ceramics (PP-6); poling voltage $U = 2.4\,\text{kV}$.
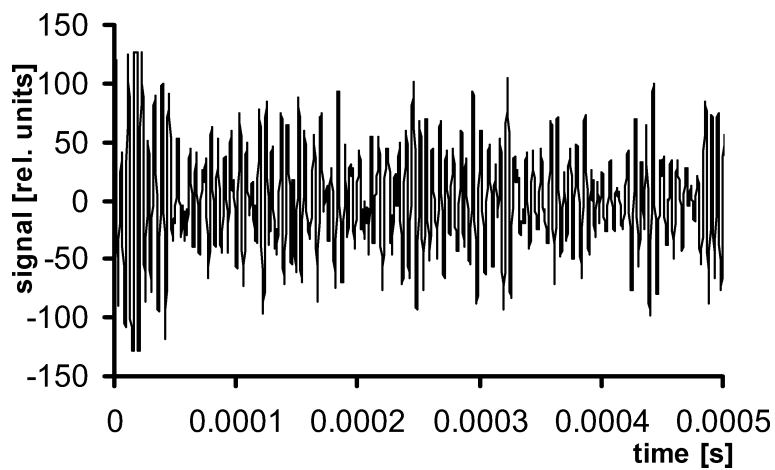
Fig. 6. AE signals of PZT ceramics (PP-6b); poling voltage $U = 2.4\,\text{kV}$.
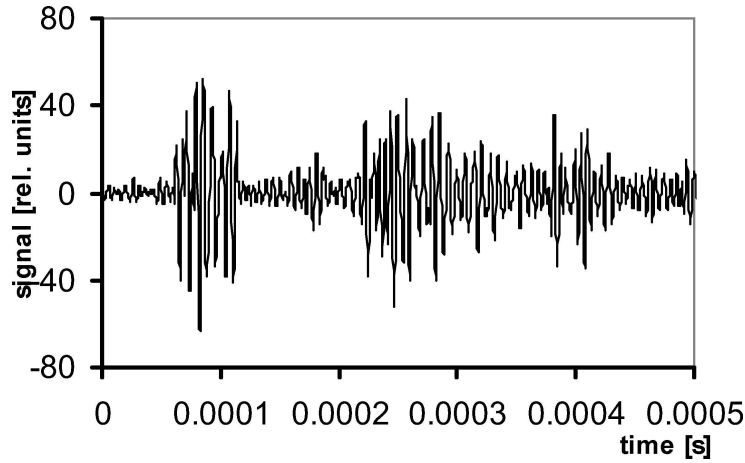
Fig. 7. AE signals of PZT ceramics (PP-9); poling voltage $U = 2.4\,\mathrm{kV}$.

emergence of clusters[11]. For magnetic materials this mechanism was observed by BITEL [12, 13]. Formation of clusters is caused by electrostatic interactions of domain walls. This interaction increases with the growth of the electric poling field in a certain range of field intensities and depends on the speed of poling of the ferroelectric material. The poling phenomenon in a material can be described in an analogy to the coherent phenomena. In the description of this phenomenon a factor is introduced which describes forced domain transitions in ferroelectric materials.

4. Spectrum analyse of acoustic emission and interpretation of results with the statistical theory

Obtained time dependencies of AE signals were subjected to spectrum analysis. In Figs. 8 – 9 examples of spectra of AE signals are presented. No repetitiveness of the AE spectra for the specimens made of ceramics of the same type was noticed. Spectrum is located in a range from $100\,\mathrm{kHz}$ to $1\,\mathrm{MHz}$ and have a fringe character. However, for a given ceramic specimen in a case of investigating the spectrum as a function of maximum electric field the acoustic emission appears at the same frequency ranges. This has been shown in Fig. 10 a – c. The dependence of spectrum for one sample of PP-6 ceramic is interesting (Fig. 11), as the spectrum structure is periodic with period $\Delta f = 75\,\mathrm{kHz}$. A spectrum with a similar appearance was obtained also for one sample of PP-9 ceramic. The period for this sample was $\Delta f = 30\,\mathrm{kHz}$, while the frequency range of AE in this second case was lower – only about $300\,\mathrm{kHz}$. In higher frequencies only two weak fringes can be seen.

To interpret the obtained results, the statistical theory of noise created for the needs of radioelectronics, which treats random processes, was used [14]. This theory treats processes in which pulses with random parameters appear in definited time periods called time intervals (Fig. 12). These processes can be nonstationary. Spectrum function which
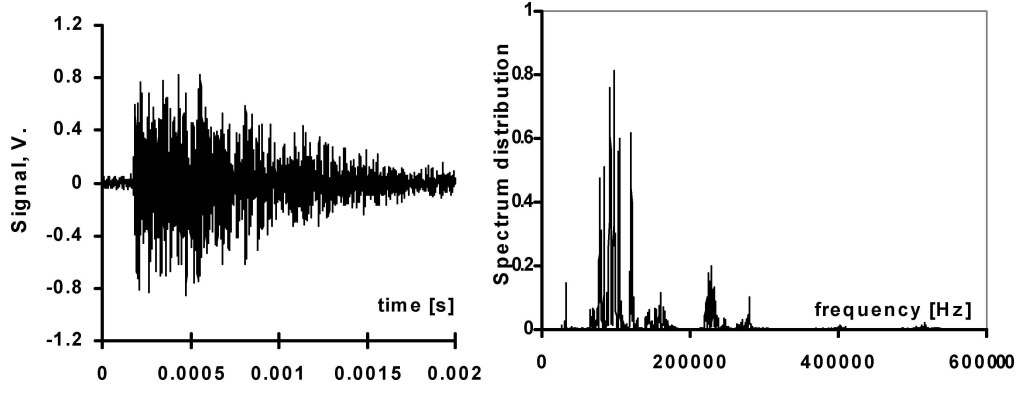
Fig. 8. Spectrum of AE signal of PZT ceramic (PP-3); poling voltage $U = 2.0\,\text{kV}$.
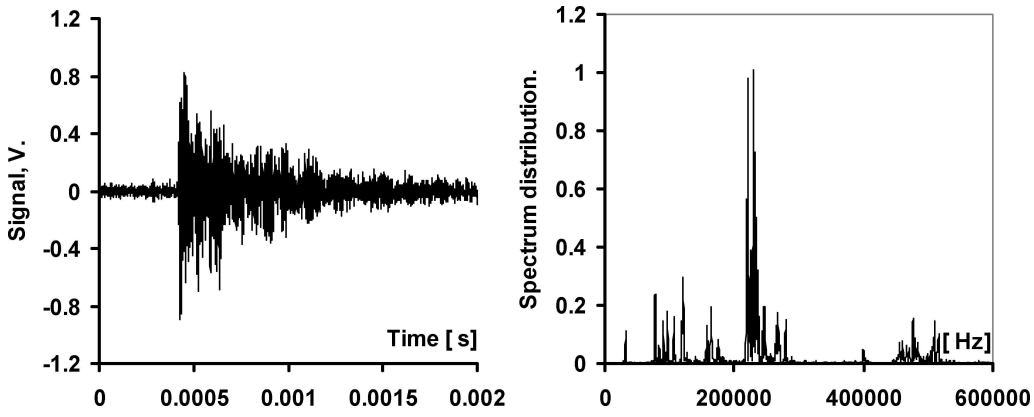
Fig. 9. Spectrum of AE signal of PZT ceramic (PP-1); poling voltage $U = 2.5\,\text{kV}$.

describes such processes is shown below:

$$F(\omega) = \frac{2}{T\left(\dfrac{1}{\tau_p^2} + \omega^2\right)}\sigma^2[1 + \psi_1(\omega)] + \frac{2\pi}{T}a^2\sum\delta\left(\omega - \frac{2\pi r}{T}\right), \tag{1}$$

where σ^2 – dispersion of amplitude of the signal, a^2 – mean value of amplitude, τ_p – constant of the transducer, r – integer value, T – time interval.

Assuming that the correlation coefficient equals:

$$R = e^{-p\beta T}\delta(p - 1), \tag{2}$$

where p – difference in numbering of pulses, β – correlation constant.

The correlation function will have the form:

$$\Psi_1(\omega) = 2\lim\sum\left(1 - \frac{p}{2N+1}\right)e^{-p\beta T}\delta(p-1)\cos p\omega T. \tag{3}$$

a

b

c
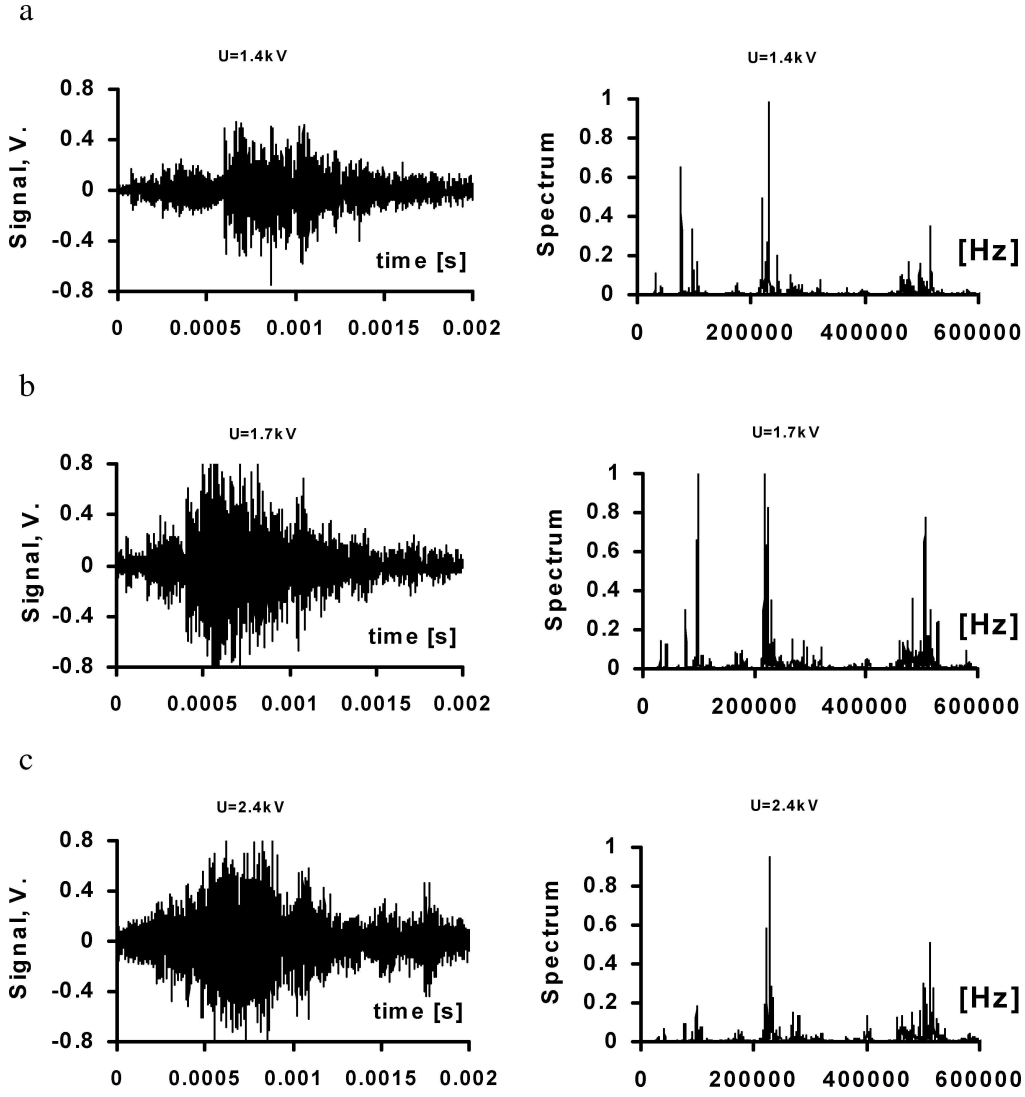
Fig. 10. AE signals and spectrum of PZT ceramic (PP-6); for different poling voltage a) $U = 1.4\,\text{kV}$, b) $U = 1.7\,\text{kV}$, c) $U = 2.4\,\text{kV}$.

Spectrum distribution takes the form:

$$g(\omega) = \frac{2\sigma^2}{T(1/\tau_p^2 + \omega^2)} \left(1 + e^{-\beta T} \cos \omega T\right). \tag{4}$$

The introduction form of the correlation coefficient of pulses in the form (2) is related to that interaction only between neighbouring pulses is taken into account, that is, during annihilation of one domain wall a new event is generated: a hop of a second domain wall (after time period T).
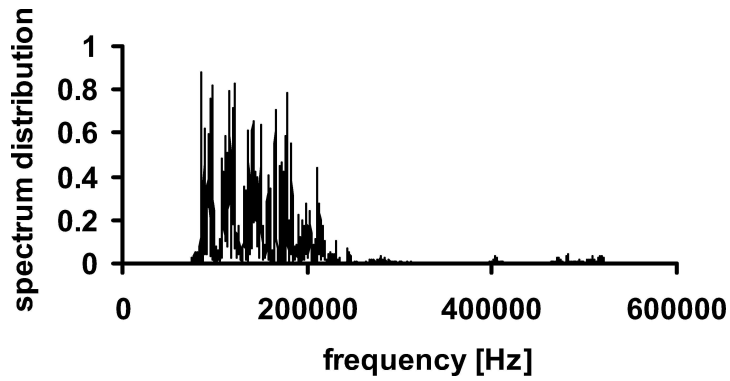
Fig. 11. Spectrum of AE signal of PZT ceramic (PP-9); poling voltage $U = 2.5\,\text{kV}$.
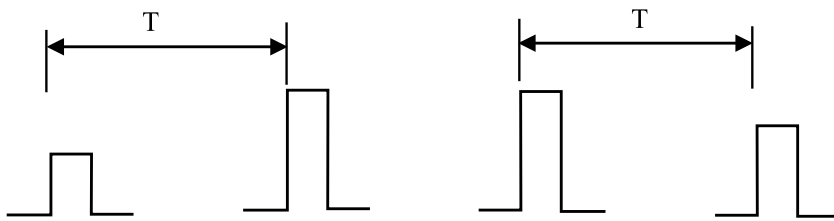
Fig. 12. Pulses with random amplitude delayed on time period T.

In Fig. 13 a theoretical spectrum obtained from formula (4) is presented. This theoretical dependence is in agreement with the dependence obtained for the sample PP-9 (Fig. 11). Time intervals obtained for these cases equal respectively: $T_1 = 300\,\mu\text{s}$ and $T_2 = 100\,\mu\text{s}$. These are times between following hops of domain walls. This results from that there is an interaction between the domain walls and the subsequent events of AE are dependent events.
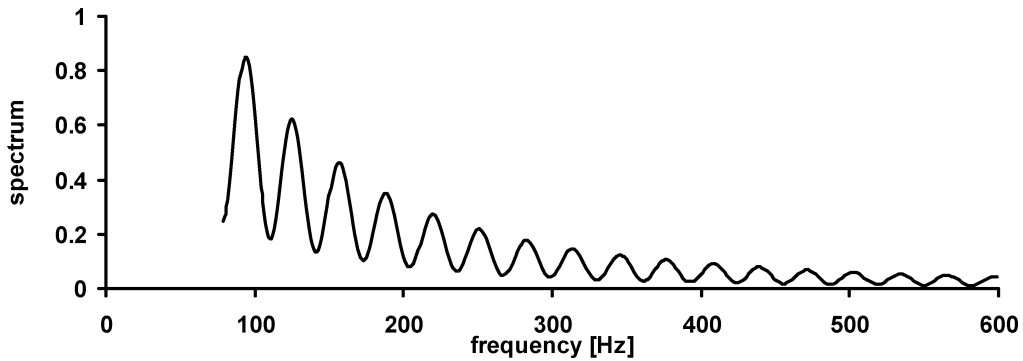
Fig. 13. Theoretical spectrum of EA signal obtained from formula (4).

5. Conclusion

From our research it results that a basis of the theory of AE in ferroelectric materials in poling processes can be the statistical theory taking into account interactions between events. Parameters of this theory are: mean value of amplitude, dispersion of amplitude and time interval T. Further studies should be carried out with this same materials. The following factors should be taken into account: changes of frequency of the poling electric field and of the internal strains caused by external factors, and the relations of the obtained results with other properties ferroelectric materials.

References

[1] R. HALMSHAW, *Non-destructive testing*, Edward Arnold, London, 2nd ed., Chap, p. 273, 1991.

[2] G.A. EVANS and M. LINZER, J. Am. Ceram. Soc., **56** (1973).

[3] P. BUCHMAN, Solid State Elektron., **15**, 142 (1972).

[4] I.J. MOHAMAD, E.F. LAMBSON, A.J. MILLER and G.A. SAUNDERS, Phys., **A71**, 115 (1979).

[5] V.A. KALITENKO, V.M. PERGA and I.N. SALIVANOV, Sov. Phys. Solid State, **22**, 1067 (1980).

[6] M. GUYOT and V. CAGAN, J. Magn. Mater., **101**, 256 (1991).

[7] M. GUYOT and V. CAGAN, J. Magn. Mater., **83**, 217 (1990).

[8] H. IWASAKI and M. IZUMI, Ferroelectrics, **37**, 563 (1981).

[9] Y. SAITO and S. HORI, Jpn. J. Appl. Phys., **33**, 9B, 5558 (1994).

[10] D.G. CHOI, J. Mater. Scien., **32**, 2, 2, 421 (1997).

[11] M. ALEKSIEJUK, [in:] New testing methods of ceramic materials, p. 260, Warszawa 1998.

[12] H. BITTEL, Physica, Bd 86, 1383, 1977.

[13] H. BITTEL and I. WESTERBOER, Annalen der Phys., **Bd 4**, 203 (1959).

[14] B.R. LEVIN, *Teoretičeskije osnovy statističeskoj radiotechniki*, pp. 550, Moskva 1974.

[15] P. MAZZETI, Il Nuovo Cimento, **25**, 6 1323 (1962).

STUDY OF THE ELASTIC PROPERTIES OF THE LITHIUM TANTALATE CRYSTAL BY THE BRILLOUIN LASER LIGHT SCATTERING

T. BŁACHOWICZ

Institute of Physics
Silesian University of Technology
(44-100 Gliwice, Krzywoustego 2, Poland)
e-mail: tblachow@zeus.polsl.gliwice.pl

This article is dedicated to prof. J. Ranachowski

The preparation of an experiment is described and measured values of elastic constants of the piezoelectric LiTaO$_3$ crystal, which belongs to the rhomboedral symmetry system, are given. As the experimental method, the Brillouin laser light scattering was applied and the constants from the hypersonic range of frequencies were measured. Appropriate conditions for the experimental configurations were determined by the use of a formalism based on the looking for eigenvalues of a so-called "characteristic matrix" which is a function of direction of the acoustic wave propagation and the elastic constants of the medium. Not all the measurement results are in full agreement with calculations based on ultrasonic data. A dispersion in the velocity of the acoustic waves can be observed for some direction of propagation due to the elastic constant changes in the hypersonic frequency range.

1. Introduction

Brillouin light scattering experiments have been well known for many years as a very useful method for the observation of acoustic phonons in the hypersonic range, both in transparent (bulk phonons) [1–4] and nontransparent media (surface phonons) [5–6]. From the quantum point of view, the creation and annihilation processes of phonons by photons are responsible for the typical Brillouin spectrum in that lines of lowered and increased frequency can be observed.

The present calculations are based on the classical theory of elasticity and classical electrodynamics, and in particular on the Newton's second law and momentum conservation which connects the wave vector of the incident light $\vec{k}$ with the wave vector of the scattered light $\vec{k}'$ and the wave vector of the acoustic wave $\vec{q}$

$$\vec{q} = \vec{k}' - \vec{k}. \tag{1}$$

The equation of motion of the acoustic wave is given in the following form

$$T_{ij,j} = \rho \ddot{u}_i \,, \tag{2}$$

where T_{ij} is the stress tensor, ρ is the density of the medium, and u_i is the displacement at the given point caused by the acoustic wave. The left side of the above equation, which is the spatial derivative of the stress tensor, is equal to

$$T_{ij,j} = c_{ijkl}^E S_{kl,j} - i\chi_j e_{nij} E_{n,j} \tag{3}$$

and was derived from the formula

$$T_{ij} = c_{ijkl}^E S_{kl} - e_{nij} E_n \,, \tag{4}$$

where, both in (3) and (4), we can recognize the elasticity tensor c_{ijkl}^E obtained at the condition of a constant electric field, at the strain tensor S_{kl}, the piezoelectric tensor e_{nij} and the electric field E_n induced by the acoustic wave due to the piezoelectric effect. The χ_j are components of a unit-length-vector in the direction of the wave vector. This vector appears in both the displacement given by

$$u_i = u_{0i} \left[e^{i(\vec{\chi}\cdot\vec{r}-\omega t)} + e^{-i(\vec{\chi}\cdot\vec{r}-\omega t)} \right], \tag{5}$$

and in the stress-induced electric field

$$E_n = E_{0n} e^{i(\vec{\chi}\cdot\vec{r}-\omega t)}. \tag{6}$$

The equality of phases in the displacement and in the electric field formulas means that the electric field is coupled by a component parallel to the direction of the acoustic wave propagation. Taking into account the dependence of the dielectric displacement on strains in a piezoelectric medium

$$D_m = e_{mkl} S_{kl} + \varepsilon_{mn}^S E_n \,, \tag{7}$$

where ε_{mn}^S is the dielectric constant (at constant strain) and taking advantage of the first Maxwell equation $D_{m,m} = 0$, where D_m are the components of the electric induction vector, we have

$$e_{mkl} S_{kl,m} + \varepsilon_{mn}^S E_{n,m} = 0. \tag{8}$$

In this way, we obtain a formula for the electric field

$$E_{n,j} = -\frac{e_{nkl} S_{kl,m}}{i\chi_m \varepsilon_{mn}^S} = -\frac{e_{mkl} \chi_k \chi_m u_l}{i\chi_m \varepsilon_{mn}^S} \,, \tag{9}$$

in that we have taken into account Eq. (5) and the following simple formulas

$$S_{kl,j} = u_{k,lj} = -\chi_l \chi_j u_k \tag{10}$$

and

$$S_{kl,j} = u_{l,kj} = -\chi_k \chi_j u_l \tag{11}$$

derived from the definition of the strain tensor

$$S_{kl} = 0.5 \cdot (u_{k,l} + u_{l,k}). \tag{12}$$

By substituting (3), (9) and (11) into the equation of motion (2) the following relation can be obtained

$$-c_{ijkl}^E \chi_j \chi_l u_k - \frac{e_{nij} e_{mkl} \chi_n \chi_m}{\varepsilon_{mn}^S \chi_m \chi_n} \cdot \chi_j \chi_l u_k = -\omega^2 \rho u_k \delta_{ik} \tag{13}$$

which is equivalent to a set of three independent linear equations, corresponding to three acoustic waves of different polarization. The equations result from the following determinant

$$\left| \left(c_{ijkl}^E + \frac{e_{nij}e_{mkl}\chi_n\chi_m}{\varepsilon_{mn}^S\chi_m\chi_n} \right) \chi_j\chi_l - \omega^2\rho\delta_{ik} \right| = 0. \tag{14}$$

The above equation defines the elastic constants modified by the piezoelectric effect and named in the literature as piezoelectrically stiffened elastic stiffness coefficients [7] or effective elastic constants [8]; an eigenproblem for the characteristic matrix defined as $Q_{ik} = c_{ijkl}^{ef}\chi_j\chi_l$ [8, 9, 10] can be recognized. Equation (14) can now be rewritten as follows

$$|Q_{ik} - X\delta_{ik}| = 0. \tag{15}$$

The eigenvectors $\vec{\gamma}$ of the Q_{ik} matrix describe states of polarization of the acoustic waves; a square root of the eigenvalues X, divided by the density of the medium, informs us about the speeds of sound.

The elastic constants can be expressed in a matrix form. Its well known symmetry for the rhomboedral crystal,

$$c_{ij} = \begin{bmatrix} c_{11}^E & c_{12}^E & c_{13}^E & c_{14}^E & 0 & 0 \\ c_{12}^E & c_{11}^E & c_{13}^E & -c_{14}^E & 0 & 0 \\ c_{13}^E & c_{13}^E & c_{33}^E & 0 & 0 & 0 \\ c_{14}^E & -c_{14}^E & 0 & c_{44}^E & 0 & 0 \\ 0 & 0 & 0 & 0 & c_{44}^E & c_{14}^E \\ 0 & 0 & 0 & 0 & c_{14}^E & 0.5\left(c_{11}^E - c_{12}^E\right) \end{bmatrix}, \tag{16}$$

is however changed for the effective elastic constants modified by the piezoelectric effect

$$c_{ij}^{ef} = \begin{bmatrix} c_{11}^{ef} & c_{12}^{ef} & c_{13}^{ef} & c_{14}^{ef} & 0 & 0 \\ c_{12}^{ef} & c_{22}^{ef} & c_{23}^{ef} & c_{24}^{ef} & 0 & 0 \\ c_{13}^{ef} & c_{23}^{ef} & c_{33}^{ef} & 0 & 0 & 0 \\ c_{14}^{ef} & c_{24}^{ef} & 0 & c_{44}^{ef} & 0 & 0 \\ 0 & 0 & 0 & 0 & c_{55}^{ef} & c_{56}^{ef} \\ 0 & 0 & 0 & 0 & c_{56}^{ef} & c_{66}^{ef} \end{bmatrix}. \tag{17}$$

The main purpose of this work was the measurement of the elastic constants of the LiTaO$_3$ piezoelectric crystal by Brillouin laser light scattering. This consists in measuring the changes of the photon frequencies by inelastic scattering on acoustic phonons near the origin of the first Brillouin zone.

The article provides information about four kinds of scattering configurations labeled by A, B, C, D (Fig. 1) in which the angle between the direction of the incident and scattered light was equal to $\pi/2$.

A configuration

[120]

[10$\bar{1}$]

$\vec{k'}$

$\vec{k}$ [101]

[10$\bar{1}$]

x

$\chi_1 = -1$

$\chi_2 = 0$

$\chi_3 = 0$

B configuration

[$\bar{1}\bar{2}$0]

[10$\bar{1}$]

$\vec{k'}$

x

$\vec{k}$ [$\bar{1}$0$\bar{1}$]

$\chi_1 = 0$

$\chi_2 = 0$

$\chi_3 = 1$

C configuration

z

$\vec{k'}$

15°

105°

[110] $\vec{k}$

$\chi_1 = 0$

$\chi_2 = -1$

$\chi_3 = 0$

D configuration

x

$\vec{k'}$

z

$\vec{k}$

[$\bar{1}\bar{2}$0]

$\chi_1 = 0$

$\chi_2 = \dfrac{\sqrt{2}}{2}$

$\chi_3 = \dfrac{\sqrt{2}}{2}$
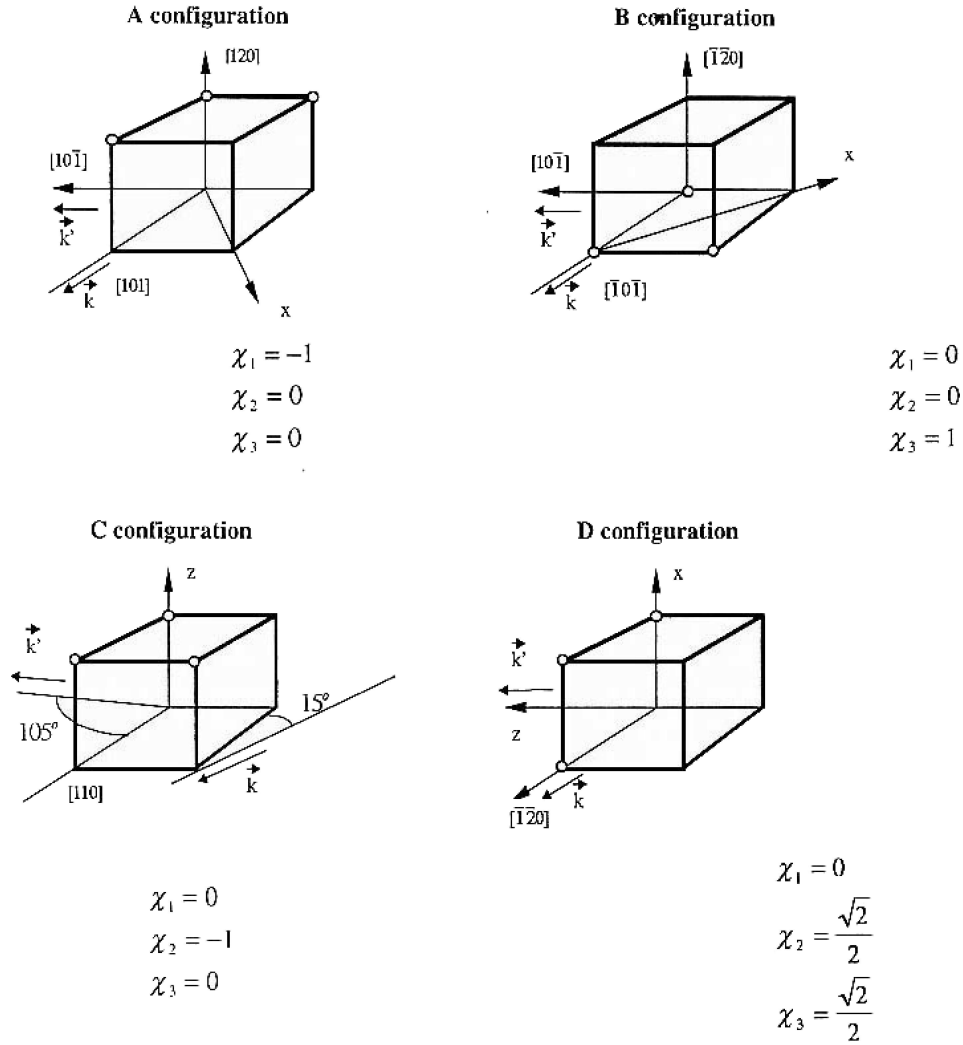
Fig. 1. Graphic definition of the experimental configurations useful for the determination of the elastic constants. Descriptions: $\vec{k}$ – wave vector of the incident light, $\vec{k'}$ – wave vector of the scattered light. The figure provides also components of the wave vector of the acoustic wave (χ_j).

2. The experimental-scattering configurations

The present section provides detailed information about the characteristic matrix for the mentioned experimental configurations and its eigenvalues. The eigenvalues contain information about frequency, polarization and velocity of the acoustic wave and, consequently, information about the investigated elastic constants.

The measurements were done on an arrangement the main elements of which are as follow: a single-mode ion-argon laser working at 514.5 nm with a power of about 100 mW, a scanned Fabry–Perot single-pass pressure interferometer and a device for single photon

counting (PTI-614 analog-digital unit from Photon Inc.) with a Hamamatsu R-4220P photomultiplier. The systematic error of the phonon frequency measurement, induced by the experimental arrangement and the numerical treatment of the data, was equal to 0.15 GHz. The statistical errors depended on the specific measurement and were in the range from 0.04 GHz to 0.27 GHz; in most cases, however they were equal to 0.08 GHz. The total error (standard deviation) for the measured frequency was calculated for the 0.7 level of confidence. All the spectra were achieved in the linear range of pressure changes [11, 12]. This means that the time scale is linearly proportional to frequency.

2.1. The A configuration — determination of the elastic constant c_{11}^E

The A configuration (see Fig. 2a) is suitable for the determination of the c_{11}^E elastic constant. It can be calculated from the Q_{11} element of the characteristic matrix because $Q_{11} = c_{11}^E$. The other values of the characteristic matrix elements are as follows:

$$
\begin{aligned}
Q_{22} &= \left[0.5 \cdot \left(c_{11}^E - c_{12}^E \right) + \frac{e_{16} e_{16}}{\varepsilon_{11}^S} \right], \\
Q_{33} &= c_{44}^E + \frac{e_{15} e_{15}}{\varepsilon_{11}^S}, \\
Q_{23} &= c_{14}^E + \frac{e_{15} e_{16}}{\varepsilon_{11}^S}, \\
Q_{31} &= 0, \qquad Q_{12} = 0,
\end{aligned}
\tag{18}
$$

where e_{ij} are the piezoelectric tensor elements written in the double-index formalism. The eigenvalues of the Q_{ij} matrix are equal to

$$
\begin{aligned}
X_1 &= c_{11}^E, \\
X_{2/3} &= 0.5 \left[\left(0.5(c_{11}^E - c_{12}^E) + c_{44}^E + \frac{e_{16}e_{16} + e_{15}e_{15}}{\varepsilon_{11}^S} \right) \right. \\
&\qquad \pm \left[\left(0.5(c_{11}^E - c_{12}^E) + c_{44}^E + \frac{e_{16}e_{16} + e_{15}e_{15}}{\varepsilon_{11}^S} \right)^2 \right. \\
&\qquad \left. \left. - 4 \left[\left(0.5(c_{11}^E - c_{12}^E) + \frac{e_{16}e_{16}}{\varepsilon_{11}^S} \right) \left(c_{44}^E + \frac{e_{15}e_{15}}{\varepsilon_{11}^S} \right) - \left(c_{14}^E + \frac{e_{15}e_{16}}{\varepsilon_{11}^S} \right)^2 \right]^{1/2} \right] \right].
\end{aligned}
\tag{19}
$$

It is easy to see that the equation $c_{11}^E = X_1$ determines the investigated elastic constant. The acoustic wave frequency observed experimentally, associated with the X_1 eigenvalue, was equal to 33.74 ± 0.16 GHz. The other eigenvalues are smaller. This means that a quasi-longitudinal acoustic wave was responsible for the X_1 value. The X_2 and X_3 values provide information about the quasi-transverse waves of frequency f and the velocity v. The formulas adequate for these parameters are as follows:

$$
f = \frac{n}{\lambda} \sqrt{\frac{2X}{\rho}}
\tag{20}
$$
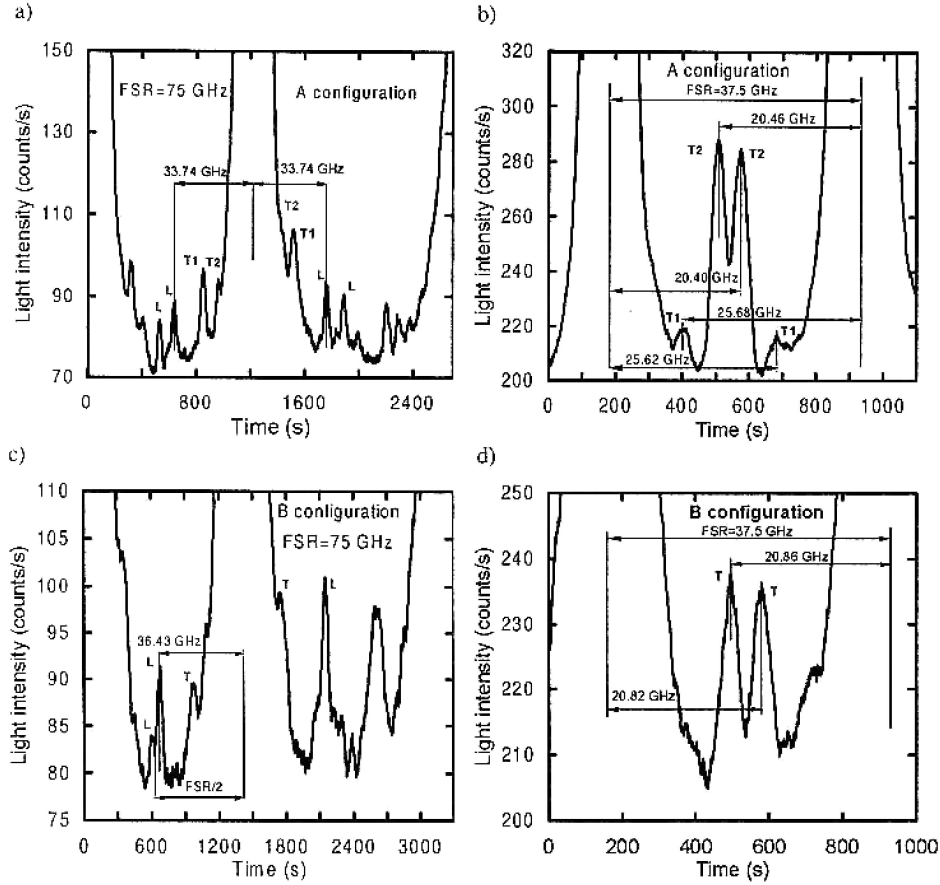
Fig. 2. Example of the Brillouin spectrum of the LiTaO$_3$ crystal: a) A configuration — full spectral range FSR equal to 75 GHz. Descriptions: L – longitudinal wave, $T1$ – quasi-transverse wave, $T2$ – quasi-transverse wave, b) A configuration — full spectral range FSR equal to 37.5 GHz. Descriptions: $T1$ – quasi-transverse wave, $T2$ – quasi-transverse wave, c) B configuration — full spectral range FSR equal to 75 GHz. Descriptions: L – longitudinal wave, T – transverse wave, d) B configuration — full spectral range FSR equal to 37.5 GHz. Description: T – transverse wave.

and

$$v = \sqrt{\frac{X}{\rho}}, \qquad (21)$$

where n is the refractive index of the medium for an ordinary beam, X is the eigenvalue of the characteristic matrix and ρ is the density of the medium. In the present paper, numerical results were obtained for the wave vector of the acoustic wave $|\vec{\chi}| = 1$. Figures 2a and 2b show examples of the Brillouin spectra for two different full FSR spectral ranges of the Fabry–Perot interferometer [12]. The spectrum in Fig. 2a shows all three lines arising from one longitudinal and two quasi-transverse acoustic waves. The FSR chosen for the next spectrum (Fig. 2b) enables a detailed observation of the two quasi-transverse frequency waves. The signal from the longitudinal wave is hidden in the strong

peak resulting from elastic scattering (the Rayleigh line). Table 1 gives the values of the calculated eigenvectors, eigenvalues, frequencies and velocities from the elastic constants of SMITH *et al.* measured ultrasonically [13], as well as a comparison with the results of the present measurements [14].

Table 1. Comparision of the acoustic wave velocity and frequency calculated from the values of the elastic constants measured ultrasonically with the velocity and frequency calculated from the hypersonic values of the elastic constants for the A configuration. Eigenvectors ($\vec{\gamma}$) and eigenvalues (X_1, X_2, X_3) calculated from the ultrasonic elastic constants.

Descriptions	Longitudinal wave (X_1)	Quasi-transverse wave (X_2)	Quasi-transverse wave (X_3)
Calculated eigenvectors	[1, 0, 0]	[0, −0.6043, 0.7967]	[0, 0.7967, 0.6043]
Calculated eigenvalues (10^{10} Pa)	23.30	12.97	8.30
Calculated velocities (m/s)	5592	4172	3338
Calculated frequencies (GHz)	33.97	25.35	20.28
Measured velocities (m/s)	5554 ± 26	4214 ± 28	3352 ± 25
Measured frequencies (GHz)	33.74 ± 0.16	25.60 ± 0.17	20.36 ± 0.15
Measured eigenvalues (10^{10} Pa)	22.98 ± 0.21	13.23 ± 0.18	8.37 ± 0.13

2.2. The B *configuration – determination of the elastic constants* c_{33}^E *and* c_{44}^E

The Q_{33} element of the characteristic matrix provides information about the elastic constant c_{33}^E. The c_{44}^E value can be determined from the Q_{11} and Q_{22} elements which are equal to one another. All the elements of the characteristic matrix and its eigenvalues are written as follows:

$$Q_11 = c_{44}^E, \quad Q_{22} = c_{44}^E, \quad Q_{33} = c_{33}^E + \frac{e_{33}e_{33}}{\varepsilon_{33}^S},$$
$$Q_{23} = 0, \quad Q_{31} = 0, \quad Q_{12} = 0, \tag{22}$$

$$\begin{aligned} X_1 &= c_{44}^E, \\ X_2 &= c_{44}^E, \\ X_3 &= c_{33}^E + \frac{e_{33}e_{33}}{\varepsilon_{33}^S}. \end{aligned} \tag{23}$$

It is obvious that the equation $c_{33}^E = X_3 - e_{33}e_{33}/\varepsilon_{33}^S$ is useful for the determination of the elastic constants c_{33}^E. The values of the piezoelectric e_{ij} constants were taken from Ref. [8] and from Ref. [9, 13] for comparison. There are no information about the experimental errors in these papers. Therefore the results of current calculations were doubled in this case. The experiment acoustic wave frequency, responsible for the X_3 eigenvalue measurement, was equal to 36.43 ± 0.19 GHz. The remaining eigenvalues are smaller. This means that a quasi-longitudinal acoustic wave was responsible for the X_3 value. The X_1 and X_2 provide information about frequencies and velocities of the quasi-transverse waves (23). Their frequencies are equal but possess perpendicular polarizations. The values are

equal to 20.94 ± 0.16 GHz. In this way, the waves are degenerated. Brillouin spectra similar to those of the A configuration can be found in Figs. 2c and 2d. Table 2 contains the values of the calculated eigenvectors, eigenvalues, frequencies and velocities from the elastic constants measured ultrasonically, as well as with the results of measurements for the B configuration for comparison.

Table 2. Comparision of the acoustic wave velocity and frequency calculated from the values of the elastic constants measured ultrasonically with the velocity and frequency calculated from the hypersonic values of the elastic constants for the B configuration. Eigenvectors ($\vec{\gamma}$) and eigenvalues (X_1, X_2, X_3) calculated from the ultrasonic elastic constants.

Descriptions	Longitudinal wave (X_3)	Transverse wave (X_1)	Transverse wave (X_2)
Calculated eigenvectors	[0, 0, 1]	[1, 0, 0]	[0, 1, 0]
Calculated eigenvalues (10^{10} Pa)	28.45	9.40	9.40
Calculated velocities (m/s)	6180	3552	3552
Calculated frequencies (GHz)	37.54	21.58	21.58
Measured velocities (m/s)	5997 ± 31	3447 ± 26	3447 ± 26
Measured frequencies (GHz)	36.43 ± 0.19	20.94 ± 0.16	20.94 ± 0.16
Measured eigenvalues (10^{10} Pa)	26.79 ± 0.27	8.85 ± 0.14	8.85 ± 0.14

2.3. The C configuration – determination of the elastic constant c_{66}^E

The C configuration is suitable for the measurement of the elastic constant c_{66}^E. Its value is given by the Q_{11} element of the characteristic matrix. All the elements of the characteristic matrix and its eigenvalues are as follows:

$$
\begin{aligned}
Q_{11} &= \frac{1}{2}\left(c_{11}^E - c_{12}^E\right), & Q_{22} &= c_{11}^E + \frac{e_{22}e_{22}}{\varepsilon_{11}^S}, & Q_{33} &= c_{44}^E + \frac{e_{15}e_{15}}{\varepsilon_{11}^S}, \\
Q_{23} &= -c_{141}^E + \frac{e_{22}e_{15}}{\varepsilon_{11}^S}, & Q_{31} &= 0, & Q_{12} &= 0,
\end{aligned}
\tag{24}
$$

$$
\begin{aligned}
X_1 =& \frac{1}{2}\left(c_{11}^E - c_{12}^E\right), \\
X_2 =& \frac{1}{2}\left[c_{11}^E + c_{44}^E + \frac{e_{22}e_{22} + e_{15}e_{15}}{\varepsilon_{11}^S} - \left(\left(c_{11}^E + c_{44}^E + \frac{e_{22}e_{22} + e_{15}e_{15}}{\varepsilon_{11}^S}\right)^2 \right.\right. \\
& \left.\left. -4\cdot\left(\left(c_{11}^E + \frac{e_{22}e_{22}}{\varepsilon_{11}^S}\right)\left(c_{44}^S + \frac{e_{15}e_{15}}{\varepsilon_{11}^S}\right) - \left(-c_{14}^E + \frac{e_{22}e_{15}}{\varepsilon_{11}^S}\right)^2\right)\right)^{1/2}\right], \\
X_3 =& \frac{1}{2}\left[c_{11}^E + c_{44}^E + \frac{e_{22}e_{22} + e_{15}e_{15}}{\varepsilon_{11}^S} + \left(\left(c_{11}^E + c_{44}^E + \frac{e_{22}e_{22} + e_{15}e_{15}}{\varepsilon_{11}^S}\right)^2 \right.\right. \\
& \left.\left. -4\cdot\left(\left(c_{11}^E + \frac{e_{22}e_{22}}{\varepsilon_{11}^S}\right)\left(c_{44}^S + \frac{e_{15}e_{15}}{\varepsilon_{11}^S}\right) - \left(-c_{14}^E + \frac{e_{22}e_{15}}{\varepsilon_{11}^S}\right)^2\right)\right)^{1/2}\right].
\end{aligned}
\tag{25}
$$

The acoustic wave frequency observed in the experiment and responsible for the measurement of the eigenvalue X_1, was equal to 21.45 ± 0.19 GHz. The values of the calculated eigenvectors, eigenvalues, frequencies and velocities as well as a comparison with hypersonic results of measurements for the C configuration are given in Table 3.

Table 3. Comparision of the acoustic wave velocity and frequency calculated from the values of the elastic constants measured ultrasonically with the velocity and frequency calculated from the hypersonic values of the elastic constants for the C configuration. Eigenvectors ($\vec{\gamma}$) and eigenvalues (X_1, X_2, X_3) calculated from the ultrasonic elastic constants.

Descriptions	Quasi-longitudinal wave (X_3)	Quasi-transverse wave (X_2)	Transverse wave (X_1)
Calculated eigenvectors	$[0, -0.9857, -0.1688]$	$[0, 0.1688, -0.9857]$	$[1, 0, 0]$
Calculated eigenvalues (10^{10} Pa)	24.39	10.88	9.30
Calculated velocities (m/s)	5722	3821	3533
Calculated frequencies (GHz)	34.76	23.21	21.46
Measured velocities (m/s)	–	3946 ± 44	3530 ± 31
Measured frequencies (GHz)	–	23.97 ± 0.31	21.45 ± 0.19
Measured eigenvalues (10^{10} Pa)	–	11.60 ± 0.26	9.28 ± 0.16

2.4. Indirect determination of the elastic constant c_{12}^E from the A and C configurations

The elastic constant c_{12}^E was calculated from the following condition

$$c_{12}^E = c_{11}^E - 2 \cdot c_{66}^E, \qquad (26)$$

where the c_{12}^E value was taken from the A configuration (19) and that of c_{66}^E from the C configuration (25).

2.5. The D configuration. Indirect determination of the elastic constant c_{14}^E from the C, B and D configurations and indirect determination of the elastic constant c_{13}^E from the A, B and D configurations

All the elements of the characteristic matrix (not equal to zero) and their eigenvalues for the D configuration are as follows:

$$
\begin{aligned}
Q_{11} &= \frac{1}{2}\left(c_{66}^E - c_{44}^E\right) + c_{14}^E, \\
Q_{22} &= \frac{1}{2}\left(c_{11}^E + \frac{e_{22}e_{22}}{\varepsilon_{11}^S + \varepsilon_{33}^S}\right) + \frac{1}{2}\left(c_{44}^E + \frac{e_{15}e_{15}}{\varepsilon_{11}^S + \varepsilon_{33}^S}\right) + \frac{1}{2}\left(-c_{14}^E + \frac{e_{22}e_{15}}{\varepsilon_{11}^S + \varepsilon_{33}^S}\right), \\
Q_{33} &= \frac{1}{2}\left(c_{44}^E + \frac{e_{15}e_{15}}{\varepsilon_{11}^S + \varepsilon_{33}^S}\right) + \frac{1}{2}\left(c_{33}^E + \frac{e_{33}e_{33}}{\varepsilon_{11}^S + \varepsilon_{33}^S}\right), \\
Q_{23} &= \frac{1}{2}\left(-c_{14}^E + \frac{e_{22}e_{15}}{\varepsilon_{11}^S + \varepsilon_{33}^S}\right) + \frac{1}{2}\left(c_{13}^E + c_{44}^E + \frac{e_{22}e_{33} + e_{15}e_{15}}{\varepsilon_{11}^S + \varepsilon_{33}^S}\right),
\end{aligned}
\qquad (27)
$$

$$X_1 = Q_{11},$$
$$X_2 = \frac{1}{2}\left[Q_{22} + Q_{33} + \sqrt{Q_{22}^2 + 4Q_{23}^2 - 2Q_{22}Q_{33} + Q_{33}^2}\right],$$ (28)
$$X_3 = \frac{1}{2}\left[Q_{22} + Q_{33} - \sqrt{Q_{22}^2 + 4Q_{23}^2 - 2Q_{22}Q_{33} + Q_{33}^2}\right].$$

The elastic constant c_{14}^E was calculated from the following formula

$$c_{14}^E = X_1 - \frac{1}{2}\cdot(c_{66}^E + c_{44}^E),$$ (29)

where the X_1 value was taken from the D configuration (28) and the remaining values, c_{66}^E and c_{44}^E, were taken from the C (25), and B configurations (23), respectively.

Table 4. Comparision of the acoustic wave velocity and frequency calculated from the values of the elastic constants measured ultrasonically with the velocity and frequency calculated from the hypersonic values of the elastic constants for the D configuration. Eigenvectors ($\vec{\gamma}$) and eigenvalues (X_1, X_2, X_3) calculated from the ultrasonic elastic constants.

Descriptions	Quasi-longitudinal wave (X_2)	Quasi-transverse wave (X_3)	Transverse wave (X_1)
Calculated eigenvectors	[0, −0.9857, −0.1688]	[0, 0.1688, −0.9857]	[1, 0, 0]
Calculated eigenvalues (10^{10} Pa)	24.39	10.88	9.30
Calculated velocities (m/s)	5722	3821	3533
Calculated frequencies (GHz)	34.76	23.21	21.46
Measured velocities (m/s)	−	3946 ± 44	3530 ± 31
Measured frequencies (GHz)	−	23.97 ± 0.31	21.45 ± 0.19
Measured eigenvalues (10^{10} Pa)	−	11.60 ± 0.26	9.28 ± 0.16

Table 5. Summary of the measurements of the elastic constants of the rhomboedral LiTaO$_3$ crystal. Comparision of the measured (hypersonic) and ultrasonic values of the elastic constants.

Elastic constant	Experimental configuration	Measured elastic constant c_{ij}^E (10^{10} Pa)	Ultrasonically measured elastic constant c_{ij}^E [13] (10^{10} Pa)	Ultrasonically measured elastic constant c_{ij}^E [8] (10^{10} Pa)
c_{11}^E	A	22.98 ± 0.21	22.98	23.3
c_{33}^E	B	26.48 ± 0.27[a] 25.84 ± 0.26[b]	27.98	27.5
c_{44}^E	B	8.85 ± 0.14	9.68	9.4
c_{66}^E	C	9.28 ± 0.16	9.29	9.3
c_{12}^E	A, C	4.42 ± 0.53	4.40	4.7
c_{14}^E	D, B, C	0.45 ± 0.29	−1.04	−1.1
c_{13}^E	D, A, B	5.36 ± 0.47[a] 5.05 ± 0.44[b]	8.12	8.0

[a] – The piezoelectric constants e_{ij} were taken from Reference [13] and permittivities ε_{ij}^S were taken from Reference [9].
[b] – The piezoelectric constants e_{ij} and permittivities ε_{ij}^S were taken from Reference [8].

The c_{13}^E value is hidden in the X_3 eigenvalue (28), and in the Q_{23} element of the characteristic matrix. To solve this problem, the values of the elastic constants c_{33}^E and c_{44}^E must to be taken from the B configuration and the c_{11}^E is available from the A configuration, so that the c_{13}^E elastic constant is calculated indirectly from 4 values. Therefore their experimental error is relatively large and equal to 8.8%. Table 4 shows the values of the calculated eigenvectors, eigenvalues, frequencies and velocities from the ultrasonic data as well as a comparison with results of the measurements. Table 5 contains values of the measured elastic constants, their experimental errors as well as a comparison with ultrasonic values.

3. Conclusions

A description of the appropriate choice of configurations required for the measurement of the elastic constants of a rhomboedral piezoelectric crystal was given above. As an example, the LiTaO$_3$ crystal was investigated. The appropriate configuration means that calculated quantities, such as eigenvalues of the characteristic matrix, frequencies and velocities of hypersonic acoustic waves, possess a simple interpretation. This means that the velocities and frequencies depending on the elastic constants in an evident form and not only by pure numerical values. The discussion of a contrary example can be found in Ref. 10.

The general conclusion is that the elastic constants c_{33}^E, c_{44}^E, c_{14}^E, c_{13}^E, for the hypersonic range stayed weaker, if to compare their values with values measured ultrasonically, then the subsequent values of velocities stayed lower. The elastic constants c_{11}^E, c_{13}^E, c_{66}^E are not changed.

It was shown that the formalism based on the determination of the eigenvectors and eigenvalues is very effective and provides a simple physical interpretation. The eigenvectors describe states of polarization of the acoustic wave and the square root of the eigenvalues divided by the density of the medium informs about the speeds of sound. However the presented calculations, based on the classical theory of elasticity and a comparison with the Brillouin scattering measurements can not describe the divergences obtained. More theoretical investigation is required to explain these facts in details.

We hope that the considerations and data given here are detailed enough to provide an adequate description of the nature of the phenomenon.

References

[1] G. Li, X.K. Chen, N.J. Tao, H.Z. Cummins, R.M. Pick and G. Hauret, *Brillouin scattering studies of the transverse acoustic modes of incommensurate* K$_2$SeO$_4$, Phys. Rev., **B44**, 13, 6621–6629 (1991).

[2] L.E. McNeil and M. Grimsditch, *Elastic constants of* As$_2$S$_3$, Phys. Rev., **B44**, 9, 4174–4177 (1991).

[3] J.J. Vanderwal, P. Zhao and D. Walton, *Brillouin scattering from the icosahedral quasicrystal* Al$_{63.5}$Cu$_{24.5}$Fe$_{12}$, Phys. Rev., **B46**, 1, 501–502 (1992).

[4] U. SCHÄRER and P. WACHTER, *Negative elastic constants in intermediate valent* $Sm_xLa_{1-x}S$, Solid St. Comm., **96**, 497–501 (1995).

[5] R. DANNER, R.P. HUEBENER, C.L. CHUN, M. GRIMSDITCH and I.K. SCHULLER, *Surface acoustic waves in* Ni/V *superlattices*, Phys. Rev., **B33**, 6, 3696–3701 (1986).

[6] M. HUES, R. BHADRA, M. GRIMSDITCH, E. FULLERTON and I.K. SCHULLER, *Effect of high-energy ion irradiation on the elastic moduli of* Ag/Co *superlattices*, Phys. Rev., **B39**, 17, 12966–12968 (1989).

[7] J. XU and R. STROUD, *Acousto-optic devices: principles, design and applications*, John Wiley & Sons Inc., 1992.

[8] A.W. WARNER, M. ONOE and G.A. COQUIN, *Determination of elastic and piezoelectric constants for crystals in class* (3m), J. Acoust. Soc. Am., **42**, 6, 1223–1231 (1966).

[9] W. SOLUCH, *Introduction to piezoelectronics*, Wydawnictwa Komunikacji i Łączności, Warszawa 1980.

[10] T. BŁACHOWICZ and Z. KLESZCZEWSKI, *Observation of hypersonic acoustic waves in a* $LiTaO_3$ *crystal*, Archives of Acoustics, **22**, 3, 351–357 (1997).

[11] T. BŁACHOWICZ, *Wykorzystanie światła laserowego do badania sprężstych własności ciał stałych w obszarze hiperdźwiękowym*, Wydawnictwo Politechniki Śląskiej, Gliwice 1999.

[12] T. BŁACHOWICZ, R. BUKOWSKI and Z. KLESZCZEWSKI, *Fabry-Perot interferometer in Brillouin scattering experiments*, Rev. Sci. Instrum., **67**, 12, 4057–4060 (1996).

[13] R.T. SMITH and F.S. WELSH, *Temperature dependence of the elastic, piezoelectric and dielectric constants of lithum tantalate and lithium niobate*, J. App. Phys., **42**, 6, 2219–2230 (1971).

[14] T. BŁACHOWICZ and Z. KLESZCZEWSKI, *Elastic constants of the lithium tantalate crystal in the hypersonic range*, J. Acoust. Soc. Am., **104**, 6, 3356–3357 (1998).

THE INFLUENCE OF PREPARATION CONDITIONS
ON THE ELECTRO-ACOUSTIC PROPERTIES OF
THE PZT-TYPE PIEZOCERAMIC SENSORS

J. DUDEK, L. KOZIELSKI, Z. SUROWIAK

Silesian University of Technology,
Department of Materials Science
(41-200 Sosnowiec, 2 Śnieżna Str., Poland)
e-mail:surowiak@us.edu.pl

M.F. KUPRIYANOV

Rostov on Don State University, Faculty of Physics
(344-104 Rostov on Don, 5 Zorge Str., Russia)

The possibilities of the application of the microstructure analysis, X-ray powder diffraction, and Raman scattering methods for the fast and reliable control of the quality of piezoelectric ceramic sensors at every stage of preparation are shown.

1. Introduction

For the past several years an intensive research effort have been made in many laboratories around the world to prepare electrically active ceramic materials intended for electromechanical transducers and other applications. Ferroelectric ceramic materials such as $Pb(Ti_xZr_{1-x})O_3$ (PZT) solid solutions have been used extensively as both sensors and actuators due to their excellent transduction capability in elastoelectric conversion $[1-4]$. Such piezoceramics have the strongest piezoelectric charge coefficients, the largest electromechanical coupling coefficients and relative permittivities as well as the lowest dielectric losses. The large permittivities of PZT ceramic materials facilitate electrical tuning and also reduce significantly the piezoelectric voltage coefficients. The PZT ceramic materials have large mechanical quality factors (Q_m) and require the addition of a damping backing in order to reduce ringing to an acceptable level.

The composition of PZT-type with conductive parameters of widespread application belongs, as a rule, to the morphotropic phase boundary (MPB) — a region of concentrations x for which a coexistence of both the rhombohedral (R) and tetragonal (T) ferroelectric phases is observed $[5-7]$. The interval of the composition parameter x at which both these phases appear is relatively wide, it may reach $15\,mol\%$. One of the characteristic properties of MPB is a small deviation from the temperature axis on the phase

diagram which corresponds to the large change of structural states with temperature for fixed concentration x. These peculiarities of MPB and of its vicinity are characterized by the most interesting properties of the corresponding materials: extreme values of the piezoelectric and dielectric parameters (Fig. 1). However, there are many problems in the processing of high quality ceramic materials on the basis of compounds from MPB.
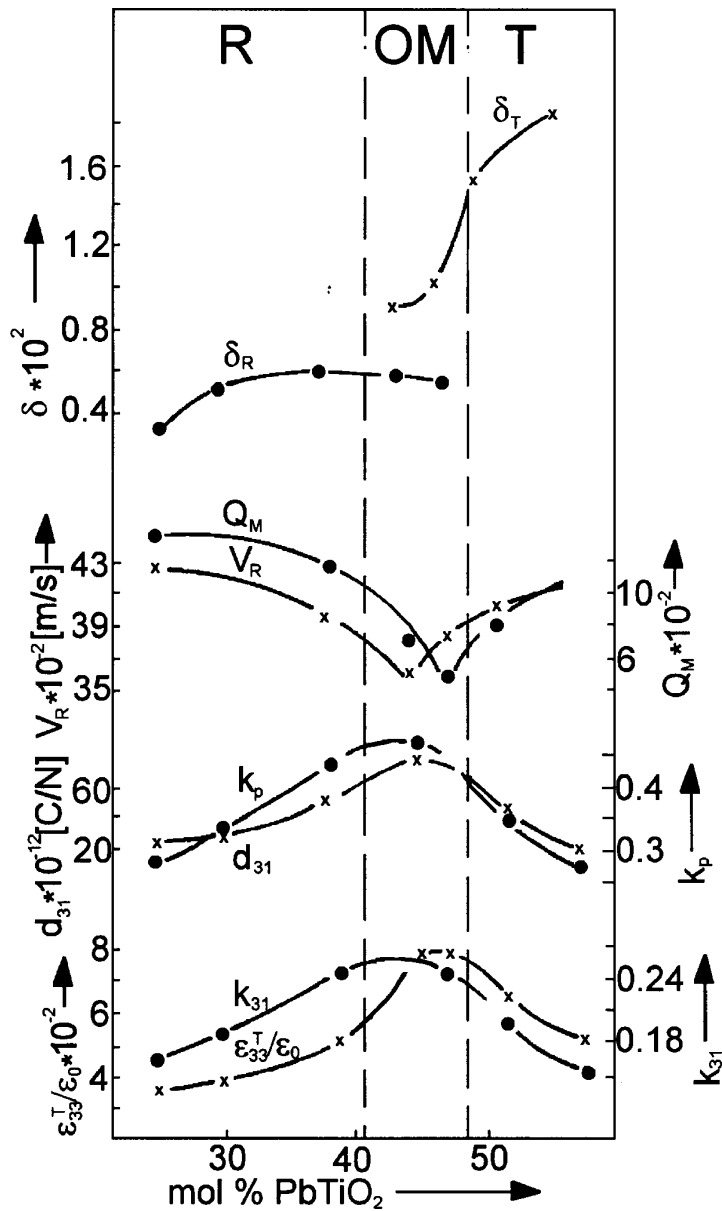
Fig. 1. The dependencies of physical parameters of the PZT-type system in the vicinity of the morphotropic phase boundary on the PbTiO₃ content.

It was shown (e.g [8 – 10]) that the properties of such ferroelectric ceramic materials depend strongly on the conditions of their preparation, i.e. on the synthesis, sintering, mechanical treatments, annealing and polarization processes. This is connected with the high sensitivity of these materials to the changes of the structural states of the MPB with small variations in composition, grain size, domain structure etc.

It is evident that at all stages of the production of the ceramics (synthesis, sintering, mechanical treatments, annealing and polarization) it is necessary to apply effective (fast, reliable, precise, nondestructive) control methods.

The aim of this paper is to analyse the possibilities of characterization of the PZT-type ferroelectric materials at every stage of the ceramic sample preparation by effective control methods. The best methods for this purpose are, in our opinion, X-ray diffraction (XRD), microstructure analysis and Raman spectroscopy.

2. Experimental

On the basis of the PZT-type solid solutions, the materials from MPB were prepared by the solid-phase synthesis methods. Ceramic samples were obtained under different conditions of preparation (varying times and temperatures) both by the usual sintering and by the hot-pressing method. The samples were investigated by the X-ray powder diffraction method at the stage of the preparation of the components for the synthesis, after synthesis, after sintering and after polarization. The investigations of the microstructure of the ceramic samples were performed led by the electron microscope method. The Raman spectra were excited by argon laser light ($\lambda = 0.488\,\mu$m).

3. Results

At the first stage, the dependencies of the piezoelectric and dielectric parameters on the conditions of the sample preparation of the PZT compositions from the MPB region were investigated. The results for one sample are presented in Fig. 2.

From the data given in Fig. 2, it results that the small differences in the conditions of preparation of the ceramic material can lead to significant differences in the physical properties. If the methods of control of the ceramic materials had not been applied during the preparation, the results of measurements of the physical properties of the fabricated ceramic samples would be rather irrational because spoilt ceramic materials hardly meet the requirements for a given application.

Control of the microstructure is done, as a rule, for the characterization of the ferroelectric ceramics at various stages of its sintering [11 – 13].

As an example in Fig. 3 the correlations between some electrophysical parameters, dimensions of the crystallites and total density (for samples obtained by hot-pressing method) are shown. It was expected that the influence of the hot pressing on the microstructure would be larger that in the case of conventional sintering.

It was found that the influence of the time and temperature of the sintering on the dimensions of grains is noticeable (Fig. 3a).
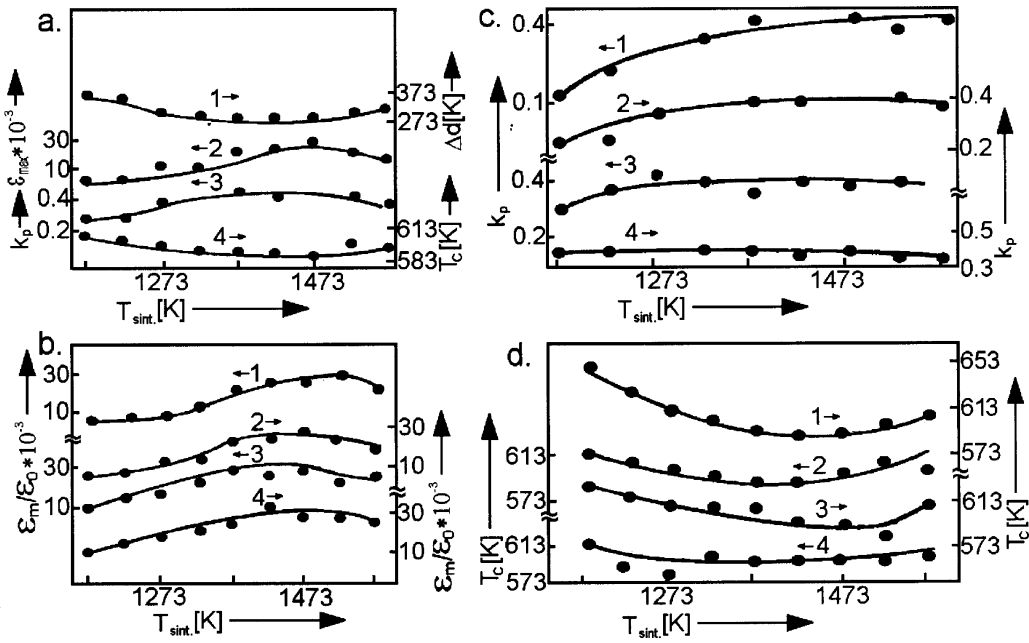
Fig. 2. The dependencies of the dielectric permittivities ($\varepsilon_{\max}$), electromechanical coupling coefficients (k_p), Curie temperature (T_c) and phase transition diffuseness parameters (Δ_d) on the sintering temperature (T_{sint}) (sintering time, $t_{\text{sint}} = 2$ hours); a) the dependencies of $\varepsilon_{\max}$, ε_0, k_p, T_c on the sintering temperature and time (t_{sint}: 1-0.25; 2-2; 3-3; 4-5 hours) (b, c, d).

The decrease in the dielectric permittivities ($\varepsilon/\varepsilon_0$) with increasing grain sizes (Fig. 3b) is due to a decrease in the internal strains of the specimen brought about by an increased domain twinning in the larger grains.

The electromechanical coupling coefficient (k_p) was practically independent of the dimensions of the grains but its value is related to the bulk density (Fig. 3c).

It is possible to explain the decrease of coercive field E_c and the monotonic decrease of the Q_m values by the grain size increase (Fig. 3d). This effects could be explained also as a result of the increased twinning during the grain size increase. The latter causes an increase in the number of the domain walls which lead to higher mechanical losses and thereby to a lower Q_m.

At the same time the analysis of the microstructure may be in general effectively used only at the stage of sintering. Its possibilities are limited to the control of other stages of preparation of the ferroelectric elements (synthesis, polarization etc).

The most suitable method of the production process control is the X-ray powder diffraction methods by that one can determine: i – the crystal phases and their concentrations in specimens; ii – the crystal phase symmetries and the cell parameters; iii – the values of spontaneous deformations; iv – mechanical and electrical (domain) texture parameters; v – microinhomogeneities (microdeformations); vi – values of coherent scattering regions (CSR).
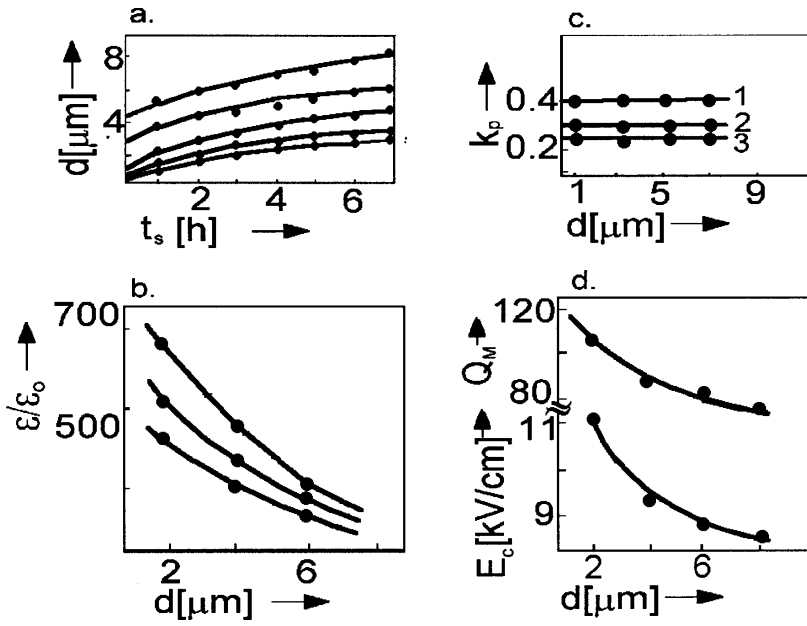
Fig. 3. The dependencies of the grain size on the sintering temperature and time (a), the dependencies of $\varepsilon/\varepsilon_0$, the electromechanical coupling (k_p), coercive fields (E_c), and mechanical quality factors (Q_m) on the grain sizes of the ceramics (b, c, d).

For the determination of the structural parameters of powder (ceramic) specimens the mathematical treatment of the diffraction profiles (Fig. 4a) has been used. Different methods of such a treatment are described in [14, 15]. Figure 4b demonstrates two examples of separation of the three diffraction peaks related to the R — (200^R), T — (200^T, 002^T) phases which coexist in MPB of the PZT-type materials.

A comparison of the diffraction profiles obtained for ceramics sintered at different τ_{sint} and T_{sint} indicates that high degree of homogeneity is possible at lower T_{sint} if the sintering time is increased. Figure 4 shows a decrease of the amount of the R-phase and narrowing of the diffraction peak of the T-phase.

A separation of the overlapped peaks allows both the determination of the cell parameters and the evaluation of the microinhomogeneities $\eta = \Delta d/d$ and the coherent scattering region (CSR) dimensions by the analysis of full width of the half maxima (FWHM) of the diffraction peaks. These parameters are very sensitive to the real state of the ferroelectric materials.

The estimation performed is due to the fact that the microinhomogeneity value in the paraelectric cubic phase does not exceed 10^{-4} and the CSR dimensions, as a rule, are found to be larger than 100 nm (for ceramics produced under the optimal conditions).

Changes of the CSR values are observed at the MPB transitions to the ferroelectric T- and R-phases.

The conditions of sintering of the ceramic materials from MPB have an influence on both the percentage of the ratio of the R to the T phases and of the FWHM as shown
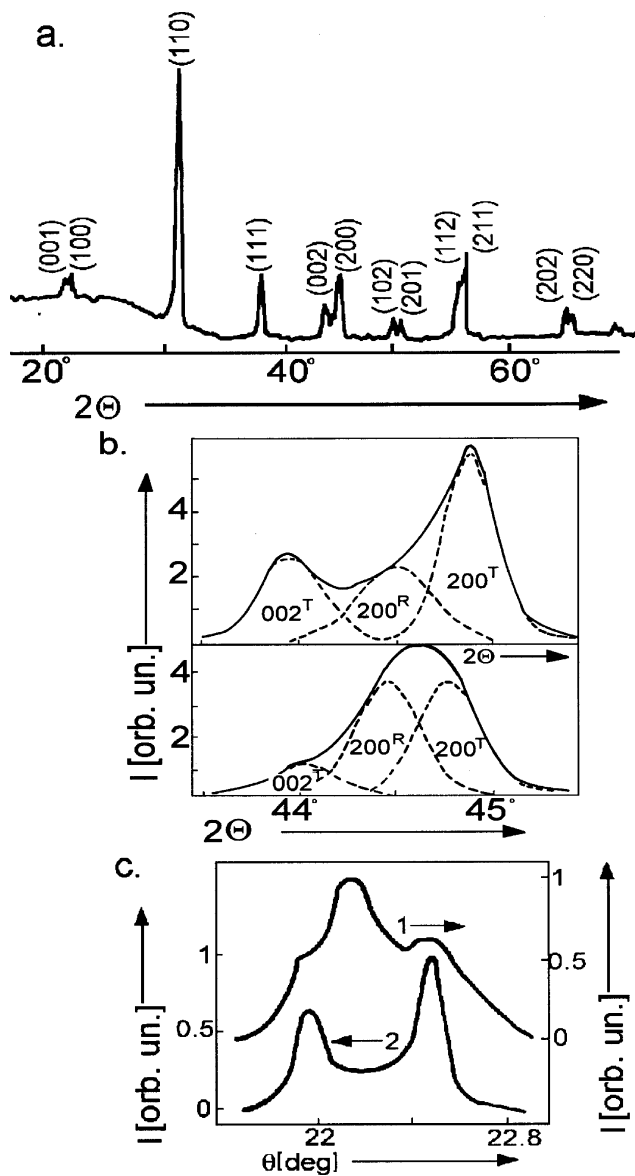
Fig. 4. The X-ray powder diffraction profile (a) and the separation method of overlapped peaks (b): 1 – sample hot pressing, 2 – classic sample technology; the change of the diffraction profile as a result of different sintering times (1 – $t_{sint} = 0.25\,\text{h}$; 2 – $t_{sint} = 5\,\text{h}$; $T_{sint} = 1223\,\text{K}$) (c).

in Fig. 4. With an increase in the sintering temperature up to 1398 K the concentration of the T phase at room temperature increases and the FWHM of the difraction peaks decreases.

The influence of the electric fields of polarization on the structure and the physical properties of the PZT-type ceramics was discussed elsewhere [16–18].

The spectra of the Raman scattering are sensitive to the dynamical state of the crystals [19–20]. In particular, by means of the IR methods, the Raman- and Brillouin-spectroscopy it is possible to investigate the softening of the transverse optical (ferroelectric) mode above the phase transition.

In this paper the preliminary results of the Raman investigations of the PZT-system samples are presented. It is worthy of noting that all samples were obtained under the same conditions of the synthesis and sintering (Fig. 5).
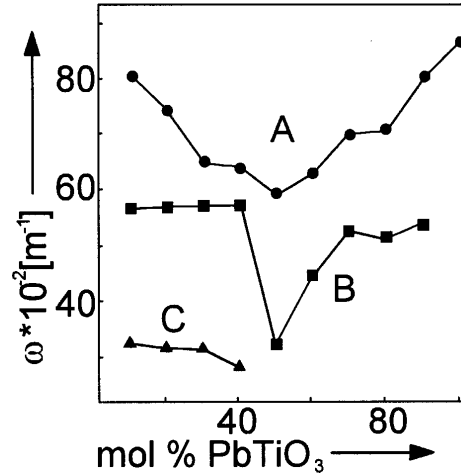
Fig. 5. The dependencies of the mode frequencies of the PZT systems on the $PbTiO_3$ concentration obtained by the Raman spectroscopy (argon laser).

It seems reasonable to assume that the A-mode is the ferroelectric E(TO) one. It becomes softer while approaching to the MPB (concentration phase transition at room temperature). The B mode may be treated as the TA-transverse acoustic one. The C-mode appears in the rhombohedral phase of the solid solutions only and may be related to RLT($R3c$) phase. It may be caused by the M_3- or R_{25}-type phase transitions.

In our opinion the further investigations of the specific vibration spectra of the PZT-type ferroelectric materials obtained under various conditions allow to separate the dependencies of the corresponding parameters on the quality of the crystallites. As a result it should give the possibility to apply the combinational light scattering method to the operative control of the quality of the material at all stages of the production.

4. Conclusion

The results of the studies of the PZT-type ceramics with compositions from MPB presented above demonstrate that the variation of preparation conditions strongly determine the physical properties of the piezoelectric ceramic sensors.

An effective control of the ceramics fabrication at the different stages of the production can be performed by the X-ray powder diffraction methods.

Acknowledgements

References

[1] B. JAFFE, W.R. COOK, H. JAFFE, *Piezoelectric ceramics*, Acad. Press, New York 1971.

[2] K. OKAZAKI, Bull. Am. Ceram. Soc, **63**, 9, 1150 (1984).

[3] C.A. ROGERS, J. Intell. Mater. Syst. Struct, **4**, 4 (1993).

[4] L.E. CROSS, J. Intell. Mater. Syst. Struct., **6**, 55 (1995).

[5] G. SHIRANE, K. SUZUKI and A. TAKEDA, Phys. Soc. Japan, **7**, 12 (1952).

[6] V.A. ISUPOV, Solid St.Commun., **17**, 1331 (1975).

[7] M. KUPRIYANOV, G. KONSTANTINOV and A. PANICH, *Ferroelectric morphotropic transitions*, RGU, Rostov-on-Don 1992.

[8] J. DUDEK and M. KUPRIYANOV, Inżynieria Materiałowa, **6**, 71, 129 (1992).

[9] A. PANICH and M. KUPRIYANOV, *Physics and technology of ferroelectric ceramics*, RGU, Rostov-on-Don 1989.

[10] Z. SUROWIAK, J. DUDEK and M. ŁOPOSZKO, Inżynieria Materiałowa, **6**, 71, 123 (1992).

[11] K. OKAZAKI, *Ceramic engineering for dielectrics*, Tokyo 1969.

[12] Z. SUROWIAK and V.P. DUDKEVICH, *Cienkie warstwy ferroelektryczne*, Uniw. Śl., Katowice 1996.

[13] R.C. BUCHANAN, T.R. ARMSTRONG and R.D. ROSEMAN, Ferroelectrics, **135**, 343 (1992).

[14] V. KOGAN and M. KUPRIYANOV, J. Appl. Cryst., **25**, 16 (1992).

[15] J. DUDEK J., YA. BOGOSOVA, D. CZEKAJ, G. KONSTANTINOV, M. KUPRIYANOV and A. PANICH, Proc. of 15th Conf. Appl. Cryst., Cieszyn, Poland, p. 278 (1992).

[16] J. KWAPULINSKI, Z. SUROWIAK, M. KUPRIYANOV *et al.*, ZTF, **49**, 1049 (1979).

[17] J. DUDEK, M.F. KUPRIYANOV, M. LOPOSZKO and E.G. FESENKO, Acta Physica Polonica, **A63**, 115 (1983).

[18] G. KONSTANTINOV, M. KUPRIYANOV, V. SERVULI *et al.*, ZTF, **59**, 80 (1989).

[19] M.E. LINES and A.M. GLASS, *Principles and application of ferroelectrics and related materials*, Clarendon Press, Oxford 1977.

[20] T. BŁACHOWICZ and Z. KLESZCZEWSKI, Akustyka Mol. i Kwantowa, **16**, 23 (1995).

APPLICATION OF THE FREQUENCY ANALYSIS OF ACOUSTIC EMISSION IN THE STUDY OF THE METAL ALLOY SOLIDIFICATION

M. GOLEC and Z. GOLEC

Poznań University of Technology,
Institute of Applied Mechanics,
Division of Dynamics and Vibroacoustics of Systems
(60-965 Poznań, Piotrowo 3, Poland)
e-mail: Maria.Golec@put.poznan.pl
e-mail: Zdzislaw.Golec@put.poznan.pl

A frequency analysis of the acoustic emission signals was applied for the investigation of the solidification of a Pb-Sb alloy. Spectra of continuous emission and short-time acoustic emission impulses were investigated. It has been stated that, together with structural changes of the Pb-Sb alloy, significant changes occur in the spectra of the acoustic emission impulses generated in different phases of solidification. Less significant changes were observed in continuous acoustic emission spectra.

1. Introduction

The research on the metal alloy solidification concerns the process of passing of alloys from the liquid to the solid state. In a solidifying metal alloy, there occur periods of separation of individual phases at particular temperature-pressure conditions. This depends on the alloy type and on how fast the heat is carried away from the solidifying area. During the research on alloy solidification, it is possible to analyse such basic phenomena as nucleation and phase growth, behaviour of a phase in the presence of other ones, and many additional phenomena which often decide about the properties of an alloy in the solid state. These include among other: things solidifying contraction phenomena, and the mass and capillary flows which compensate them; segregation phenomena; separation of endogenous pollution; sedimentation of endogenous pollution; convection phenomena; solidifying contraction in the solid state. The phenomena mentioned above do not occur simultaneously in the whole alloy, and their intensity depends on the direction and speed of carrying the heat away. Many of them cause a deterioration of mechanical and operational properties of the alloy. In order to reduce these negative effects, researches make use of different research methods; measurable physical quantities have been carried out. Scientists have still searched for new methods of investigation of the alloy solidifi-

cation. However, the knowledge about the phenomena occurring in such processes and their interpretation is still limited to some hypotheses.

To identify the phenomena occurring in a real time in solidifying alloys, researchers have looked for unconventional methods. The acoustic emission (AE) method, which consists of recording and analysing the AE time signals generated in a solidifying alloy, is one of them.

Generally, acoustic emission can be defined as a phenomenon that consists in the generation and propagation of elastic waves, inside or on the surface of a medium, which can be characterised by a broad frequency band within the limits of 1 Hz to 100 MHz, i.e. from infrasounds to ultrasounds.

The previously mentioned phenomena accompanying the solidification can be sources of AE in a solidifying alloy.

2. Research on the alloy solidification by means of the AE method

Acoustic signals emitted during phase transitions in the solid state were observed in the 1930 s. The first researches concerned martensite transformation in steel during hardening [1] and were repeated many times. WLODAWER [2] investigated solidification of cast steel observing acoustic effects generated during casting mould filling, convection of the liquid alloy and its crystallisation, and during a reaction inside the material of a mould. For the last few years now, of the fast development of new methods of signal acquisition and processing, the number of studies in that AE signals are used for the identification of phenomena accompanying the alloy solidification has been growing. The authors of the papers [3 – 7] investigated the solidification of metals applying the sum of AE impulses as a measure of its intensity. In the papers [5] and [6], the mean value of root mean square values (RMS) of the AE signals were used additionally and in the paper [6] the maximum amplitude was applied as well. Since 1990, the analysis of AE signals in the frequency domain has been used more and more often for the investigation of the metal alloy solidification. It has been stated, in the research report [10], basing on the analysis of the time function of the AE signals, that it is possible to identify phase transitions in solidifying alloys. As a continuation of the research started and described in [10], the authors tried to assess structural changes in solidifying alloys basing on the frequency analysis of AE signals [11].

3. Scope of the research on Pb-Sb alloy solidification

It was tried to identify the phase transitions in the alloy during its passing from the liquid to the solid state. To this end the AE method, based on the amplitude-frequency analysis of AE signals received from two different micro-regions of the alloy and on a simultaneous analysis of the self-cooling curves (thermal analysis), was used (Figs. 1 and 2).

The Pb-Sb alloy was obtained by smelting products containing 8% Sb. The liquid metal was smelted in ceramic-graphite melting pots in an electric chamber furnace. Thick-
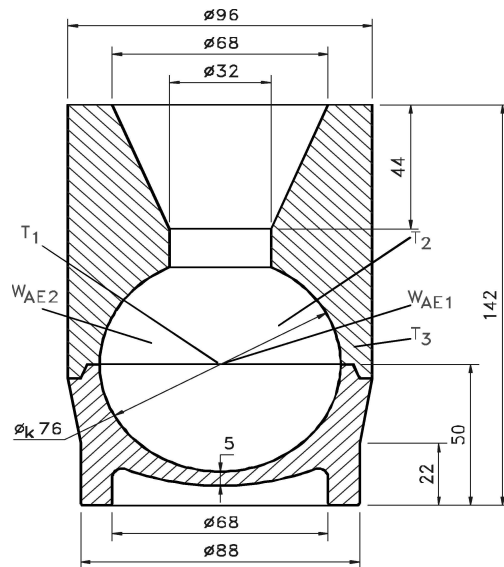
Fig. 1. Ball shaped grey iron mould with the feeding system end temperature and one AE measuring points: T_1, W_{AE1} — thermocouple and AE wave-guide in the sphere centre, T_2, W_{AE2} — thermocouple and AE wave-guide 15 or 20 mm away from the alloy surface, T_3 — thermocouple 5 mm away from the internal surface of the mould.
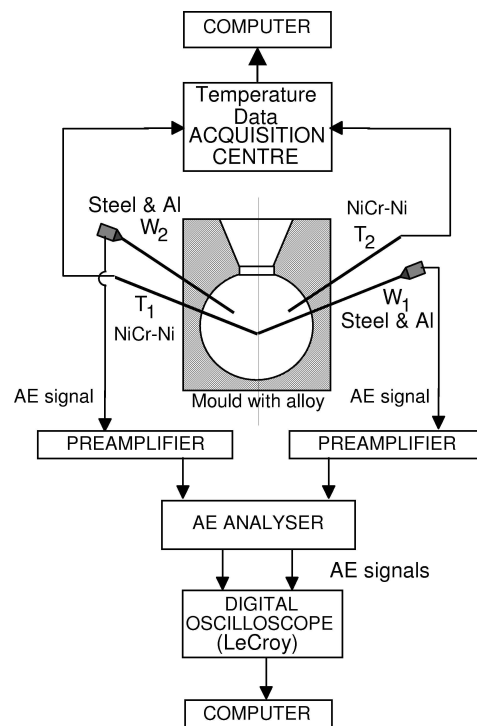
Fig. 2. Measuring system for two-channel acquisition of temperature and AE from the solidifying alloy.

walled grey cast iron moulds with a metal supply system were used (Fig. 1). During the pouring of the moulds the following parameters were used:

— pouring temperature: $T_z = 438 - 464°C$,

— initial mould temperature: $T_p = 197 - 215°C$,

— pouring time: $t_z \approx 5\,s$.

The internal surfaces of the moulds were not coated by any protective coating.

The wave-guides for the AE signals consisted of steel bars length $l = 193\,mm$ and diameter $\o = 1.5\,mm$ coated with glass fibre jackets of length $l = 120 - 140\,mm$. There were aluminium cones with AE transducers mounted on the tips of the wave-guides.

To create files containing temperature, the authors' own computer programs were used. The analysis of AE signals was performed using MATLAB software.

4. Results of the experiments

Basing on the self-cooling curves of the Pb-Sb alloy, the time of the occurrence of individual phases of the solidification process in the thermal centre of the casting (the sphere centre) was determined. The alloy solidification phases were difficult to identify at a distance of about dozens of millimetres away from the surface of the mould.

For the individual phase transitions in the solidifying alloy (the sphere centre), the following points were determined:

— Beginning of the separation of the hypo-eutectic phase at the crossing of the liquidus line: $-25\,s$ after the mould was poured.

— The end of the temperature hold in the range of the liquidus temperature: $-65\,s$ after the mould was poured.

— Beginning of the eutectic transformation: $-220\,s$ after the mould was poured.

— The end of the eutectic transformation: $-435\,s$ after the mould was poured.

There were two kinds of AE signals observed during the solidification of Pb-Sb alloy: a continuous emission with an almost constant root mean square value overlapped by single impulses with various amplitudes. Therefore, the amplitude spectra for both the continuous AE and AE impulses have been recorded.

Figure 3 shows the time functions for the continuous AE and the respective amplitude spectra in the frequency band $(0-1)\,MHz$ made for different times of solidification t_0.

In the spectra shown three frequency bands were marked off:

— $(120 - 180)$ kHz,

— $(500 - 650)$ kHz,

— $(720 - 750)$ kHz.

Changes in the components for different solidification phases were observed in these bands.

In order to present the components in the above frequency bands more clearly, the spectra have been performed in different scales (Fig. 4) This allowed to observe the shift of the characteristic components in the first and second frequency bands. At this stage it was impossible to identify unambiguously the components. Their appearance and frequencies

to = 21 s

to = 76 s

to = 244 s
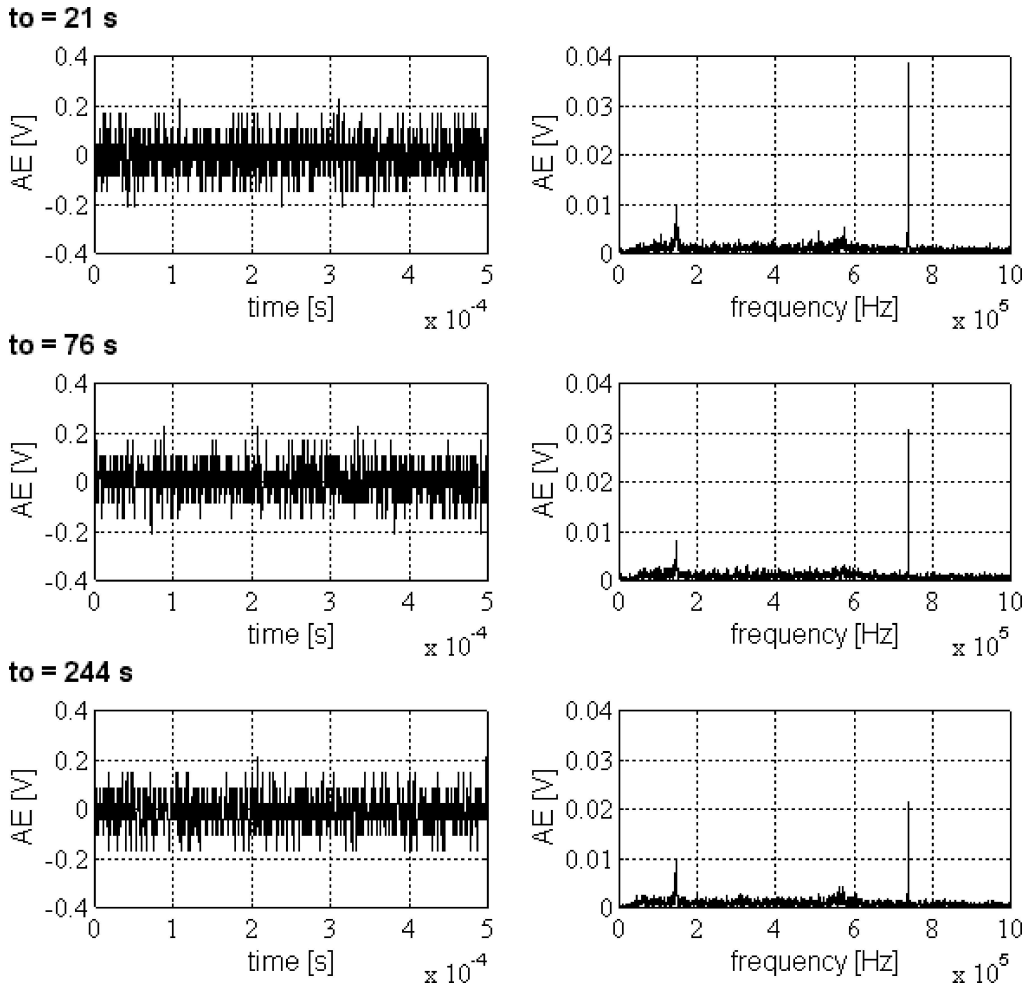
Fig. 3. Continuous AE time functions and their respective amplitude spectra.

can be connected not only with the alloy properties in the respective solidification phase, but also with the alloy defects or with other phenomena occurring during the solidification processes. In the third frequency band there was no shift of the component of a frequency of 738 kHz (Fig. 4) during the solidification. Therefore, it can be inferred that this component is connected with the properties of the measuring system (this component appears also in the AE impulse spectra — Fig. 5).

The AE impulse spectra (Fig. 5) for different alloy solidification phases differ much more and contain much more components. The spectrum with clear components in the frequency band up to 200 kHz (21 s after the mould was poured) corresponds to the beginning of the pre-eutectic phase separation.
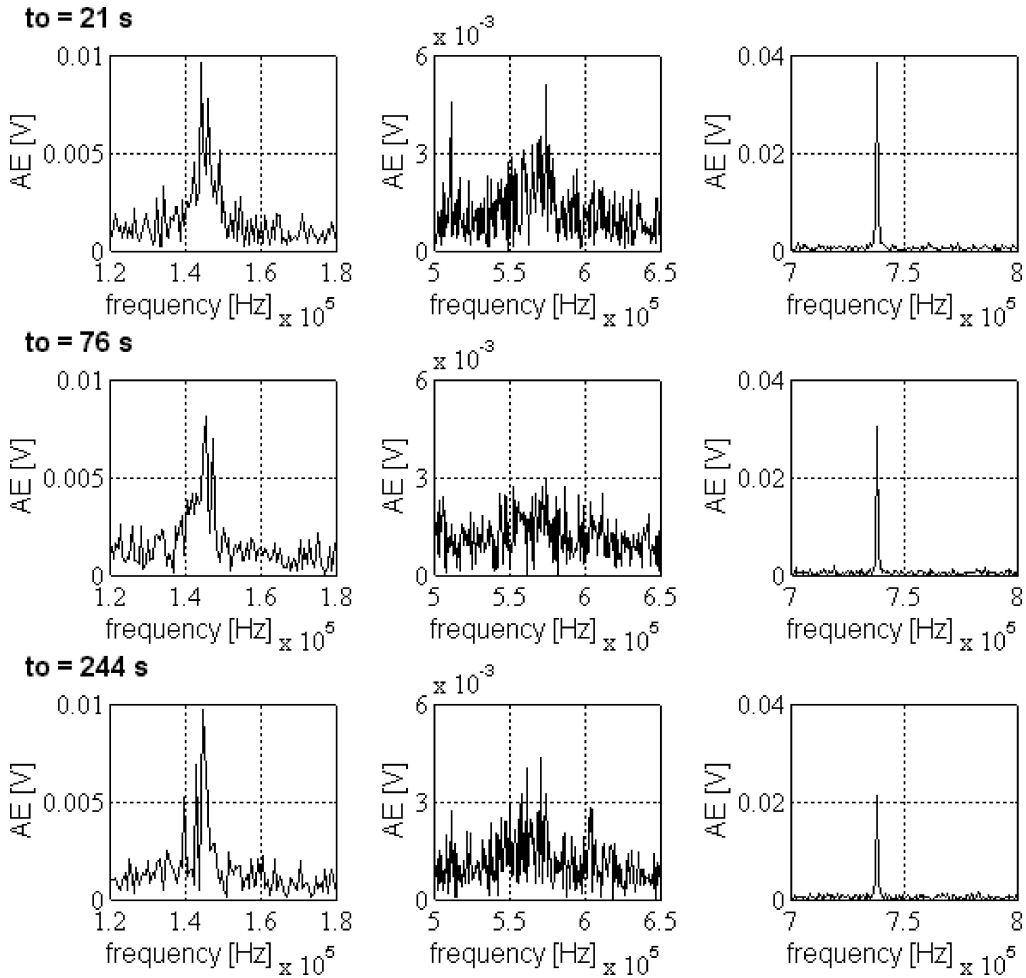
Fig. 4. Continuous AE spectra for the different solidification phases.

The AE impulse spectrum in the subsequent solidification phase (after the temperature hold at the liquidus temperature range and before the eutectic transformation) contain many components in the frequency band up to 600 kHz.

During the eutectic transformation, the number of components in the AE impulse spectrum decreases. There is only one clear-cut component in the frequency band up to 200 kHz and several others in the frequency band (400 − 600) kHz.

to = 21.00497 s
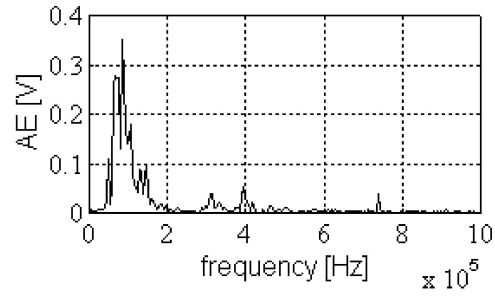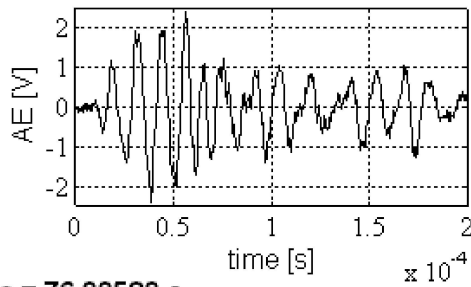
to = 76.00580 s
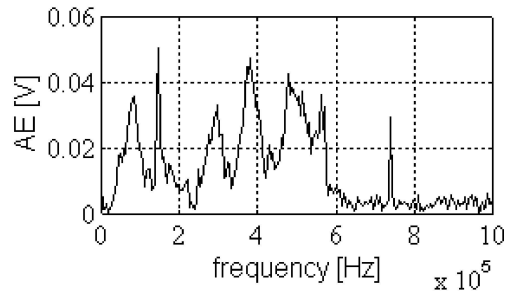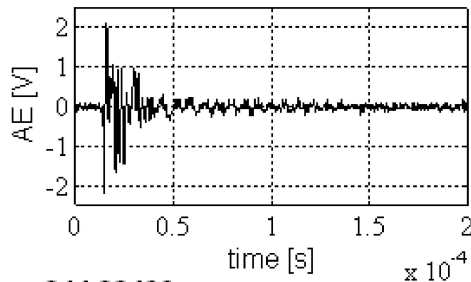
to = 244.00499 s
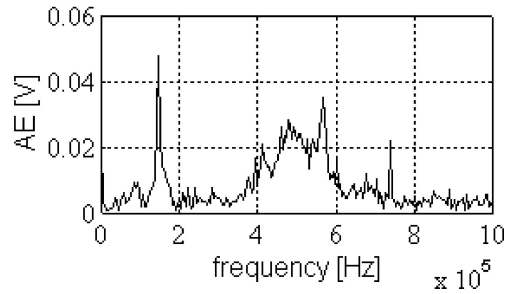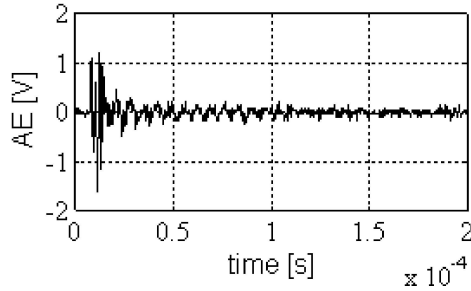
Fig. 5. Time functions of AE impulses and their respective amplitude spectra.

5. Conclusion

The thermal analysis and its respective frequency analysis of the AE signals show that structural changes of Pb-Sb alloys are accompanied by significant changes in the AE impulse spectra generated in different solidification phases. There are less clear changes observed in the continuous AE spectrum.

The results shown allow the authors to say that changes in AE signals have been found which enable the observation of structural changes in the solidifying alloy. However, a comprehensive identification of the solidification phases based on the AE spectrum changes needs further research taking into account other alloys.

References

[1] F. Forster and E. Scheil, *Acoustic of the Study Formation of Martensite Needles*, Zeitschrift für Metallkunde, **9**, 245–247, 1936.

[2] R. Wlodawer, *Gelenkte Erstarrung von Gußeisen*, Giesserei-Verlag, GmbH, pp. 436–438, Düsseldorf 1977.

[3] U. Feuer and R. Wunderlin, *Observation of Porosity Formation During Solidification of Aluminium Alloys by Acoustic Emission Measurements*, Proceedings of International Conference Solidification and Casting of Metals, pp. 340–344, Sheffield 1977.

[4] T.S. Prosanna Kumar and O. Prabhakar, *Acoustic Emission during Solidification of Aluminium Alloys*, AFS Transactions, **93**, 13–22 (1985).

[5] A.L. Purvis, E. Kannatey Asibu and R.D. Pehlke, *Evaluation of Acoustic Emission from Sand Cast Aluminium Alloy 319 During Solidification and Formation of Casting Defects*, AFS Transactions, **98**, 1–7 (1990).

[6] A.L. Purvis et al., *Acoustic Emission Signal Characteristics from Casting Defects Formed During Solidification of Al. Akkoy 319*, AFS Transaction, **99** (1991)

[7] B. Xiufang et al., *Acoustic Emission during Solidification of Al.-Si Alloy*, Proceedings of Second International Conference on Aluminium Alloys, Beijing 1990.

[8] A.L. Purvis, E. Kannatey Asibu, Jr. and R.D. Pehlke, *Linear Discriminant Function Analysis of AE Signals Generated During Solidification*, AFS Transactions, **1**, 1–8 (1995).

[9] A. Vinogradov, M. Nadtochly, S. Hashimoto and S. Miura, *Comparative Analysis of the Acoustic Emission Spectra in Copper and Copper-aluminium Single Crystals*, La Revue de Métallurgie-CIT/Science et Génie des Matériaux, pp. 215–223, Févier 1996.

[10] Multi-author work, Acoustic Emission (AE) in identification and investigation of the metal alloy solidification and crystallization. Final statement PB 1244/S2/93/04[in Polish], Poznań University of Technology, Institute of Applied Mechanics, Division of Dynamics and Vibroacoustics of Systems, Poznań 1994.

[11] M. Golec and Z. Golec, *Frequency analysis of the acoustic emission applied to investigation of the metal alloys solidification* [in Polish], [in:] New trends in technology and material investigations, Polish Academy of Sciences Institute of Fundamental Technological Research, J. Ranachowski [Eds.], pp. 65–72.

APPLICATION OF ACOUSTIC EMISSION FOR DETERMINATION OF INITIAL TEMPERATURE OF CASTING MOULD

M. GOLEC, Z. GOLEC

Poznań University of Technology,
Institute of Applied Mechanics
(60-965 Poznań, Piotrowo 3, Poland)
e-mail: office_iam@put.poznan.pl

M. HAJKOWSKI

Poznań University of Technology,
Institute of Material Technology
Division of Dynamics and Vibroacoustics of Systems
(60-965 Poznań, Piotrowo 3, Poland)
e-mail: office_imt@put.poznan.pl

It was shown in this paper that, thermal stresses and accompanying them plastic strains, generated during solidification and cooling of casts of metal alloys, were the sources of acoustic emission. For casts, which phase α is deformed by slip, there is a possibility of determination of initial temperature of casting mould by means of acoustic emission.

1. Introduction

While cooling there arise thermal stresses in the metal alloy castings, which are caused by different temperatures of casting parts. The temperature difference depends on thickness of a casting walls and initial temperature of a mould. Thermal stresses should not cause plastic strain of material, which may lead to micro- and macro-cracks of the casting. In [1] the authors dealt with a problem of influence of plastic strain type of a solidified casting layer on acoustic emission (AE). For the research on casting solidification and cooling two alloys with different plastic strain type of a solidified layer were chosen: aluminium alloy AK9 and zinc alloy Z41.

The α phase (metallic matrix) in aluminium alloys undergoes a deformation by slip, and the η phase in zinc alloys undergoes a deformation by twinning.

2. Description of the experiment

Components of a synthetic AlSi8,6 (AK9) alloy were melted in a graphite melting pot under deoxidising and covering slay (degasal T200) in a chamber furnace. Metal oxides in the liquid alloy were refined by means of degasal T200, which in a quantity of 0.1% of charge was immersed and mixed with the metal. For gas refining "Probatem fluss Al 224" in a quantity of 0.1% of the charge was used and placed in a graphite bell. The process was carried out at the temperature of $740°C - 745°C$. The mould was poured with the alloy of which the temperature was $755°C - 760°C$.

The zinc alloy Z41 was melted in a graphite melting pot under the cover of charcoal. The mould was poured with the alloy at $490°C$. Castings were made in a truncated cone mould with a volume of $79\,cm^3$ (castings solidifying with a free contraction) and a cone-with-rings mould with a volume of $97\,cm^3$ (castings solidifying with an inhibited contraction). Application of different materials for different parts of the mould allowed the authors to obtain directional solidification of the castings. The base of the mould was made of aluminium alloy AK11, the middle part — of carbon steel, and the upper part — of cast iron Zl200. In the upper part of the mould, for feeding of a casting, there was a feedhead which dimensions allowed to have metal in the liquid state for long enough.

The researches were carried out in different technological conditions. The castings made of AK9 alloy solidifying with a free contraction were tested changing in the consecutive experiments the initial temperature of the mould: $22°C$, $155°C$ and $270°C$. The initial temperature of the mould for castings solidifying with an inhibited contraction was $20°C$. The Z41 alloy castings were tested in the mould with the initial temperature of $22°C$ for both solidification with a free contraction and solidification with an inhibited contraction. The temperature measured in two points of the casting axis and the mould temperature were recorded during solidification. The elastic wave of acoustic emission (AE) was received by means of two steel wave-guides, the tops of which were placed in the casting axis with a distance of about $3\,mm$ from the tips of thermocouples. The wave-guides 1 and 2 were placed $17.5\,mm$ and $52.5\,mm$ from the base of the casting respectively. The AE signal was recorded as an envelope by means of Teac Data Recorder in the frequency band to $20\,kHz$. This recorder was connected to a PC equipped with an input card Data Recorder Interface Board model Quik Vu II, the software of which enabled automatic acquisition of the AE envelope.

3. Results of the experiments

During solidification of AK9 castings a slow increase in RMS value of continuous AE envelope was observed. A sudden decrease in RMS value of AE was observed during their cooling (see Fig. 1 a, b, d). The biggest decrease occurred in the castings, which solidified with an inhibited contraction, and it was not observed in the case of solidification in the mould with the initial temperature of $270°C$ (see Fig. 1 c). In this case the RMS value of continuous AE was slowly decreasing.
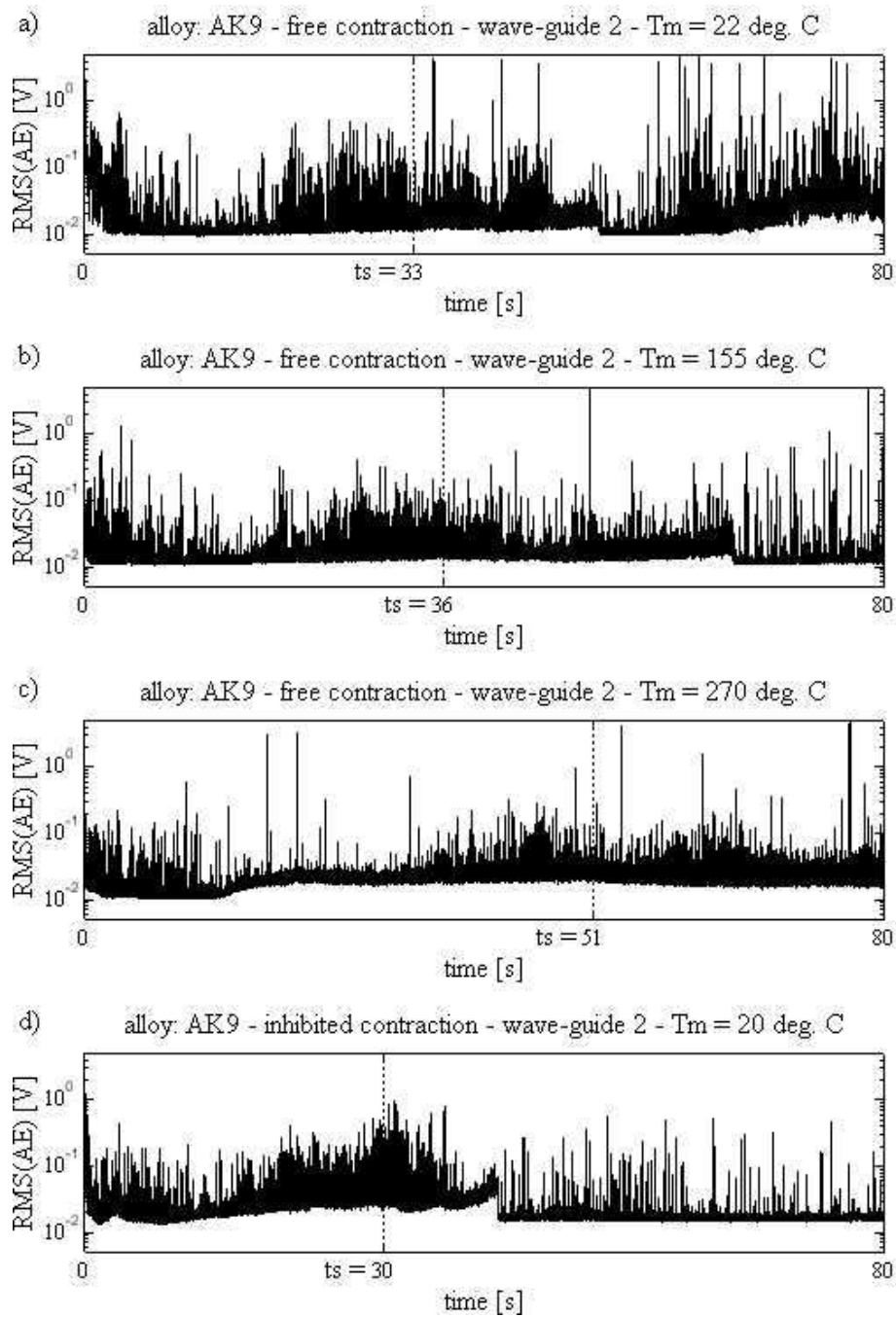
Fig. 1. AE signal envelope generated during solidification of AK9 alloys: a) casting solidifying with a free contraction, $T_{\text{in.mould}} = 22°C$, b) casting solidifying with a free contraction, $T_{\text{in.mould}} = 155°C$, c) casting solidifying with a free contraction, $T_{\text{in.mould}} = 270°C$, d) casting solidifying with an inhibited contraction, $T_{\text{in. mould}} = 20°C$. ts — the end of the solidification.

For the Z41 castings solidifying both with a free and with an inhibited contraction any sudden changes of the AE envelope were not observed. The influence of the contraction inhibition in the solidified layer (the resistance of the mould) can be seen as continuous AE. The inhibited contraction of the solidified layer is observed in the form of subsequent AE impulses.

There is a continuous strain of the material. In the castings solidifying without contraction inhibition this phenomenon is less intensive (see Fig. 2).
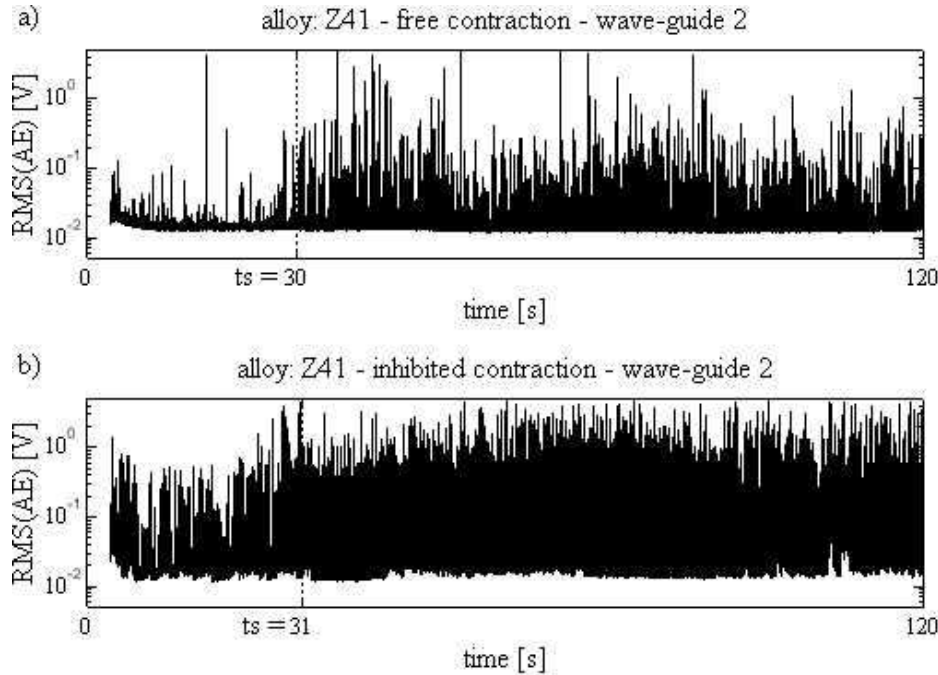
Fig. 2. Envelopes of the AE signal generated during solidification of Z41 alloy castings: a) casting solidifying with a free contraction, b) casting solidifying with an inhibited contraction. ts — the end of the solidification.

4. Conclusions

The results of research on solidification and cooling of AK9 castings show that the initial temperature of the mould, which ensures minimisation of thermal stresses in the casting, can be determined basing on the analysis of AE signals. In the experiment, in order to minimise plastic strain of the material and to avoid micro- and macro-cracks the initial temperature of the mould should be between $155°C$ and $270°C$.

The explanation of the problem of influence of plastic strain in solidifying castings on acoustic emission and the development of a method of selection of the initial temperature of the mould basing on the analysis of AE signals, need further research and taking more alloys and more initial temperatures of moulds into account.

References

[1] *Emisja akustyczna jako narzędzie badania procesów krzepnięcia i krystalizacji stopów metali*, Sprawozdanie końcowe z realizacji projektu Nr 7 T07B 005 09. Politechnika Poznańska, Poznań 1999.

[2] M. GOLEC, Z. GOLEC and M. HAJKOWSKI, *Zastosowanie emisji akustycznej do określenia początkowej temperatury formy odlewniczej*, XLVI Otwarte Seminarium z Akustyki OSA'99, Kraków – Zakopane 14-17.09.1999, 225–228.

DETERMINATION OF INITIATING AND CRITICAL STRESS LEVELS IN COMPRESSED PLAIN AND HIGH-STRENGTH CONCRETE BY ACOUSTIC METHODS

J. HOŁA

Institute of Building Engineering
Wrocław University of Technology
(50-370 Wrocław, Wybrzeże Wyspiańskiego 27, Poland)

New criteria suitable for determining the levels of initiating stress σ_i and critical stress σ_{cr} in plain and high-strength concrete under compression by acoustic materials testing methods have been established. Also the criteria known from the literature on the subject have been verified. On the basis of the author's own research results obtained by the ultrasonic method and the acoustic emission (AE) method the limits of the applicability of the two above methods have been determined. The new criteria, classified according to their suitability for plain concrete or high-strength concrete, have been defined using such descriptors as: the velocity of longitudinal ultrasonic waves, AE counts, the rate of AE counts, the energy of short AE impulses and the RMS value of AE.

1. Introduction

Initiating stress σ_i and critical stress σ_{cr} should be treated as certain stress levels in concrete subjected to loading which delimit qualitatively different stages in the damage to its structure. Three such stages can be distinguished in the course of the failure of concrete under compression. According to [1] they are: the stable initiation of microcracks, the stable development and propagation of the microcracks and the unstable propagation of the microcracks. The validation of the above can be found in many papers, especially monographs [2–9]. It should be noted here that the multistage character of the failure of concrete subjected to compression has not been confirmed by researchers who favour the Palmgren–Miner theory of damage accumulation as expounded, for example, in [10].

Initiating stress σ_i and critical stress σ_{cr} levels are not the same in all the concretes subjected to compression. Several technological and service conditions have a bearing on the above stress levels [7–9, 11–18]. The considered stress levels are regarded to be two fatigue characteristics which give us a clue as to the susceptibility of compressed concrete to signalled or not signalled cracking. Furthermore, research has indicated that the level of stress σ_i in compressed concrete can be regarded as equal to the safe fatigue life [19] and that of stress σ_{cr} — as equal to the long-lasting fatigue strength [20, 21].

In order to determine levels σ_i and σ_{cr} it is necessary to trace the failure of concrete in the whole range of loading. For this purpose indirect methods have been used with

much success. These include: the strain measurement method, the ultrasonic method and the acoustic emission (AE) method. As regards the strain measurement method, the criteria for determining the considered stress levels in compressed plain concrete have been defined and they can be found in the literature on the subject [7, 11, 12, 22, 23]. But they have been shown to be unsuitable for determining levels of critical stress σ_{cr} in compressed high-strength concrete [18, 24]. Practically no descriptions of such criteria for determining levels of stress σ_i and stress σ_{cr} on the basis of results obtained by acoustic methods can be found. This is probably due to the continuous improvements made in measuring equipment which open up new research possibilities. Another factor here is the introduction of all kinds of additives and admixtures into concrete which affect the strength characteristics (broadly understood) of this material.

Since the ultrasonic method and the AE method have been used more and more frequently to investigate the failure of compressed concrete, both plain and high-strength one, the author of the present paper deemed it proper to assess the usefulness of these methods and the suitability of their criteria for the determination of levels of stress σ_i and stress σ_{cr}. The assessment is based on the author's own experimental results.

2. Ultrasonic method

The descriptors used in the ultrasonic method to describe the failure of compressed concrete and to determine the levels of stress σ_i and stress σ_{cr} are the time of passage or the velocity of propagation of a longitudinal ultrasonic wave perpendicularly to the direction in which the load acts. Experimental research has shown that the values of these descriptors are causally linked to the course of failure.

In papers [12, 25], among others, it is suggested that the level of stress σ_i in concrete should be the level at which a longitudinal ultrasonic wave propagated perpendicularly to the direction of compressive load passes through the concrete in the shortest time. The level of stress σ_{cr} is assumed to be the stress level at which this wave's time of passage reaches again initial value t_0. This is illustrated in Fig. 1.

The above criteria have been found to be inapplicable to plain concrete with average or increased compression strength or to high-strength concrete [14–16, 18]. It cannot be ruled out that they are applicable to plain concrete with very low compression strength.

It has also been found that it is not possible to establish a definite criterion for determining levels of stress σ_i in concretes belonging, by reason of their compression strength and deformability, to plain concretes. Such a criterion can, however, be established for stress σ_{cr}: it is the vanishment of the possibility of measuring the velocity of a longitudinal wave propagated perpendicularly to the direction in which the load acts, as illustrated by curve 1 in Fig. 2. The criteria established for high-strength concretes are represented by curve 2 in Fig. 2 [18].

The stress level above which a marked decrease in the longitudinal ultrasonic wave's velocity occurs (it becomes apparent that there is no linear relationship between the velocity and the compressive stress) in concretes of this kind is the level of stress σ_i. The stress level at which the possibility of measuring the wave's velocity vanishes is that of stress σ_{cr}.
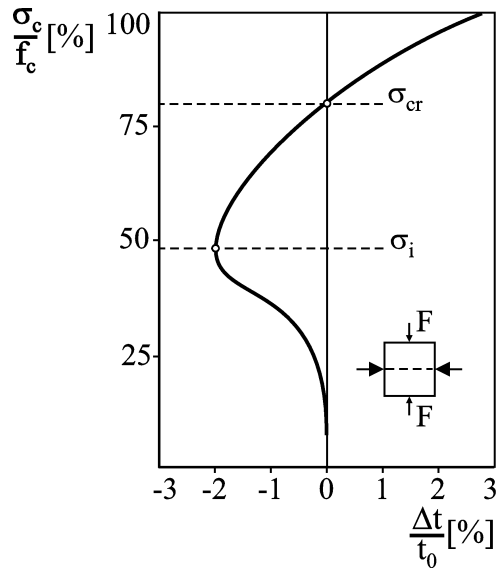
Fig. 1. Criteria for determining levels of stresses σ_i and σ_{cr} in compressed concrete by ultrasonic method [12, 25].
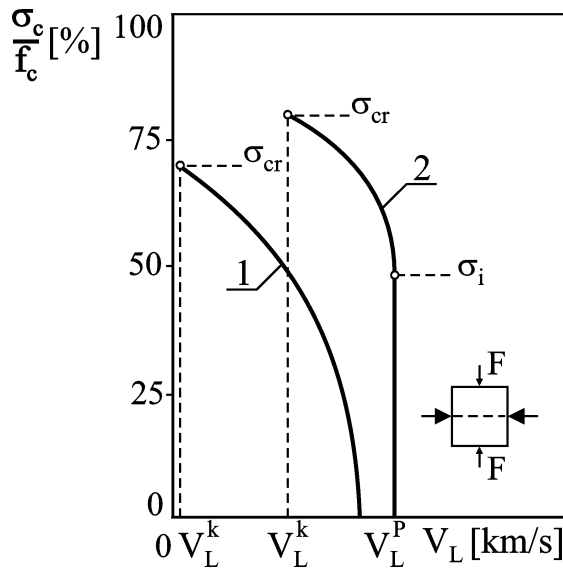
Fig. 2. Criteria established by the author for determining levels of stresses σ_i and σ_{cr} in compressed plain concrete (1) [14, 16] and high-strength concrete (2) [18].

3. Acoustic emission method

The descriptor which has been used with success to determine the levels of initiating stress σ_i and critical stress σ_{cr} in compressed plain concrete is AE counts [14–17, 26–28].

As it follows from source work [26], AE counts in concrete subjected to compression should be measured as a function of, for example, stress increment. Then the rate of AE counts, also as a function of stress increment, is determined. This can be written as [27]:

$$\mathrm{IN} = \sum N_{n+1} - \sum N_n \,, \tag{1}$$

where IN — a rate of AE counts, $\sum N_{n+1}$ — AE counts recorded for stress levels $n+1$, $\sum N_n$ — AE counts recorded for stress levels n.

Stress intervals in which the rate of AE counts is determined can be as large as, for example, $0.05\sigma_c/f_c$. A sample course of the rate of AE counts determined in this way is shown in Fig. 3. Three stages can be distinguished in it: a stage of steady increment of AE counts, a stage of stable increment of AE counts and a stage of rapid increment of AE counts.
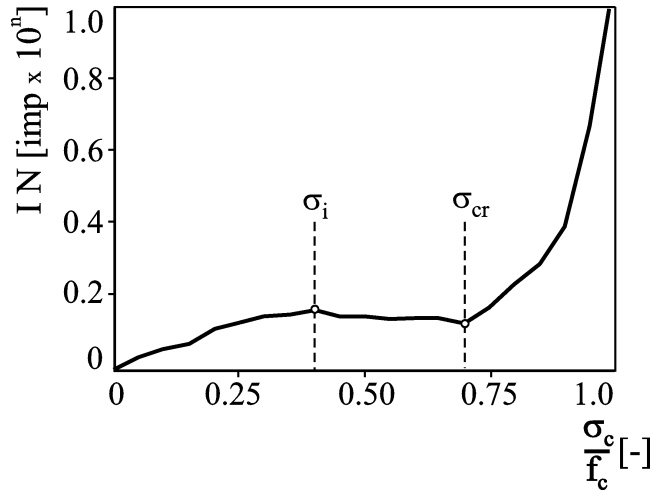
Fig. 3. Determination of levels of stresses σ_i and σ_{cr} in compressed plain concrete on basis of measured AE counts [14–17, 26, 27].

Knowing the rates of AE counts as a function of compressive stress, levels of stresses σ_i and σ_{cr} can be read directly from the plotted graph. To increase the accuracy of reading the above stress levels, the stress intervals in which the rate of AE counts is determined can be narrowed locally to, for example, $0.025\sigma_c/f_c$. As Fig. 3 shows, the stress level at which the stage of steady increment of AE counts and that of stable increment of AE counts are clearly delimited corresponds to the level of stress σ_i. At the level of stress σ_{cr} the stage of stable increment of AE counts and that of rapid increment of AE counts can be clearly distinguished. This way of determining the considered stress levels can be called graphic.

Knowing the rate of AE counts as a function of compressive stress increment, the levels of stresses σ_i and σ_{cr} in concrete can be determined also by statistical methods. Then it should be assumed that a specified rate of AE counts is a function of acoustic impulses in a certain time interval corresponding to a certain increment in compressive

stress. The points of inflexion of this function occur at the places at which the stages of steady, stable, and stable and rapid increment in the number of the impulses become delimited. By determining these points we determine the levels of stresses σ_i and σ_{cr}. This represents a criterion for determining the above stresses. Then it is enough to assume the following model:

$$Y = f(x) + \varepsilon, \tag{2}$$

where $Y = (Y_1, ..., Y_n)^t$ — (a dependent variable) observed changes in the rate of AE counts (IN); $x = (x_1, ..., x_n)^t$ — (an independent variable) relative stress in compressed concrete (σ_c/f_c); $\varepsilon = (\varepsilon_1, ..., \varepsilon_n)$ — such a random vector having dimension n (measuring errors) that ε_1 has distribution $N(O, \sigma^2)\sigma <\propto$ for $i = 1, ..., n$; n — a number of observations.

Since the aim of the statistical analysis is to determine the points of inflexion of the function, it is not possible to apply the least squares method to the whole observation area. Thus this domain of function $f(x)$ should be divided into three intervals in which, we surmise, the function has three different forms. The author has determined experimentally that the regression curves can be estimated by the least squares method, assuming model form $Y = ax + b$ for intervals I and II and model form $Y = \exp(ax + b)$ or $Y = ax + b$ for interval III. Eventually, a model better fitted to the data (for which coefficient R^2 will have a higher value) should be assumed for interval III. Ultimately, the value of stress σ_i is obtained as the intersection of the estimated curves in intervals I and II and the value of stress σ_{cr} — as the intersection of the estimated curves in intervals II and III, as illustrated in Fig. 4.
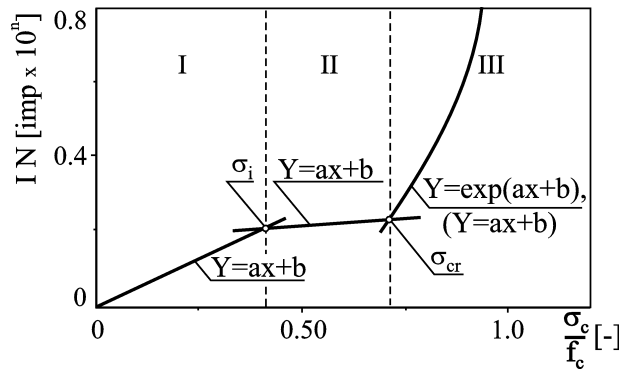
Fig. 4. Determination of points of inflexion of AE counts rate function by statistical methods for compressed plain concrete.

It follows from [18] that the rate of AE counts is less useful for the determination of the considered stresses in high-strength concrete since the number of AE counts recorded during the initial stage and the intermediate stage of loading in this case is small. And small increments in AE counts per unit of length make it difficult to determine the level of initiating stress σ_i. But, as Fig. 5 shows, it is possible to determine the level of critical stress σ_{cr} corresponding to the level of compressive stress at which AE counts begin to increase rapidly.
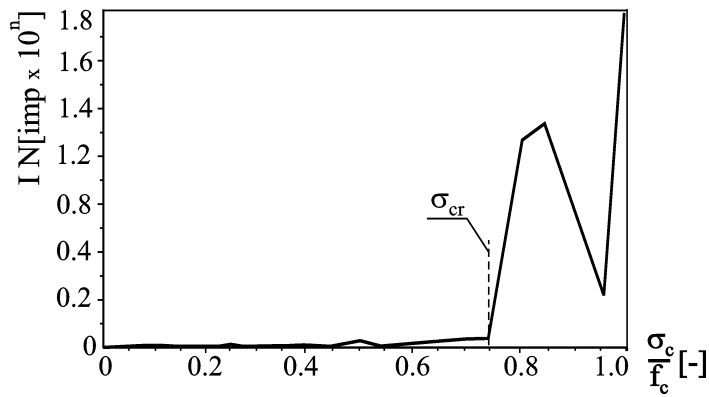
Fig. 5. Determination of critical stress σ_{cr} in compressed high-strength concrete based on measurements of AE counts [18].

The AE method allows one to determine levels of stresses σ_i and σ_{cr} in compressed concrete on the basis of other than AE counts descriptors. One can use the rate of AE counts, the energy of short AE impulses or the RMS value of the AE signal for this purpose [18]. Below it is described how to do it for high-strength concrete.

As regards the rate of AE counts and the energy of short AE counts, they should be measured as a function of failure time. Also a graph of absolute or relative compressive stress versus failure time should drawn. The AE signal's RMS value should be measured as a function of, for example, relative compressive stress. Figures 6, 7 and 8 show typical traces, with distinguishable three stages, of the above AE descriptors in high-strength concrete subjected to compression. Figures 6 and 7 include an exemplary graph of compressive stress, denoted by σ_c/f_c, versus failure time.
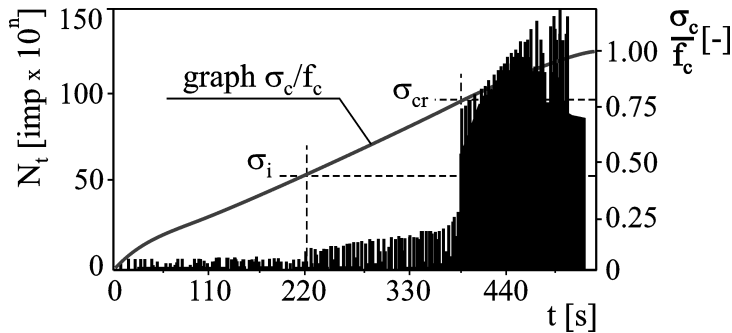
Fig. 6. Determination of levels of stress σ_i and σ_{cr} in compressed high-strength concrete based on measurements of AE counts rate [18].

As one can see in Figs. 6, 7 and 8, the values of all the above AE descriptors are low initially. Then a the rate of AE counts and the energy of short AE impulses increase moderately and the AE signal's RMS value increases quite sharply. In the final stage the increases are rapid and in the case of the AE signal's RMS value, the increase is very
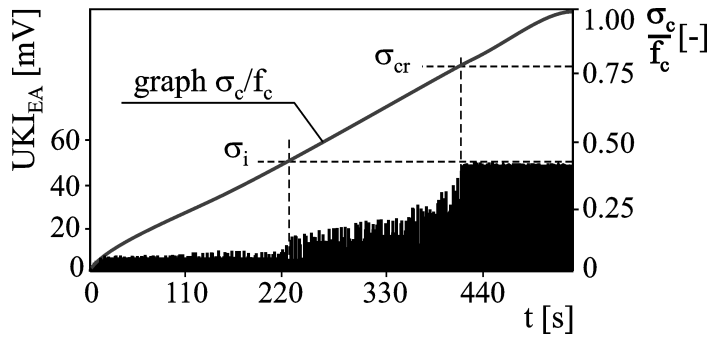
Fig. 7. Determination of levels of stress σ_i and σ_{cr} in compressed high-strength concrete based on measurements of energy of short AE impulses [18].
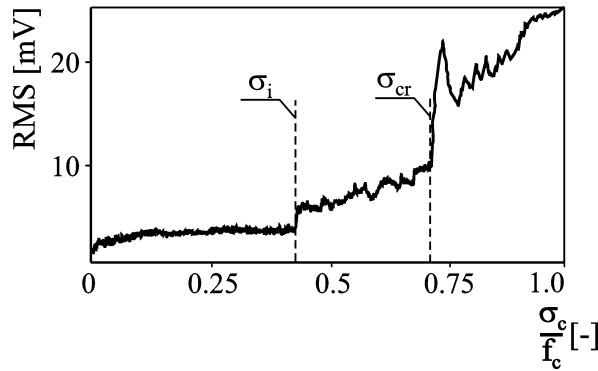
Fig. 8. Determination of levels of stress σ_i and σ_{cr} in compressed high-strength concrete based on measurements of AE signal's RMS value [18].

sharp. To establish the levels of stresses σ_i and σ_{cr}, the failure time after which the rate of AE counts and the energy of short AE impulses start to increase, first moderately and then rapidly, should be determined. By plotting the determined times on the graph of σ_c/f_c versus failure time one can establish the considered stress levels. In the case of the AE signal's RMS value one should locate the points at which moderately sharp and very sharp increase in the value of this descriptor occurs. These points, plotted on the axis of relative compressive stress σ_c/f_c, indicate the sought levels of stress σ_i and σ_{cr}.

4. Conclusions

1. The criteria for determining the levels of initiating stress σ_i and critical stress σ_{cr}, which divide the qualitatively different stages in the course of failure of concrete subjected to compression, found in the literature are based mainly on the experimental results obtained by the strain measurement method. Very few such criteria are available for acoustic methods which have been applied more and more frequently — especially the acoustic emission method — to investigate the failure of concrete. Furthermore, not

all of the literature criteria based on experimental results obtained by acoustic methods are useful for either plain or high-strength concrete. This problem has been addressed by the author of the present paper on the basis of his own experimental results.

2. In the case of the ultrasonic method it is impossible to establish a definite criterion which would enable the determination of stress σ_i levels in plain concrete under compression. It is possible, however, to establish such a criterion for stress σ_{cr} in this kind of concrete. Whereas in the case of compressed high-strength concrete the ultrasonic method is suitable for the determination of both stress σ_i and stress σ_{cr}.

3. As regards the AE method it is possible to establish definite criteria enabling the determination of the levels of stresses σ_i and σ_{cr} in plain concrete subjected to compression. It is enough to use AE counts for this purpose. Whereas the usefulness of this AE descriptor for the determination of the levels of stress σ_i in high-strength concrete is problematic due to the fact that the number of AE counts recorded in the initial stage and in the intermediate stage of loading this kind of concrete is small. Apart from AE counts, other AE descriptors, such as the rate of AE counts, the energy of short AE impulses and the AE signal's RMS value, can be used successfully to determine the levels of both initiating stress σ_i and critical stress σ_{cr}.

References

[1] K. NEWMAN and I.B. NEWMAN, *Failure theories and design criteria for plain concrete*, Proceedings of the Civil Engineering Materials Conference, Southampton, 1969, M. TE'ENI [Ed.], Wiley-Interscience, London, Part 2, 963–996.

[2] A.M. BRANDT et al., *Cracking and failure mechanism in concrete-like composites* [in Polish], [in:] Mechanical Properties and Structure of Concrete Composites, PAN, Ossolineum, Warszawa 1974, 163–209.

[3] S. MIMDESS and J.F. YOUNG, *Concrete*, Prentice-Hall, 1981.

[4] T. GODYCKI-ĆWIRKO, *Mechanics of concrete* [in Polish], Arkady, Warszawa 1982.

[5] A.M. BRANDT, *Experimental fracture mechanics as applied to test composites with cement matrices* [in Polish], [in:] Mechanics of Concrete-Like Composites, PAN, Ossolineum, Wrocław 1983, 449–501.

[6] S. MINDESS, *Application of failure mechanics to cement slurry, mortar and concrete* [in Polish], [in:] Mechanics of Concrete-Like Composites, A.M. BRANDT [Ed.], Polish Academy of Sciences, Ossolineum, Wrocław 1983, 377–407.

[7] K. FURTAK, *Bearing capacity of normal cross-sections in flexural reinforced concrete elements subjected to variable loading with reference to bridges* [in Polish], Scientific Papers of Cracow Polytechnic, No. 4, Cracow 1985.

[8] B. BILISZCZUK, *Concrete — a material for bridge building* [in Polish], Scientific Papers of the Institute of Civil Engineering of the Technical University of Wrocław, No. 32, Monographs, No. 10, 1986.

[9] J. KASPERKIEWICZ [Ed.], *Structure and properties of concrete and concrete-like composites. State of knowledge in Poland* [in Polish], PWN, Warszawa 1989.

[10] D.C. SPOONER and J.W. DOUGILL, *A quantitative assessment of damage sustained in concrete during compressive loading*, Magazine of Concrete Research, **27**, 92, 151–160 (1975).

[11] S.P. SHAH and S. CHANDRA, *Critical stress, volume change and microcracking of concrete,* ACI Journal, **65**, 9, 770–781 (1968).

[12] K. FLAGA and K. FURTAK, *Influence of aggregate grading on critical stress levels in compressed concrete* [in Polish], Arch. Civil Eng., **27**, 4, 653–666 (1981).

[13] K. FLAGA and K. FURTAK, *Effect of aggregate quality on cracking of reinforced concrete beams* [in Polish], Arch. Civil Eng., **28**, 1–2, 113–133 (1982).

[14] J. PYSZNIAK and J. HOŁA, *Application of acoustic methods to assessment of concrete humidity influence on the process of concrete destruction*, Archives of Acoustics, **16**, 2, 343–353 (1991).

[15] A. MOCZKO, *The age effect in cracking behaviour of plain concrete*, [in:] Brittle Matrix Composites 3, A.M. BRANDT, L. MARSHALL [Eds.], Elsevier Applied Science Publishers, London 1991, 234–239.

[16] J. HOŁA, *Effects of aggregate grading on the stress degradation of compressed concrete*, Arch. Civil Eng., **38**, 1–2, 85–101 (1992).

[17] J. HOŁA, *Role of thermal treatment in stress failure of concrete differing in its aggregate grain composition*, Engineering Transactions, **44**, 1, 17–29 (1996).

[18] J. HOŁA, *Studies of failure of high-strength concrete*, Engineering Transactions, **46**, 3–4, 333–351 (1998).

[19] L. BERES, *Fracture of concrete subjected to cyclic and sustained loading*, ACI Journal, **69**, 4, 304–305 (1971).

[20] Z.P. BAŽANT, *Theory of creep and shrinkage in concrete structures: a precis of recent developments*, Mechanics Today, 2, Pergamon Press (1975).

[21] B.L. MEYERS, F.O. SLATE and G. WINTER, *Relationship between time-dependent deformation and microcracking of plain concrete*, ACI Journal, **66**, 1, 60–68 (1969).

[22] O.YA. BERG, *Nekotorye rezultaty issledovaniya fiziko-mekhanicheskikh svoistv betona*, Trudy Koordinacionnykh Soveshchanii po Gidrotekhnike, Vypusk XIII, Moskva 1964.

[23] O.YA. BERG, G.N. PISANKO and YU.N. KHROMEC, *Issledovanie fizicheskogo processa razrusheniya betona na prochnost i deformativnye svoistva betona transportnykh sooruzhenii*, Moskva 1966, 5–41.

[24] J. BILISZCZUK and O. RAJSKI, *Deformability testing of high-strength concrete* [in Polish], Inżynieria i Budownictwo, **12**, 623–627 (1997).

[25] G.YA. POCHTOVIK, *Ispolzovanie ultrazvuka dla ocenki napryazhennogo sostoyaniya i strukturnykh izmenenii v obychnom keramzitovom betone*, Dissertaciya, Moskovskii Avtomobilno-Dorozhnyi Institut, Moskva 1962.

[26] J. HOŁA and A. MOCZKO, *Analysis of failure of selected kinds of concrete structure by ultrasonic method and AE method* [in Polish], Doctoral Dissertation. The Institute of Civil Engineering of the Technical University of Wrocław, Wrocław 1984.

[27] J. HOŁA, *Acoustic emission in concrete: Acoustic emission — sources, application, methods* [in Polish], J. MALECKI and J. RANACHOWSKI [Eds.], IFTR, Polish Academy of Sciences, Biuro Pascal Publisher, Warszawa 1994, 223–240.

[28] Z. RANACHOWSKI, *Methods of acoustic emission signal measuring and analysis* [in Polish], Thesis Qualifying for Assistant-Professorship, IFTR, Polish Academy of Sciences, Warszawa, No. 1, 1997.

THE ANALYSIS OF THE INFLUENCE OF THE THERMAL SHOCKS ON ACOUSTIC EMISSION SIGNAL GENERATED IN CORDIERITE CERAMICS

Z. RANACHOWSKI and P. RANACHOWSKI

Polish Academy of Sciences
Institute of Fundamental Technological Research
(00-049 Warszawa, Świętokrzyska 21, Poland)

The paper describes a raw materials composition and manufacturing technology of cordierite material, applied to manufacturing of welding backing strips. The resistance of the cordierite specimens to thermal shock within the range of $150 - 320°$C was analysed. Shocked samples, submitted to three — point mechanical stress, have been investigated by acoustic emission method. The results let the authors to conclude that there is a correlation between the Acoustic Emission (AE) signals parameter, describing the AE activity during the loading and the stage of material degradation caused by the applied thermal shock.

1. Introduction

The thermomechanical durability of ceramics is highly influenced by the critical microcraks growth due to thermal shock. One of the efficient methods to control that process is the Acoustic Emission measurement [1]. The latter method let us to determine the stress level corresponding with the initiation of the critical destruction processes in the investigated composition. The aim of this paper is to combine the initial stages of crack formation processes and their growth with the descriptors of the AE signal due to the increasing temperature difference of the applied thermal shock. The similar investigations were done on the alumina and the magnezite–zirconic ceramics [2]. The authors of this paper investigated the resistance to thermal shock of the cordierite ceramics and measured the AE activity of this material during three-point bending test after shocking.

Cordierite ceramics was chosen for the investigation due to its wide application in manufacturing of the elements with high thermal shock durability — for example the welding backing stripes.

The welding backing stripes are wide applied in one — operator welding, especially in shipyard and pressurized vessel construction. The stripes should meet several requirements: its shape and dimensions should stimulate the right formation of the welding path, they should not interact with the welding substrates by gas production or intermediate layer formation. Their expansion coefficient should be less than 4×10^{-6}K^{-1}, they should also withstand the thermal shock at the temperatures higher than $250°$C and its bending

strength should be higher than 100 MPa. All these requirements are optimally met by the cordierite ceramics.

For the perfect stechiometric composition the melting point is situated relatively high at 1545°C. The real compositions with additions of glass phase or other cristallites melt at lower temperature. The higher contents of the stechiometric cordierite represent the better thermal shock durability but at the real conditions there is mullite as a major addition. The stechiometric contents of the cordierite is following: 13.7% of MgO, 34.9% of Al_2O_3 and 51.4% SiO_2. The latter list indicates the low contents of SiO_2 when comparing to other ceramic compositions. That implies the low liquidity of the cordierite in the sintering process what increases the sensivity of the material on the slight inhomogeneities of the oven temperature distribution.

2. The structure and the thermomechanical durability of cordierite

The contents of the cordierite composition was prepared in accordance to the remarks stated in the previous paragraph. The composition used in following research fulfils the requirements of the Polish Standard No 86/E-06301 for the materials belonging to Group No 410. At the other hand, the mechanical parameters of prepared material are also sufficient for the demands of welding technology. The detailed contents of the composition is as follows: plastic fireproof clay 42%, rough Chinese talc 23%, ceramic alumina 20%, quartz sand 10%, kalium feldspar 5%.

The material contents stated above was designed in the way to obtain reduction of expansion coefficient and immunity for the sintering temperature variations. This was realized by the additional stabilization of the cordierite phase by mullite $(3Al_2O_3 \cdot 2SiO_2)$ what caused additional mechanical durability increase. Dimensions of the prepared welding strip bases had the dimensions of $105 \times 25 \times 8$ mm. Their plain shape and relatively small size enabled for using a press in shaping of the details. Two stage grinding process was applied for the substrates — preliminary grinding of hard cristallites and — finally — the whole mass grinding in the presence of plasticizers. The products were sintered in tunnel oven at temperature of 1280 ± 10.

The porosity of the backing strips was in the range of 9.5 — 10%, the average pore size was 5.5 µm and the mulite grain diameter was in order of 4 µm. At the microscopic image of the structure there are oval pores, numerous long mulite crystals placed in glassy cordierite matrix with slight contents of quartz relicts.

To discuss the resistance of the prepared material to thermal shocks according to the Polish Standard, mentioned above it has to be observed that the sample shocked with the temperature 250°C should perform not less than 75% of its normal mechanical strength. The compositions used at high temperature ranges usually can be applied up to threshold shock temperature difference, ΔT_{max} and beyond this value the major structural damages arise in the material volume. ΔT_{max} depends on mechanical parameters of the compositions according to the following formula:

$$\Delta T_{\max} = \frac{\lambda \cdot R_r}{\alpha \cdot E}(1 - \mu),\tag{1}$$

where: λ — heat conductivity, $-R_r$ tensile strength, α — linear expansion coefficient, E — Young's modulus, μ — Poisson's ratio.

The basic mechanical parameters of the investigated materials were following: specific density — $2540\,\text{kg/m}^3$, Young's modulus, measured with ultrasound method — $91\,\text{GPa}$, critical stress intensity ratio — $2.9\,\text{MPa·m}^{1/2}$, average bending strength — $132\,\text{MPa}$, Weibull's coefficient of the bending strength distribution — 21, linear expansion coefficient at $200-700°\text{C}$ — $2.9 \div 3.9{\times}10^{-6}\,\text{K}^{-1}$. Calculating the formula (1), using the typical values for the cordierite — $R_r = 1000\,\text{GPa}$, $\lambda = 10^{-4}\,\text{J/m\,s}°\text{C}$, $\mu = 0.1$ one can obtain the result that the ideal shaped cordierite sample should withstand the shock $\Delta T_{\max} \sim 1000°\text{C}$. In real conditions, the measured value of $\Delta T_{\max}$ reaches 25% of its theoretical value. The thermal shocks were applying to the samples, preheated to the temperature T_1 by placing them in water bath in temperature T_0. The determination of $\Delta T_{\max}$ was undertaken measuring the three-point bending strength R_b of the samples as a function of shocking temperature difference. The measurements of R_b were made on the loading machine type Zwick 1446. The traverse velocity during the measurements was $1\,\text{mm/min}$ and the sample supporting prisms were placed at the distance of $60\,\text{mm}$ from each other. The results of R_b measurements are shown in Table 1 and in Fig. 1. The accuracy of the R_b measurements was ca. 2%.

Table 1. Results of the measurements of three-point bending strength R_b for the cordierite samples, as a function of shocking temperature difference ΔT.

ΔT [°C]	0	100	150	200	220	250	280	300	320	400
R_b [MPa]	102.9	102.3	103.2	107.5	105.9	33.5	29.6	27.7	35.4	24.5
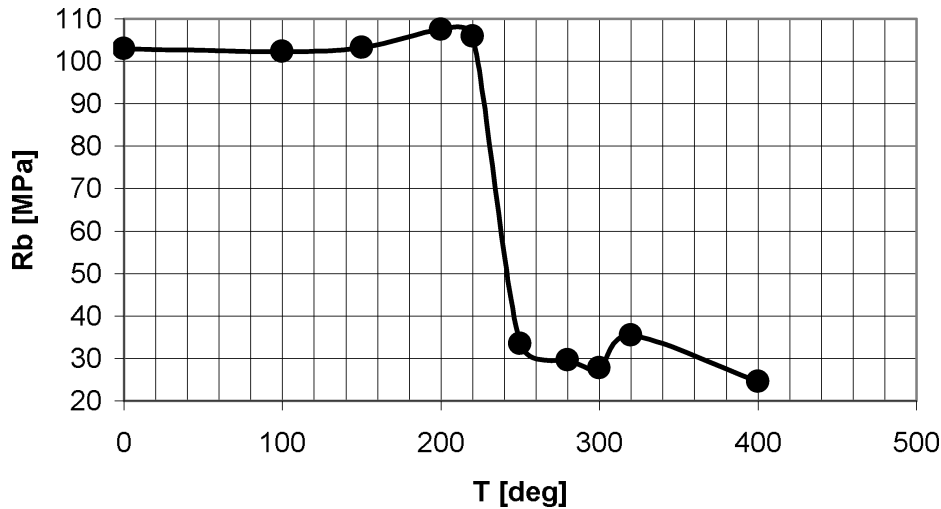
Fig. 1. Results of the measurements of three-point bending strength R_b for the cordierite samples, as a function of shocking temperature difference ΔT, visible value of threshold shock temperature difference $\Delta T_{\max}$.

3. Acoustic Emission measurements

In the course of bending test a wideband AE sensor (Physical Acoustic Corp., WD Type) was attached to the loaded cordierite samples. Acoustic Emission signal processor consisted of the band-pass amplifier, working in the frequency band $500-2000\,\text{kHz}$ and AE counts processor, connected with personal computer via fast parallel interface. Because of rapid character of microcrack propagation in cordierite the EA counts registration was made at a rate of 100 measurements per second. For the purpose of further analysis of AE activity in different regions of bending stress, current level of loading force was also registered in the computer. Eighteen samples were tested for each shocking temperature difference ΔT indicated in Table 1. For all ΔT levels the large variations in measured counts sum per entire loading process were observed. Therefore no correlation between AE counts sum and shocking temperature difference ΔT could be found. The most probable reason of this effect could be the fact that the sensivity of EA sensor remarkably depended on the direction of crack propagation and the influence of termal shock structure degradation was weaker than the factor mentioned above. However AE activity was indicated both at the low levels of bending stress and at the critical levels of that stress (comparable to rupture level). Figure 2 illustrates typical time dependence of AE counts rate at three-point bending test. Current AE count recordings are marked as triangles, the black line indicates the stress applied to the sample.
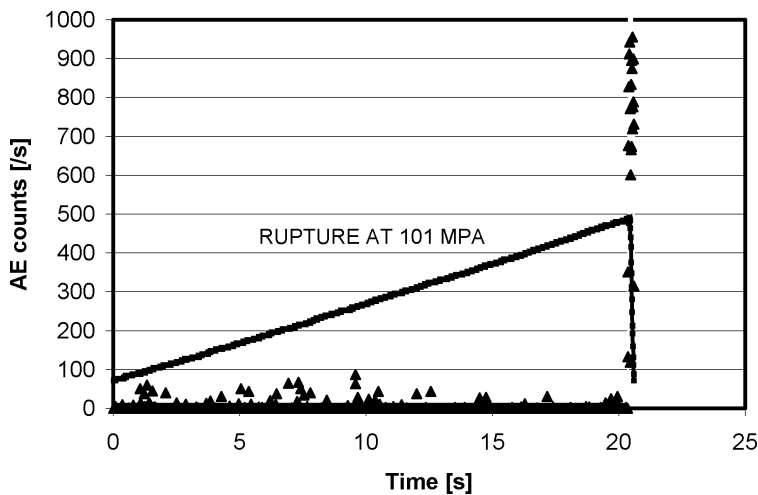
Fig. 2. Typical time dependence of AE counts (triangles) and applied bending stress (solid line) registered in investigated cordierite sample.

The authors of this paper processed the AE data putting into account the feature shown in Fig. 2 — recordable AE activity at the entire process of mechanical loading of the samples. For each sample AE counts were totalized in two separate regions. The first region, denoted as N_I included AE counts totalized from the load start up to 95% of the bending stress. The second region, denoted as N_R included AE counts from 95% of the

bending stress to the rupture. The calculations indicated that N_I and N_R are proportional to each other within the group of the samples treated with the same thermal shock temperature difference. In each group only 25% of the samples failed to present the trend described above (probably they were defected at the manufacturing process). Therefore the ratio N_I/N_R could be treated as acoustic measure of material degradation due to thermal shock. The average N_I/N_R ratios for each sample group (at least 18 members) together with averaged bending strength and shocking temperature difference ΔT are shown in Table 2. The dependence N_I/N_R ratio on shocking temperature difference ΔT are shown in Table 2.

Table 2. The average N_I/N_R ratios for each sample group shown together with averaged bending strength and shocking temperature difference ΔT measured for the group.

ΔT [°C]	0	150	200	220	250	280	320
R_b [MPa] (averaged)	106.2	102.4	102.7	104.3	34.2	35.1	30.7
$N_I/N_R \times$ 100%	40	36	83	66	5	0.6	0.4

The dependence N_I/N_R ratio on shocking temperature difference ΔT is also presented in Fig. 3.
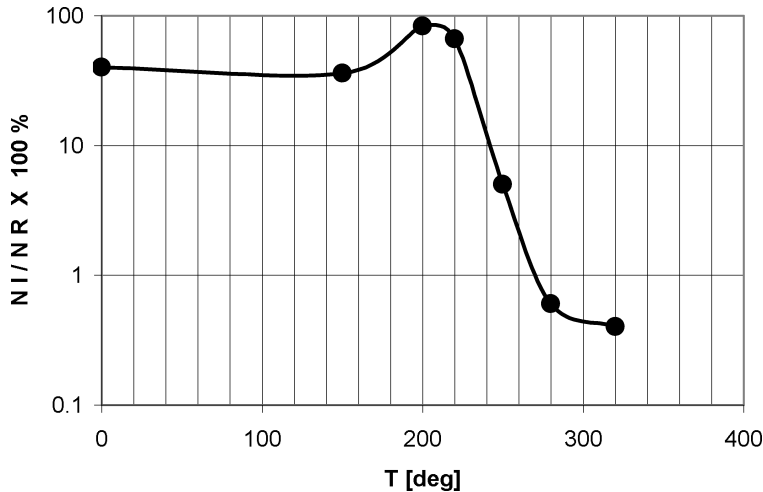
Fig. 3. The dependence N_I/N_R ratio on shocking temperature difference ΔT for the investigated cordierite samples.

There are remarkable similarities in the shape of the curve shown in Fig. 1 and in the shape of the curve shown in Fig. 3. The first curve presents the results of the mechanical strength test. The latter presents the data derived from the acoustical measurements. To fulfil the requirements of the Polish Standard No 86/E-06301, mentioned in second paragraph — according to the results presented in Fig. 1 — the shocking temperature difference should not exceed 230 degrees. The same result with accuracy of ±5% is possible to obtain using the data submitted in Fig. 3 if we modify the definition of significant

structure degradation what was assumpted in the Polish Standard described above. For the results of AE measurements it should be specified that the significant structure degradation appears if the N_I/N_R ratio measured in logarithmic scale as a function of shocking temperature difference ΔT falls down to 75% of its initial value.

The investigation of material resistance to thermal shock with application of mechanical loading is expensive kind of testing. The additional problems with application of the described method are caused by the dispersion of the mechanical strength of the investigated specimens. Therefore, application of acoustic method of shocking stress monitoring during mechanical test might provide the additional verification of the obtained experimental results.

Acknowledgement

References

[1] C.Y. JIAN, T. SHIMIZU, T. HASHIDA et al., *Development of thermal shock and fatigue tests of ceramic coatings for gas turbine blades*, J. of Acoustic Emission, **13**, 3-4, S68–S74 (1995).

[2] K. KONSZTOWICZ, *Acoustic emission study of the resistance to thermal shock of ceramic materials*, J. Am. Ceramic Soc., **73**, 3, 502–508 (1990).

[3] K. ONO, *AE Arising from Plastic Deformation and Fracture*, Fundamentals of AE, Univ. of California, Los Angeles 1979, pp. 167–207.

[4] Polish Standard No. PN–86/E–06301 "Insulating ceramic materials. Classification and requirements", Alfa, Polish Standard Publ., 1986.

[5] J. RANACHOWSKI, P. RANACHOWSKI and J. BERTRAND, *Acoustic emission in thermomechanic tests of line insulators* [in Polish] [in:] New Methods of Technology and Materials Science, IFTR PAS, Warszawa 1999, pp. 47–59.

[6] Z. RANACHOWSKI, *Acoustic emission measurements in ceramic, wood and metals* [in Polish], Scientific Bulletins of University of Mining and Metallurgy, **14**, 2, Kraków 1995, pp. 130–142.

DIRECTIONAL CHARACTERISTICS OF A PLANAR ANNULAR PLATE FOR AXIALLY–SYMMETRIC FREE VIBRATIONS

W.P. RDZANEK, JR.

Pedagogical University, Department of Acoustics
(35-310 Rzeszów, ul. Rejtana 16a, Poland)
wprdzank@atena.univ.rzeszow.pl

Z. ENGEL

University of Mining and Metallurgy
Department of Vibro-Acoustics
(30-059 Kraków, Al. Mickiewicza 30, Poland)
engel@uci.agh.edu.pl

There is solved a coastal problem of the acoustic wave radiation at Fraunhofer zone for a planar annular plate vibrating harmonically. It is assumed that a plate is clamped with both its banks, inner and outer, into a planar rigid baffle. There is an analysis of axially-symmetric free vibrations. There are directional-frequency characteristics for both kinds of sources — annular plate and annular membrane.

1. Introduction

Many of substantial factors should be taken into consideration during theoretical analysis of complex surface vibrating systems generation and propagation phenomena. These factors are acoustic influences of source surface particular elements, individual sources of a system and of vibration form upon vibrating system radiation resultant field. There are many scientific works considering these problems. E.g. works of Levin and Leppington [6] in case of axially-symmetric sources. In works [9, 10] authors considered analytic active and reactive radiation power of a planar annular membrane for axially-symmetric vibrations forms. In work [8] there are presented directional characteristics of vibrating annular plate. Natural frequencies of transversely vibrating plates analysis is contained in work [11]. Energetic radiation aspect of an annular plate is transformed to integral form with Hankel transform in work [1]. Authors analyzed in detail non-dimensionalized added virtual mass incremental (NAVMI) factors. A considerable part of works contain problems of radiation conditions optimization of vibrating systems (comp. Engel [3], Fuller [4], Nelson and Deffayet [2]).

More complex, in respect of analytic research, is acoustic wave radiation of vibrating annular plate. There is a theoretical analysis of linear and sinusoidal in time phenomena. As a result acoustic pressure at Fraunhofer zone formula of elementary form of is produced. The source of pressure is a planar annular plate clamped with both its banks into a planar rigid baffle. Frequency-directional characteristics of annular plate radiation are presented in respect of source sizes. These characteristics are also compared with corresponding characteristics of annular membrane.

2. Free vibrations of an annular plate

In the plane $z = 0$, which is perfectly rigid, there is a planar thin annular plate. It is clamped with its banks, i.e. for $r = r_1$ and $r = r_2$, and $s = r_2/r_1 > 0$. There are considered axially-symmetric free vibrations, sinusoidal in time. Transverse deflection of plate surface points $\eta(r,t) = \eta(r)\exp(i\omega t)$ with boundary conditions

$$\eta(r_2, t) = \eta(r_1, t) = 0, \qquad \left.\frac{\partial \eta(r, t)}{\partial r}\right|_{r=r_2} = \left.\frac{\partial \eta(r, t)}{\partial r}\right|_{r=r_1} = 0, \qquad (2.1)$$

there is

$$\frac{\eta_n(r)}{A_n} = J_0\left(x_n \frac{r}{r_1}\right) + B_n I_0\left(x_n \frac{r}{r_1}\right) - C_n N_0\left(x_n \frac{r}{r_1}\right) - D_n K_0\left(x_n \frac{r}{r_1}\right). \qquad (2.2)$$

There are here functions of null order: J_0 — Bessel, N_0 — Neumann, I_0 – modified Bessel and K_0 — McDonald. A value $x_n = k_n r_1$ $(k_n^4 = \omega_n^2 \varrho h/B)$ is n–th root of frequency equation

$$[sN(sx_n) - N(x_n)][sT(sx_n) - T(x_n)] = [sS(sx_n) - S(x_n)][sR(sx_n) - R(x_n)], \qquad (2.3)$$

where

$$\begin{aligned}
S(x) &= J_1(x)I_0(x) + J_0(x)I_1(x), \\
T(x) &= N_1(x)I_0(x) + N_0(x)I_1(x), \\
N(x) &= J_1(x)K_0(x) - J_0(x)K_1(x), \\
R(x) &= N_1(x)K_0(x) - N_0(x)K_1(x).
\end{aligned} \qquad (2.4)$$

There are constants in the vibration equation (2.2)

$$\begin{aligned}
B_n &= sx_n \frac{R(sx_n)N(x_n) - R(x_n)N(sx_n)}{sR(sx_n) - R(x_n)}, \qquad C_n = \frac{\lambda S(sx_n) - S(x_n)}{sT(sx_n) - T(x_n)}, \\
D_n &= sx_n \frac{T(sx_n)S(x_n) - T(x_n)S(sx_n)}{sT(sx_n) - T(x_n)}.
\end{aligned} \qquad (2.5)$$

The constant A_n is calculated from normalization condition (comp. [9])

$$\int_{r_1}^{r_2} \eta_n^2(r)\, r\, dr = \frac{1}{2}(r_2^2 - r_1^2). \qquad (2.6)$$

There is obtained

$$A_n^2 = \frac{1}{2}(s^2 - 1)\left\{s^2[J_0(sx_n) - C_n N_0(sx_n)]^2 - [J_0(x_n) - C_n N_0(x_n)]^2\right\}^{-1}. \qquad (2.7)$$

In Table 1 there are given values of frequency equation several roots (2.3).

Table 1. Roots x_n of the frequency equation (2.3).

n	s
	1.1	1.2	1.5	2	3	5
1	47.299	23.648	9.4554	4.7236	2.3579	1.1766
2	78.531	39.264	15.703	7.8477	3.9200	1.9569
3	109.96	54.976	21.988	10.991	5.4923	2.7433
4	141.37	70.685	28.272	14.134	7.0640	3.5295
5	172.79	86.393	34.555	17.276	8.6354	4.3154
6	204.20	102.10	40.839	20.418	10.207	5.1013

3. Acoustic pressure at the Fraunhofer zone

An annular plate, which transverse vibration distribution is calculated from the formula (2.2), radiates a wave of acoustic pressure into a half space $z \geq 0$ which is filled with a perfect gas medium of rest density ϱ_0 and wave propagation velocity c_0.

Acoustic pressure distribution of vibrating source clamped into a planar rigid baffle at the Fraunhofer zone is [7]:

$$p(R, \vartheta, \varphi) = \frac{i\varrho_0\omega}{2\pi} \frac{\exp(-ik_0R)}{R} \int\limits_{\sigma_0} v(r_0, \varphi_0) \exp[ik_0 r_0 \sin\vartheta \cos(\varphi - \varphi_0)] \, d\sigma_0 \qquad (3.1)$$

and $\frac{1}{2}k_0 r_0\{r_0/R\} \ll 1$, R, ϑ, φ are spherical coordinates of field point and r_0, φ_0 are polar coordinates of source point, $k_0 = 2\pi/\lambda$, λ is radiated wavelength, $v(r_0, \varphi_0)$ is a normal component of surface source vibration velocity.

In case of axially-symmetric vibrations $v(r_0) = i\omega\eta(r_0)$ the formula (3.1) is of form

$$p(R, \vartheta) = -\varrho_0\omega^2 \frac{\exp(-ik_0R)}{R} \int\limits_{r_1}^{r_2} \eta(r_0) J_0(k_0 r_0 \sin\vartheta) r_0 \, dr_0. \qquad (3.2)$$

As a result of calculation of this integral, with specified vibration distribution (2.2), there is

$$p_n(R, \vartheta) = -\varrho_0\omega_n^2 A_n \frac{\exp(-ik_0R)}{R} \frac{2(r_1 x_n)^2}{x_n^4 - u^4}$$
$$\times \left\{x_n[sC_1'(sx_n)J_0(su) - C_1'(x_n)J_0(u)] - u[sC_0'(sx_n)J_1(su) - C_0'(x_n)J_1(u)]\right\}, \qquad (3.3)$$

where $u = k_0 r_1 \sin\vartheta$, $C_0'(x) = J_0(x) - C_n N_0(x)$ and $C_1'(x) = J_1(x) - C_n N_1(x)$.

Result (3.3) presents an elementary form of an acoustic pressure expression at the Fraunhofer zone of an annular plate, which is activated to axially-symmetric form of vibrations $(0, n)$.

At the main direction there is

$$p_n(R, 0) = -2\varrho_0 r_1^2 A_n \frac{\omega_n^2}{x_n} [s C_1'(s x_n) - C_1'(x_n)] \frac{\exp(-i k_0 R)}{R} , \qquad (3.4)$$

where A_n is the normalization constant defined by formula (2.7).

Directional characteristic of an annular clamped plate is in the form

$$K_n(\vartheta) = \left| \frac{p_n(R, \vartheta)}{p_n(R, 0)} \right|$$

$$= \frac{s C_1'(s x_n) J_0(s u) - C_1'(x_n) J_0(u) - (u/x_n)[s C_0'(s x_n) J_1(u) - C_0'(x_n) J_1(u)]}{[1 - (u/x_n)^4][s C_1'(s x_n) - C_1'(x_n)]} , \qquad (3.5)$$

where $u = \beta \sin \vartheta$.

If an annular membrane is stimulated to axially-symmetric form of vibrations $(0, n)$ then pressure at the Fraunhofer zone is (comp. [9])

$$p_n(R, \vartheta) = -i \varrho_0 \omega_n W_n(\vartheta) \frac{\exp(-i k_0 R)}{R} , \qquad (3.6)$$

where

$$W_n(\vartheta) = \sqrt{s^2 - 1} \frac{i \omega_n x_n}{N_0(x_n)} \left\{ \frac{1}{N_0^2(s x_n)} - \frac{1}{N_0^2(x_n)} \right\}^{-1/2}$$

$$\times \frac{\alpha_n J_0(s \beta \sin \vartheta) - J_0(\beta \sin \vartheta)}{x_n^2 - \beta^2 \sin^2 \vartheta} , \qquad (3.7)$$

where $\alpha_n = J_0(x_n)/J_0(s x_n)$, x_n is a root of characteristic equation (comp. [5] and [9, 10])

$$\frac{J_0(x_n)}{J_0(s x_n)} = \frac{N_0(x_n)}{N_0(s x_n)} . \qquad (3.8)$$

Annular membrane directional characteristic for mode $(0, n)$ is in the form

$$K_n(\vartheta) = \left[1 - (\beta/x_n \sin \vartheta)^2 \right]^{-1} \frac{\alpha_n J_0(s \beta \sin \vartheta) - J_0(\beta \sin \vartheta)}{\alpha_n - 1} . \qquad (3.9)$$

4. Numerical analysis and concluding remarks

Diagrams of annular plate radiation direction indicator of axially-symmetric vibration forms are presented in Figs. 1–4. In case of odd vibrations forms $(n = 1, 3, 5, ...)$ the direction indicator is calculated from the formula [7]

$$K_n(\vartheta) = \left| \frac{p_n(R, \vartheta)}{p_n(R, \vartheta_0)} \right| \qquad \text{where} \quad \vartheta_0 = \begin{cases} 0 & \text{for } n = 1, 3, 5, \dots , \\ \max_{p_n(R, \vartheta)} \vartheta & \text{for } n = 2, 4, 6, \dots . \end{cases} \qquad (4.1)$$
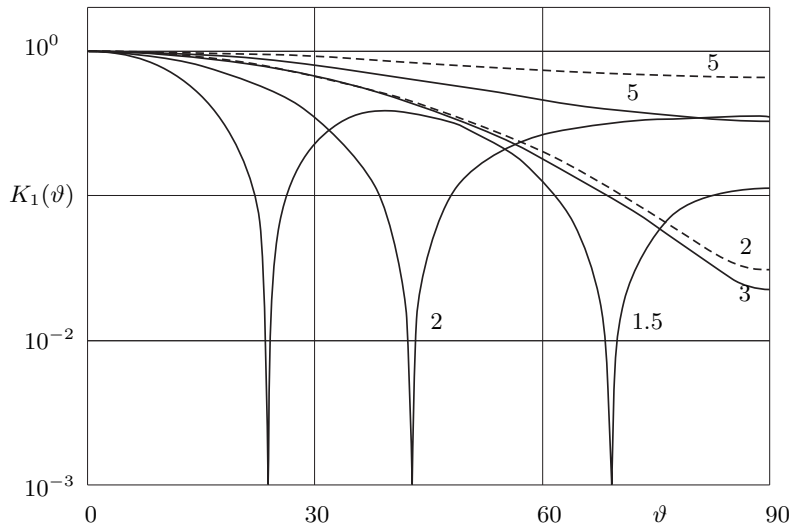
Fig. 1. Directional characteristics of annular source radiation for $\beta/x_1 = 0.5$, $s = 5, 3, 2$ and 1.5.
Attention for Figs. 1–4, 7: Curves in figures are: solid — vibrating plate is a source, dashed — vibrating membrane is a source.
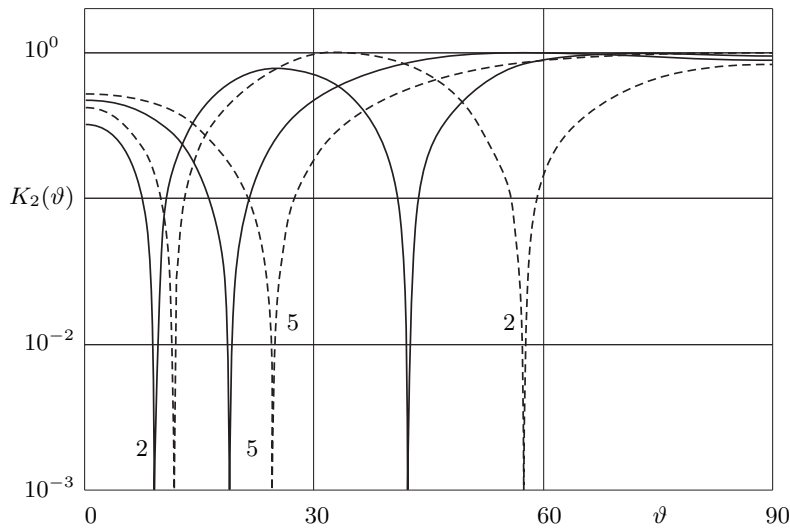
Fig. 2. Directional characteristics of annular source radiation for $\beta/x_2 = 0.5$, $s = 5$ and 2.

If an annular plate is stimulated to one of the even forms of vibrations ($n = 2, 4, 6, ...$), then pressure $p_n(R, \vartheta)$ is related to pressure $p_n(R, \vartheta_0)$. Angle ϑ_0 determines the direction of the maximal radiation.

Directional characteristics are also presented graphically in case of vibrating annular membrane. It allows comparing directional characteristics of two different annular sources
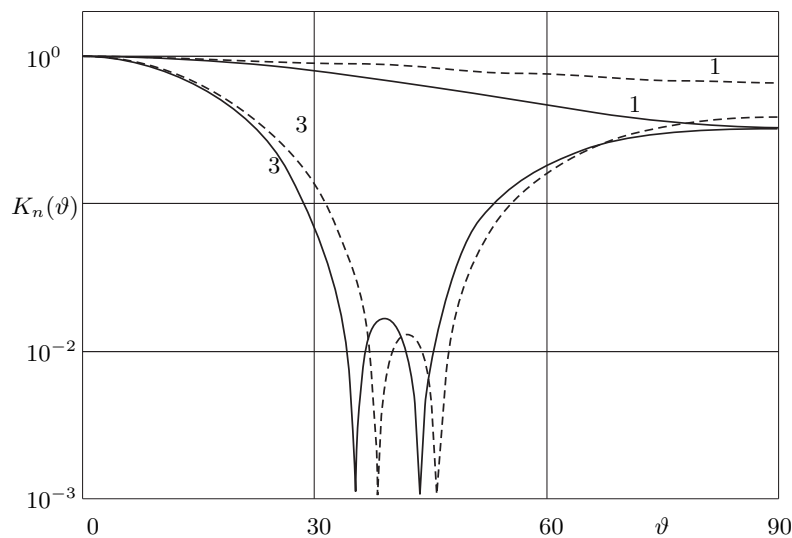
Fig. 3. Directional characteristics of annular source for $s = 5$, $\beta/x_n = 0.5$, $n = 1$ and 3.
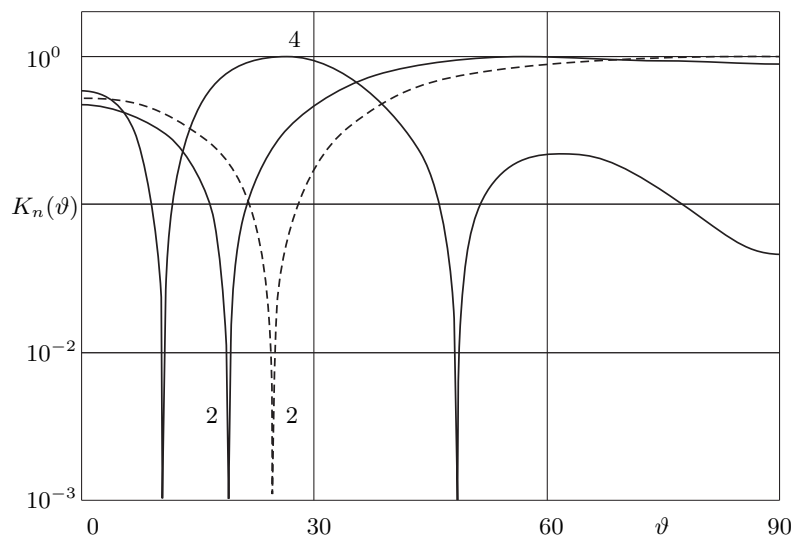
Fig. 4. Directional characteristics of annular source for $s = 5$, $\beta/x_n = 0.5$, $n = 2$ and 4.

— the plate and the membrane. There are diagrams of $K_n(u)$ versus variable $u = \beta \sin \vartheta$ in Figs. 5, 6 and versus variable $u = \beta/x_n \sin \vartheta$ in Fig. 7.

In boundary case, when $r_1 \to 0$ and $r_2 = a$, there are formulas describing a circular source (membrane or plate) instead of formulas describing an annular source (membrane or plate). Instead of characteristic equation (2.3) there is characteristic equation for a
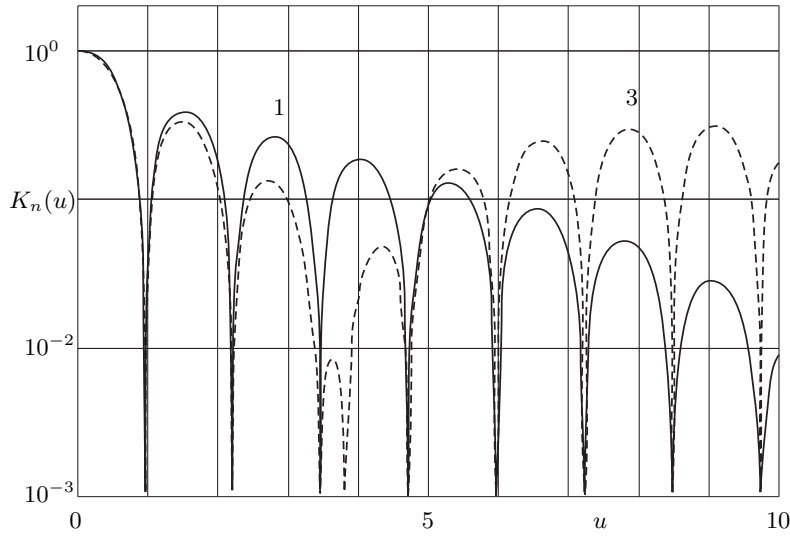
Fig. 5. Diagrams of $K_n(u)$ function versus variable $u = \beta \sin \vartheta$ for annular plate. It is assumed that $s = 1.5$, $n = 1$ and 3.
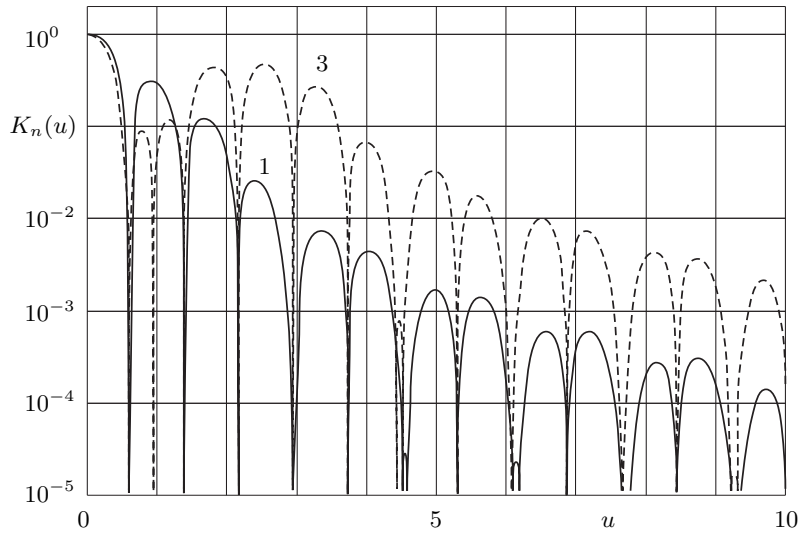
Fig. 6. Diagrams of $K_n(u)$ function versus variable $u = \beta \sin \vartheta$ for annular plate. It is assumed that $s = 3$, $n = 1$ and 3.

circular plate of radius $r = a$, i.e. when $r_1 \to 0$, $C_n \to 0$,

$$S(sx_n) = S(k_n a) = J_1(k_n a)\, I_0(k_n a) - J_0(k_n a)\, I_1(k_n a) = 0, \qquad (4.2)$$

where $k_n^2 = \omega_n \sqrt{\varrho h / \beta}$. There is also that $\lim_{r_1 \to 0} A_n(r_1) = 2^{-1/2} J_0^{-1}(k_n a)$.
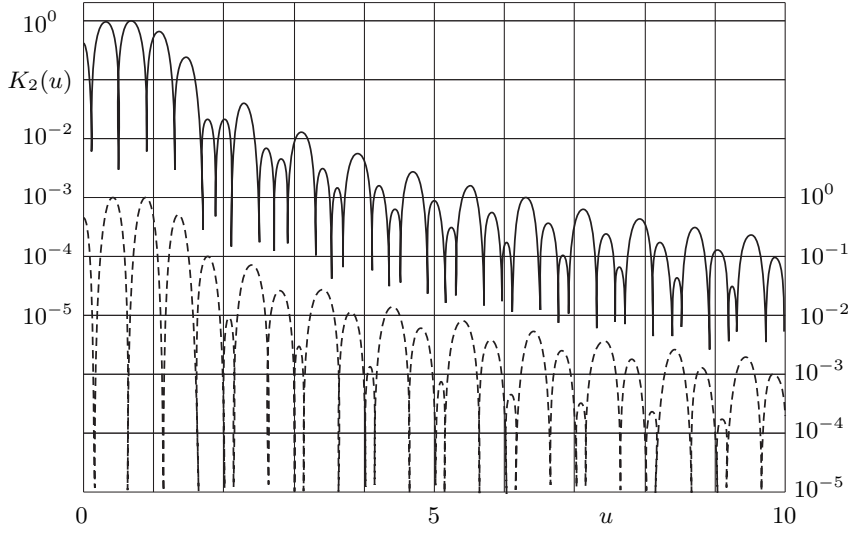
Fig. 7. Diagrams of $K_2(u)$ function versus variable $u = \beta/x_2 \sin \vartheta$ for annular source. It is assumed that $s = 3$.

From the formula (3.5) there is

$$\lim_{r_1 \to 0} K_n(r_1, \vartheta) = \frac{J_0(k_0 a \sin \vartheta) - \dfrac{k_0}{k_n} \dfrac{J_0(k_n a)}{J_1(k_n a)} \sin \vartheta\, J_1(k_0 a \sin \vartheta)}{1 - (k_0/k_n)^4 \sin^4 \vartheta} . \tag{4.3}$$

Instead of characteristic equation (3.8) there is a characteristic equation for a circular membrane of radius $r = a$, i.e.

$$J_0(k_n a) = 0, \tag{4.4}$$

where $k_n = \omega_n \sqrt{\sigma/T}$, σ is the membrane surface density, T is the stretching force. From the formula (3.9) there is

$$\lim_{r_1 \to 0} K_n(r_1, \vartheta) = \frac{J_0(k_0 a \sin \vartheta)}{1 - (k_0/k_n)^2 \sin^2 \vartheta} . \tag{4.5}$$

Acknowledgement

References

[1] M. Amabili, G. Frosali and M.K. Kwak, *Free vibrations of annular plates coupled with fluids*, J. of Sound and Vibration, **191**, 5, 825–846 (1996).

[2] C.D. Deffayet and P.A. Nelson, *Active control of low-frequency harmonic sound radiated by a finite panel*, J. of the Acoustical Society of America, **84**, 6, 2192–2199 (1996).

[3] Z. Engel, *Development of active methods in Poland* [in Polish], Materials of III-rd School "Active Methods of Vibration and Noise Reduction", Zakopane 1997, pp. 53–57.

[4] C.R. Fuller, *Active control of sound transmition/radiation from elastic plates by vibration inputs, I. Analysis*, J. of Sound and Vibration, **136**, 1, 1–15 (1990).

[5] E. Janke, F. Emde and F. Lösch, *Tafeln höherer funktionen*, B.G. Teubner Verlagsgesellschaft, Stuttgard 1960.

[6] H. Levine and F.G. Leppington, *A note on the acoustic power output of a circular plate*, J. of Sound and Vibration, **121**, 2, 269–275 (1988).

[7] I. Malecki, *Physical foundations of technical acoustics*, Pergamon Press, Oxford 1969.

[8] W.P. Rdzanek Jr. and Z. Engel, *The acoustic radiation power of a planar annular plate for the form of vibrations* $(0, n)$ [to be published in proceedings of Forum Acusticum '99, Berlin 1999, This work is realized within a framework of the KBN project no T07B01812.

[9] W.J. Rdzanek and W.P. Rdzanek, Jr., *The real acoustic power of a planar annular membrane radiation for axially-symmetric free vibrations*, Archives of Acoustics, **22**, 4, 455–462 (1997).

[10] W.J. Rdzanek and W.P. Rdzanek, Jr., *The acoustic reactance radiated by a planar annular membrane for axiallysymmetric free vibrations*, [to be published in Archives of Acoustics].

[11] S.M. Vogel and D.W. Skinner, *Natural frequencies of transversely vibrating uniform annular plates*, J. of Applied Mechanics, **32**, 926–931 (1965).

THE POSSIBILITY OF APPLYING OF ACOUSTIC METHODS
FOR THE MONITORING OF SOL-GEL PROCESSES

J. RZESZOTARSKA

Department of Chemistry, University of Warsaw
(02-093 Warszawa, ul. Pasteura 1, Poland)

J. RANACHOWSKI

Polish Academy of Sciences
Institute of Fundamental Technological Research
(00-049 Warszawa, Świętokrzyska 21, Poland)

Models simulating the propagation of acoustic waves in the successive stages of the gelation process are presented. The early stage of gelation has been considered with scattering theory for very low concentrations of suspensions. The system may be simulated by the line of the independent Maxwell elements. When concentration of the suspension increases, the interaction of the particles can be presented by an acoustic model, which consist of a chain of coupled Maxwell elements. After the gelation point, the system becomes rigid, and three dimensional tensoral fields distribution of stress and strain was used.

1. Introduction

This paper is aimed at the presentation of the possible applications of the ultrasonic methods to the monitoring of the gelation process. New trends in material science of the last years concern, among other things, the manufacturing of materials and composites arranged in a nanometric scale. The application of nanotechnology has opened perspectives of manufacturing materials of unique mechanical, electrical, optical and catalytic properties. The application of the sol-gel method enabled the creation of materials of parameters that can not be obtained by traditional methods, e.g. the titanic-silica glass. Ceramic materials produced by this method are similar to the natural ones, e.g. to bones and shells.

The gelation process has not been fully known so far, therefore its monitoring is essential for both the practical and scientific reasons. The application of acoustic methods to this purpose requires an improvement of both the measuring methods and the theoretical analyses.

The peculiarity of the problem lies in the fact that during the separate stages of the gelation process, the two-phase medium changes its structure continually. Beginning from the nuclei present in the liquid, growing agglomerates of fractal structure are formed. After reaching the gelation point, the system becomes a rigid spatial structure immersed in a liquid. The knowledge of the propagation of acoustic waves in such a system is still incomplete and requires further research.

This paper is confined to the general presentation of models simulating the propagation of acoustic waves in the separate stages of gelation.

2. Stages of the gelation process

Gelation may be defined as a secondary phase transition of the sol to a gel. In the sol phase, there exist molecules or particles consisting of several monomers in the solution. Approaching the gelation point, aggregation of the particles occurs and the measured physical values achieve critical sizes.

After this phase of the transformation, an unique state of matter arises characterised by a spatial expanded lattice filled up with gel. Macroscopically, the medium shows elastic properties similar to solid bodies. The liquid phase contained in gel enables, after exceeding a critical point, comparatively a relatively fast transport of ions. It means that the diffusion coefficients are only slightly lower than in a liquid.

After the transition, the transport of the liquid phase contained in the gel is relatively fast. This means that the diffusion coefficients of the ions in the gel are only a little smaller than in a liquid. The evaporation velocity of the liquid from the system is so fast as if there were only a liquid in the vessel. The energy of this transition is rather small, for example, for silica gel it equals 10–20 kcal/mole depending on the conditions under which the process occurs.

Together with the progress in the aging process, after crossing the gelation point the rigidity increases, because residual oligomers of the gel present in the solvent, are bonded in the main lattice, forming additional cross-links. This phenomenon is responsible for the appearance of the elasticity of the system. The elastic properties of the gel on the molecular level depend on the structure of the network, especially on the cross-links.

The sol-gel transitions discussed occur in several consecutive stages listed below:

• molecular aggregation and forming of clusters; the cluster is defined as a collection of mutually connected bonds and nodes,

• further aggregation and growing of clusters; the life time of this stage depends on the distribution and expansion of the clusters,

• proper transformation of the sol to gel, i.e. the formation of a large cluster that consists of a continuous network filling the whole volume of the vessel; a space structure of the system is formed,

• the formed extensive cluster becomes dense as the result of the formation of new cross-linking bonds; this stage is named ageing during which the elastic properties of the medium increase significantly.

3. The fractal concept of gelation

The classical Flory's theory of gelation has been applied until now to answer the following question: what is the fraction of all bonds (p_c) that must formed before continuous network structure appears. The general equation is

$$p_c = \frac{1}{z-1},\tag{1}$$

where p_c — gel point, z — number of bonds in the monomer. This model predicts that $p_c = 1/3$ when $z = 4$ (for silica). This means that the point of gelation occurs when one third of all the possible bonds are formed. The disadvantage of this theory is that it neglects the formation of rings within the growing clusters and that it does not consider the kinetics of gelation. Thus, the classical model does not provide a realistic image of the cluster growth. These properties are considered in the fractal growth model of gelation.

A fractal is a paradigm for describing the morphology and evolution of the shape and the growth processes. A fractal dimension of 1.0 which defines the cluster growth (D) represents a linear growth. If the fractal dimension is equal to 3, the cluster density is uniform (nonfractal growth). A fractal growth imply a decrease in the density with increasing radius of the cluster ($D < 3$).

The mass (M) in the gelation process with fractal radius (r) is growing according to the relation

$$M = kr^D,\tag{2}$$

where k is a constant.

The rate of the cluster growth and the cluster–cluster aggregation growth for silica gels, according to Connel and Aubert, increases exponentially

$$\begin{aligned}
r &= r_0 \exp(q_r t),\\
M &= M_0 \exp(q_r t),
\end{aligned}\tag{3}$$

where t is time and q_r is a constant, M is the fractal mass or the average molecular weight, M_0 is the mass (molecular weight) of the monomer, r_0 is the radius of the monomer (core radius).

Below the gel point, the molecular weight and cluster size can be calculated from the viscosity as a function of time.

The decrease in density (ρ), as the fractal increases in size, can be calculated from the relation

$$F = \frac{\rho}{\rho_0} = \left(\frac{r_0}{r}\right)^{3-D}.\tag{4}$$

In the evolution of solids from solutions, a different type of structures, depending on the degree of cross-linking, can be formed. Recently, various experimental techniques of microscopy, small-angle X-ray scattering, small-angle neutron scattering and rheology have been applied to elucidate fractal structures in the aggregation and gelation of systems. According to the fractal theories, the network structure of gels is a collection of
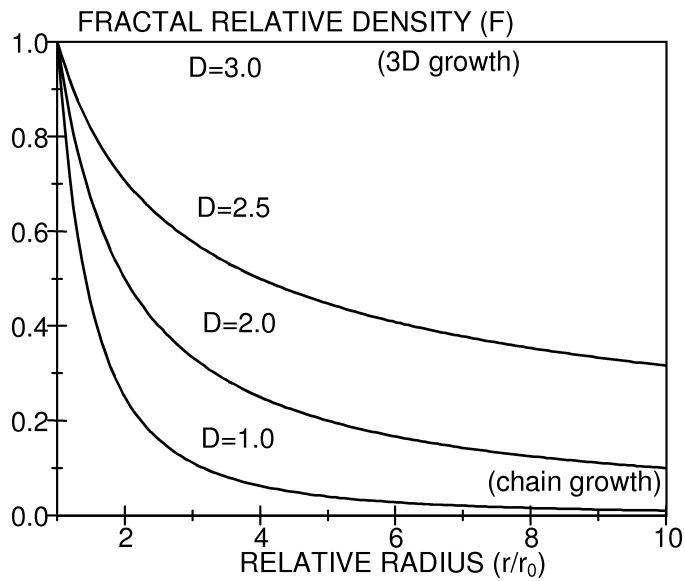
Fig. 1. Fractal relative density versus relative radius as a function of variations in the fractal dimension. From E.J.A. POPE [2].

fractal aggregates closely packed throughout the system. The rheologic measurements are easy, especially in the high concentration range of the clusters.

During the thermal treatment at small oscillatory deformation with shear strains of frequency (ω), the shear modulus (G^*), which is a complex number with a real part G' (stiffness modulus) and an imaginary part G'' corresponding to shear losses, is measured for gels. The G' values are larger that the G'' this generally only one of the characteristic properties of gel is described.

4. Models simulating the propagation of acoustic waves in the successive stages of the gelation process

From the acoustical point of view, the whole gelation process can be divided in several stages. For each of them, somewhat different models of the acoustic wave propagation give the best simulation. These stages correspond to the stages of the cluster nucleation and the particles aggregation presented in Sec. 2 of this work.

There are no sharp limits between the ranges of evolution where the acoustic model fits best, except the rapid change of the system at the gelation point. The models simulate the behaviour of the propagation velocities and the attenuation of acoustic waves. The generation of acoustic emission was beyond the scope of the present investigations.

The main problem is the dependence of the parameters of the acoustic wave propagation on the elastic or visco-elastic moduli of the two-phase network in the sol-gel system.

The following consecutive models are taken into account.

4.1. A fluid with very low concentration of suspensions

This case corresponds to an initial state of the sol with few suspended particles (nuclei) per volume unit of very small size (compared with the acoustic wave length). The system can be considered to be homogeneous; if is a liquid phase with a volume elasticity (bulk elasticity modulus) K and the viscosity η related to the imaginary part G'' of the shear modulus G^*. The imaginary part of the modulus, K^*, which corresponds to the volume viscosity, K'', and the real part of the shear modulus related to the shape stiffness can be omitted. The system has the same parameters as a pure liquid not affected by the suspension. The usual classical model of a homogeneous fluid is valid.

4.2. A fluid with the increasing concentration of suspensions

The system becomes a two phase system, its viscosity depends on the number and size of particles according to the Einstein formula. The formula is applicable for a uniform concentration and size of particles when the volume concentration is less then 0.1. When the formation of the surface fractal structure of the clusters takes place, this process can be expressed in the acoustic model by assuming a change in the size and density of the particles, as already shown.

The main feature of the system at this stage is that the vibrations of the particles are independent from each other, and there is no mutual interaction between the particles.

The system may be simulated by the line of the independent Maxwell elements (Fig. 2).
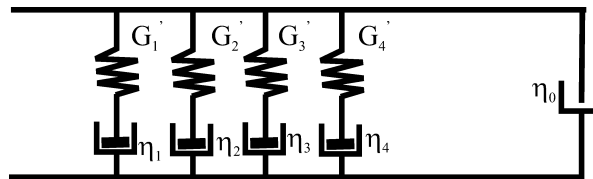
Fig. 2. The line of the independent Maxwell elements, as a model of a fluid with concentration of suspensions less than 0.1.

Each element has its own relaxation time with a random spectral distribution, however the previous, still valid, assumption of a uniform size of the particles suggest that the distribution has a distinct maximum. The shear modulus is treated here as a complex number, $G^* = G' + jG''$, and the system viscosity is $\eta = G''/\omega$, but its real part G' is still not significant.

The bulk viscosity K'' and the scattering of the longitudinal wave on the suspended particles can be neglected. The system should be analyzed as a inhomogeneous visco-elastic liquid.

4.3. The beginning of the interaction between particles

When the concentration of the suspension increases, the appearance of the mutual links is caused by changes of the particles structure. They are no longer uniform balls

but mass fractals of very complicated shape connected by chemical bonds. An exact theoretical evaluation of the scattering and attenuation of an acoustic wave is impossible in this case, however acoustic measurements provide valuable information about changes in the behaviour of the whole system. The interaction of the particles can be presented by an acoustic model which consist of a chain of coupled Maxwell elements, i.e. the so-called "ladder" model (Fig. 3) equivalent to a delay-line model used in electronics. Due to the interacting particles, the discrete spectrum of relaxation times (DRS) is an ordered one, in contrast to the random spectrum as in the previous stage. The links between the particles (clusters) has still a large compliance, nevertheless the shear modulus should be count as a complex number, $G^* = G' + jG''$, and the measurements of velocity and attenuation of the shear wave are relevant for the evaluation of the viscosity. The system is a two-phase system but the solid state phase is not yet stiff enough to be treated as a solid framework, rather the presentation as a visco-elastic-liquid with the "bounded" mass fractals is more correct. The scattering of the longitudinal wave on the clusters is now perceptible. The general theory of the acoustic wave scattering is applicable. The particle is considered to be an inclusion of defined cross-section. The calculation of the size and number of the cross-sections as complex units enable the evaluation of the attenuation and dispersion of the acoustic wave.
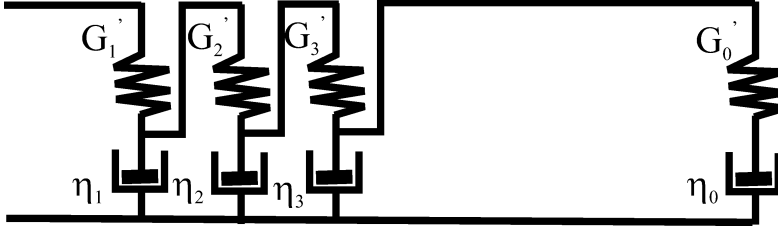
Fig. 3. The chain of coupled Maxwell elements, i.e. the "ladder" model of a fluid with interacting clusters of a mass fractal structure.

4.4. Increase of the bonds stiffness between the clusters

The two-phase system is now similar to a solid elastic space framework plunged in the liquid. The large number of the relaxation times τ, has a statistical distribution H_τ, and the resultant viscosity can be evaluated from the formula

$$(5) \qquad \eta = \int\limits_0^\infty H_\tau(\ln \tau).$$

To take into account both the solid state and fluid parameters of the system, an acoustic model similar to that of Mervin seems to be most convenient (Fig. 4).

The model can be applied to transverse (shear) waves and to longitudinal ones. For this reason, it can be considered, assuming certain simplifications, as the joint Maxwell–Voigt model (Burgers model).
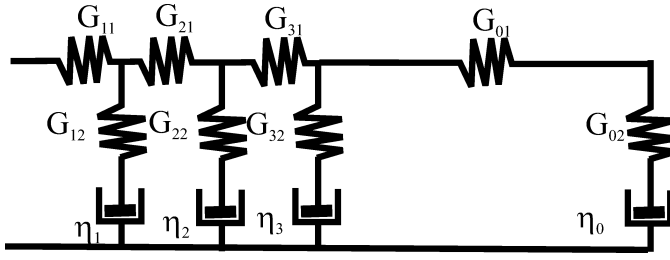
Fig. 4. The chain of Burgers elements; the completed Mervin model of the solid elastic network planged in a fluid.

4.5. The rigid porous structure saturated by the fluid

This case corresponds to the system after crossing the gelation point. The pores of the solid structure are partially open; thus the flow of the fluid is possible. The previous one-dimension models are not applicable, because it is necessary to analyze three dimensional tensoral fields of stress and strain. The approach, presented first by Biot completed by Willis, is used as the basis of the following investigation. The idea consist in a stepwise consideration of the quasistatic and dynamical system treated first as a purely elastic one and than as a viscoelastic one.

The quasistatic case. When the system is treated as a homogeneous two-phase one, its elastic properties are determined by four constants: λ and μ — the Lamé coefficients, B — the penetration volume coefficient defined as the pressure required to force a certain volume of the fluid into the porous structure while the total volume remain constant. Q — the coefficient characterizing the coupling between the volume change of the solid and that of the fluid. The second Lamé constant, μ, is equivalent to the shear modulus G, but for the description of the continuous medium it is more convenient.

An important parameter is also the porosity. The mass porosity β is defined by the formula

$$\rho_1 = (1 - \beta)\rho_s \,, \qquad \rho_2 = \beta\rho_f \,, \qquad \rho = \rho_1 + \rho_2 \,, \tag{6}$$

where ρ_s — solids state density, ρ_f — fluid density, ρ_1 and ρ_2 the solid and fluid parts of the resultant density of the system ρ, respectively.

The dynamic case. The system parameters are evaluated when an acceleration of the system as a whole occurs. In general case, when the mobilities of the solid and fluid are different, the corresponding displacements are u_s and u_f. This is caused by the additional force, F, caused by the flow resistance of the fluid through the solid framework

$$F = \rho_{12} \frac{\partial^2 u}{\partial t^2} \,, \tag{7}$$

when $u = u_f - u_s$.

The factor ρ_{12} corresponds to the apparent additional density (with positive of negative sign) of the parts ρ_{11} and ρ_{22} of the resultant density ρ; this means:

$$\rho_{11} = \rho_1 + \rho_{12} \qquad \text{and} \qquad \rho_{22} = \rho_2 + \rho_{12} \,. \tag{8}$$

The substitutional dynamic moduli of the system can be calculated by usual method of the theory of elasticity.

Acoustic wave propagation in the lossless system. The velocity of the acoustic wave propagation is calculated from the dynamic parameters of the system described above. The shear waves excite the rotational acoustic fields in the coupled fluid and solid; the apparent density of the system is smaller than in the quastistatic case. The velocity of the transverse (shear) wave is equal to

$$c_T^2 = \frac{\mu}{\rho_{11}} \left(\frac{1}{1 - \dfrac{\rho_{12}^2}{\rho_{11}\rho_{12}}} \right). \tag{9}$$

The dilatational wave can be described approximately as a longitudinal plane wave propagating in the x-direction. It is convenient to introduce a reference velocity c_{0L}, calculated for the dilatational wave in the system when the so-called "dynamic compatibility" is fulfiled, and the mutual solid-fluid displacements are equal to zero

$$c_{0L} = \frac{\lambda + 2\mu + B + 2Q}{\rho} . \tag{10}$$

In the general case, the bulk dilatations of the solid, ε_s, and of the fluid, ε_f, are different for the longitudinal wave

$$\varepsilon_s = C_s \exp(kx + \omega t) \qquad \text{and} \qquad \varepsilon_f = C_f \exp(kx + \omega t). \tag{11}$$

The expression for the wave velocity should fulfil the usual equations of motion for a solid and fluid. This condition yield to the complicated second order equation for the variable

$$w = \left(\frac{c_{0L}}{c_L} \right)^2.$$

The two roots of this equation define the two dilatation waves having the different velocities

$$c_{1L} = w_1^{-1/2} c_{0L} \qquad \text{and} \qquad c_{2L} = w_2^{-1/2} c_{0L} . \tag{12}$$

The terms of the high-velocity or first kind wave for c_{1L} and the low-velocity or second kind wave for c_{2L} are admitted.

Acoustic wave propagation in the visco-elastic system. The energy dissipation depend only on the relative motion of the solid framework in relation to the saturated fluid and can be expressed by the formula

$$D = b(v_f^2 - v_s^2). \tag{13}$$

The coefficient b is a measure of the degree of viscosity of the system and has the value

$$b = \frac{\eta \beta^2}{q} , \tag{14}$$

where η — viscosity of the fluid, β — mass porosity of the solid framework, q — the coefficient of permeability.

It is worth introducing several reference values and to express the acoustic wave parameters as relative magnitudes.

a) For the shear wave the reference velocity

$$c_{0T}^2 = \frac{\mu}{\rho} \qquad (15)$$

corresponds to the condition $v_f = v_s$.

b) The reference frequency of the acoustic sinusoidal wave corresponds to the coefficient b

$$f_c = \frac{b}{2\pi\rho} \, . \qquad (16)$$

c) The reference attenuation coefficient results from the preceding quantities

$$\alpha_{0T} = \frac{2\pi f_c}{c_{0T}} \, . \qquad (17)$$

For given values of the reference velocity and the reference frequency, the numerical solution of the complicated theoretical formula are calculated by M.A. Biot. It enables the evaluation of the frequency dependence of the shear wave velocity. The attenuation coefficient for this wave versus frequency is equal approximately to

$$\frac{\alpha_T}{\alpha_{0T}} = \frac{1}{2}(\rho_{22} + \rho_{12}) \left(\frac{f}{f_0}\right)^2 . \qquad (18)$$

However, the assumed here exponent is for some systems less than 2.

For the dilatational wave, a similar method can be applied. The reference velocity is the same as for the lossless system, c_{0L}, the reference frequency is equal to f_0, and the reference attenuation coefficient

$$\alpha_{0L} = \frac{2\pi f_0}{c_{0L}} \, . \qquad (19)$$

However, the problem is much more complicated, because the two kinds of waves have different frequency dependences and the variable w in the second order equation of motion has roots with the complex magnitudes for the second kind wave; the attenuation coefficient and propagation velocity are both proportional to the factor $(f/f_0)^{1/2}$. For the wave of the first kind the attenuation coefficient is, similarly as for the shear wave, proportional to $(f/f_0)^2$, but the reduced velocity is proportional to the term $\left[1 - A(f/f_0)^2\right]$, while the factor A can be either positive or negative.

The present theoretical investigation serves for the evaluation of the general behaviour of the acoustic wave propagation during the consecutive stages of the gelation process. An exact quantitative evaluation of the velocity and attenuation of those waves (usually ultrasonic waves) can be achieved only by experiment.

Acknowledgement

References

[1] C.J. Brinker and G.W. Schere, *Sol-gel science*, Academic Press, New York 1990.

[2] *Chemical processing of ceramics*, B.J. Lee, E.J.A. Pope [Eds.], New York 1994.

[3] D. Stauffer, *Gelierungstheorie — Versäumte Zusammenarbeit von Physik und Chemie*, Ber. Bunsenges. Phys. Chem., **102**, 1672–1678 (1998).

[4] Farady Discussions-Gels, **101** (1995).

[5] J. Ranachowski and T. Łaś, *Non-destructive testing of some dielectric solids materials* [in Polish], [in:] The Present Problems of the High Voltage Technology, PWN, Warszawa 1965, 365–397.

[6] J. Ferguson and Kembłowski, *Applied rheology of fluids*, MARCUS, Łódź 1995.

[7] R. De Boer and W. Ehlery, *A historical review of the formulation of porous medies theories*, Acta Mech., **74**, 1–8 (1998).

[8] M.A. Biot, *Theory of propagation of elastic waves in a fluid-saturated porous solid*, J. Acoust. Soc. Am., **28**, 168–191 (1956).

[9] M.A. Biot and D.G. Willis, *The elastic coefficients of the theory of consolidation*, J. Appl. Mech., **24**, 594–601 (1957).

[10] W. Phillipoff, *Relaxations in polymer solutions. Liquids and gels*, Physical Acoustics, P. Mason [Ed.], New York, Vol. II, part B (1965), 1–90.

[11] R.S. Marvin and H. Oeser, *Distribution of relaxation times*, J. Research Nat. Bur. Standards, **B66**, 171–177 (1962).

[12] J. Lewandowski, *Acoustic and effective material parameters of heterogeneous viscoelastic bodies*, Acta Mech., **57**, 143–158 (1985).

[13] J. Lewandowski, *Acoustic and dynamic properties of two-phase media with non-spherical inclusions*, Ultrasonics, **33**, 61–68 (1995).

[14] J.J. McCoy, *A theory of stress wave propagation through inhomogeneous solids*, J. Appl. Mech., **44**, 462–471 (1977).

[15] I. Malecki and J. Ranachowski, *The acoustic cross-section method for evaluation of porous material parameters*, Bull. Pol. Ac. Sci., Ser. Tech. Sci., **45**, 43–56 (1997).

[16] P.R. Williams and R.L. Williams, *Rheometrical aspects of the viscoelastic dispersion of shear waves in gel-like mechanical network*, J. Non-Newtonian Fluid Mech., **78**, 203–225 (1998).

ACOUSTIC EMISSION OF THE BRIGGS–RAUSCHER OSCILLATORY REACTION: EFFECT OF STIRRING

J. RZESZOTARSKA

Department of Chemistry, University of Warsaw
(02-093 Warszawa, ul. Pasteura 1, Poland)

F.R. REJMUND

Polish Academy of Sciences
Institute of Fundamental Technological Research
(00-049 Warszawa, Świętokrzyska 21, Poland)

The acoustic emission method has been applied to the investigation of the dependence of the oxygen release in the Briggs-Rauscher oscillatory reaction on the rate of stirring. The oxygen distribution does not increase toward a limiting value but achieves a maximum and decreases afterwards. There exists a low stirring rate at which the release of oxygen from the solution proceeds in the form of "fountains". This can be observed before the disappearance of the iodine oscillations. The results obtained by the acoustic emission method can be useful in the description of the unknown mechanism of the Briggs-Rauscher reaction.

1. Introduction

Regular periodic reactions and reactions showing a very complicated and chaotic progress occur first of all in systems being far away from the equilibrium state; irreversible physicochemical processes take place during those reactions. Until quite lately, only processes in that the reactants change monotonically towards equilibrium quantities in a closed system have been investigated. However already in 1921, Bray discovered the phenomenon of the periodic release of iodine and oxygen during the decomposition of hydrogen peroxide in the presence of iodate as catalytic agent [1]. These processes could not be described by the mechanisms accepted at that time in chemical kinetics. The oscillatory oxidation of organic acid by bromate in the presence of cerium ions, discovered by Bielusov-Zhabotynski, has aroused a growing interest in oscillatory reactions and other non-linear phenomena of irreversible processes. The main stimulus for the development of chemical kinetics was the need to explain periodic biological processes caused by chemical reactions, e.g. the enzymatic catalysis of redox reactions occurring in living

organisms or the oscillatory course of the glykolysis (which is one of the most important metabolic processes).

The oscillatory Briggs-Rauscher process (BR), known also as the "iodine clock", is a coupling of Bray-Liebhafsky oscillators (BH) and the well-konwn Bielusov-Zhabotynski oscillator (BZh) $[2-6]$. The substrates of the BR reaction are potassium iodate, KJO_3, hydrogen peroxide, H_2O_2, a manganese (II) salt, $MnSO_4$, malonic acid, $CH_2(COO)_2$, and sulphuric acid, H_2SO_4. The number of oscillations of the concentrations of iodine and iodide ions, and of the accompanying oscillations of oxygen release, depends on the initial concentrations of the reactants, the reactor type, temperature and on the rate of stirring of the reaction system. Both the oscillation processes are mutually phase shifted. [6]. The reaction mechanism is very complex and has been cleared only to a small extent. The main global reactions may be written:

$$2\,IO_3^- + 5\,H_2O_2 + 2\,H^+ \;\rightarrow\; I_2 + 5\,O_2 + 6\,H_2O_2\,,$$

$$2\,H_2O_2 \;\rightarrow\; 2\,H_2O + O_2\,.$$
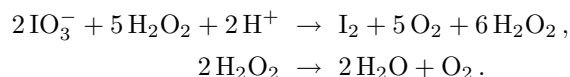
The mechanism includes a large number of elementary reactions, among them being radical reactions (autocatalytic production of HJO_3) and non-radical ones (iodation of the malonic acid). From the viewpoint of the problems discussed in this paper, the most important process is the velocity of transfer of oxygen from the solution to the atmosphere:

$$O_{2(aq)} \leftrightarrow O_{2(g)}\,.$$
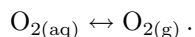
This is why the kinetics of this reaction depends on stirring.

Stirring is a very complicated phenomenon occurring in the time and space scales. The space aspect of macroscopic stirring consists in the superimposing of flows of different initial reactant streams leading to a homogeneous system. In the micro-scale, imperfect mixing causes the formation of local swirls with small gradients of the reactant concentrations in the elementary flux. The initiation time and the spot of vortex peculiarities in the space are difficult to predict, however their occurrence is the source of extreme processes of different dynamic runs. Among other things, this is the reason why a standardization of the mixing process would be very much needed. It should be stressed that not homogeneity but heterogeneity is the normal phenomenon in biology and inanimate nature (geologic processes). The effect of mixing in non-linear reaction systems, particularly in the BZh reaction, is the subject of frequent studies. A decrease in stirring causes increasing in the heterogeneity of the reaction system and, because of the increasing non-linearity, the occurrence of new phenomena such as reaction clocks and homogeneous chaos. Thus, the mixing rate is an example of a parameter of bifurcation in non-linear reaction systems. In the BR reaction, the transport of the gas released in the solution to the atmosphere depends first of all on the stirring rate. For a given reaction system, there exists a rate at that the thin superficial liquid layer can be neglected; the transport of the gas from the solution occurs immediately and without any drag [9]. If, however, the mixing is very slow, the liquid flows are laminar and supersaturated gas solutions are likely to appear. Consequently, the nucleation of gas bubbles becomes spontaneous; the bubbles increase very quickly and are emitted to the atmosphere in an

explosive way. Those phenomena are visually attractive and because of their periodicity the name *fountain effect* is rather justified [10].

In this work, the time of gas release in the BR reaction was studied at different stirring rates. Oscillatory processes in chemical systems are measured mainly by potentiometric methods. In our opinion, the acoustic emission method seems to be reliable for the study of the gas release in chemical reactions [11, 12]. In the literature, there exists only one paper dealing with the application of acoustic emission, namely for the study of the oscillatory Bray reaction [13].

2. Experiment

Reactants: analytically pure potassium iodate (V), KIO_3, malonic acid, $CH_2(COOH)_2$, manganese sulphate (II), $MnSO_4$, sulphuric acid, H_2SO_4 and hydrogen peroxide, H_2O_2 have been used without further purification. The stock solutions have been prepared using redistilled water. The amounts of solutions purred in a cylindrical vessel have been chosen so as to obtain the following concentrations: $[KIO_3]_o = 0.067$; $[CH_2(COOH)_2]_o = 0.050$; $[MnSO_4]_o = 6.7 \times 10^{-3}$; $[H_2SO_4]_o = 0.026$; $[H_2O_2]_o = 1.200$ mol/l. The final volume of the solutions studied was 50 ml. The $MnSO_4$ solution was added at the end. The solutions were stirred using a mechanical stirrer with 20×10 mm paddles. The minimum and maximum mixing rates were 50 and 2500 r.p.m., respectively.

The parameters of the acoustic emission (rate of counting, RMS values) were registered by a measuring set shown in Fig. 1.
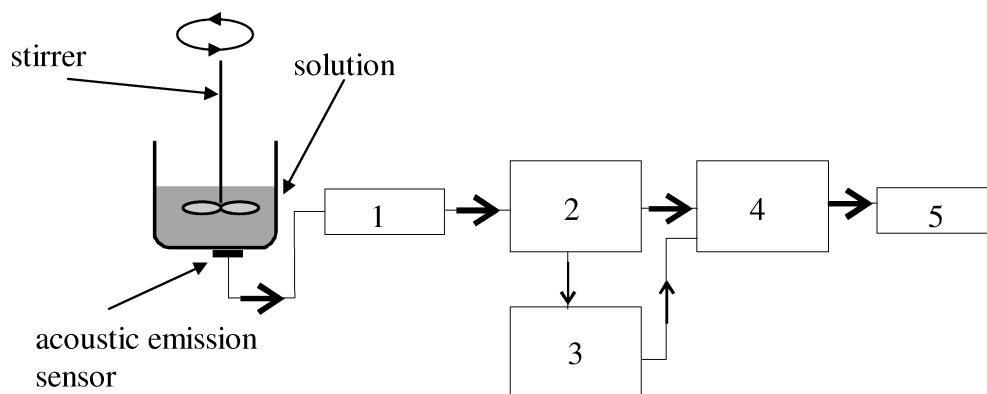
Fig. 1. Diagram of the measuring set: 1 — pre-amplifier, 2 — AE analyser of DEMA type, 3 — oscilloscope with memory of IWATSU OS-6612C type, 4 — computer, 5 — printer.

The counting rate and RMS values were registered at a time base of 0.1 s with the exception of the stirring process for which the values were collected in 1-second intervals. The single signals for the frequency analysis were registered by a digital oscilloscope of IWATSU OS-6612C type. The Fourier analysis of those signals was performed in the frequency range $0 \div 500$ kHz.

sensitivity [dB]
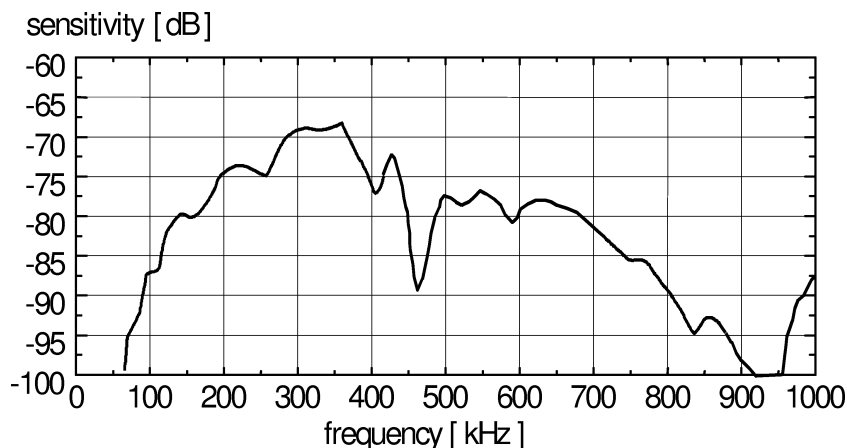
Fig. 2. Frequency characteristic of the broad-band transducer, type NANO-30, produced by PAC.

Mean spectra of a few or a few dozen of acoustic emission signals taken from selected time intervals of the BR reaction at room temperature have been put to the tests. The broad-band PZT transducer from the PAC company (Fig. 2) was attached to the outside of vessel bottom. The amplification and the discrimination threshold of the AE analyser and oscilloscope were the same for all the specimens.

3. Results and discussion

The periodic variations of the iodine concentration, observed by change of the color of the solution, start immediately after the addition of $KMnO_4$. The colorless solution becomes yellow-tawny and then again colorless. The color change cycle was repeated sixteen times and lasted for about 200 s. At the same time gases have been liberated, mainly oxygen. The oxygen release has become most intensive after the termination of the iodine oscillations. The complete characteristics of the acoustic emission are different depending on the stirring rate (Fig. 3). In a very narrow range of the stirring rates, oxygen is released in the form of periodic fountain-like explosions (Fig. 3B).

The rate of the AE countings in a range selected from the course shown in Fig. 3B, in that a fountain-like oxygen emission occurs, is shown in Fig. 4. Beside the five oscillating explosions lasting for about 54 s, a distinct splitting of the maxima is observed. The latter is probably due to the fact that the counting rate base is 0.1 s and the liberation of unit volumes of oxygen from the solution is not synchronised with the stirring rate (ca. 1 r.p.m.).

This result shows that the AE method is suitable for the monitoring of the dynamics of the gas release from solutions.

The dynamics of the gas release during the iodine oscillations, i.e. during the first 200 s, characterised by the RMS values, shows a monotonic AE energy increase and the rate of the energy increase depends on the stirring rate (Fig. 5). Furrow and Noyes, measuring the oxygen volume by a thermostatic burette joined to the reaction solution [14],
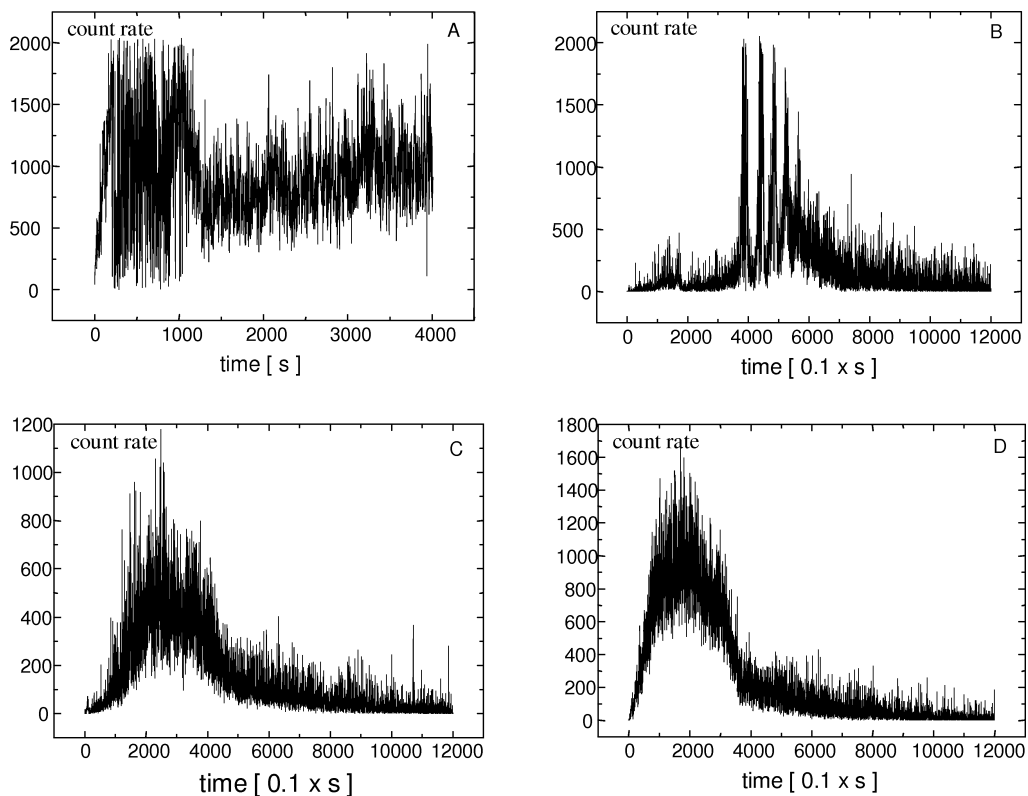
Fig. 3. Dynamic of the oxygen release in the BR reaction for different stirring rates: A — without stirring, B — 50 r.p.m., C — 800 r.p.m., D — 1500 r.p.m.
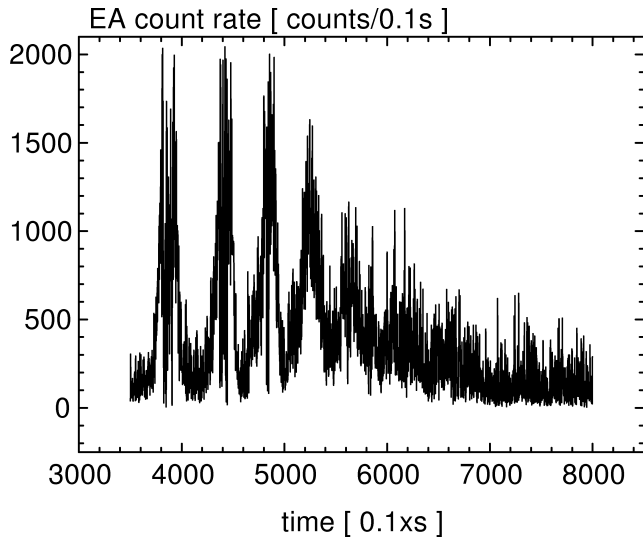
Fig. 4. Rate of AE countings during the fountain-like release of oxygen (as in Fig. 3B).
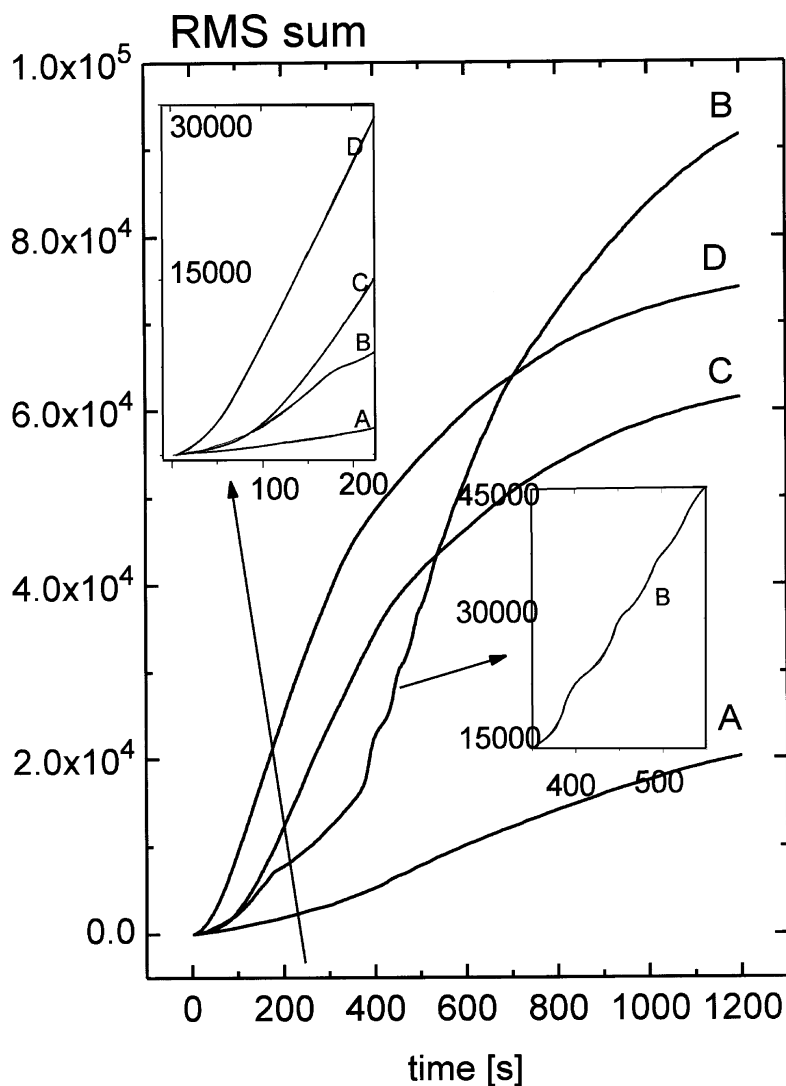
Fig. 5. Dependence of the AE energy on time during the BR reaction at different mixing rates.

observed a non-oscillating oxygen release in the BR reaction. Assuming the hypothesis of a monotonic increase in the oxygen release, the values due to the monotonic increase have been separated form the real RMS values; in this way the AE course, probably characterising the dynamics of the process of iodine oscillations, have been obtained (Fig. 6).

The averaged spectra of a dozen of single AE signals collected from different time intervals of the BR reaction were similar. In all the studied reactions, there appears a 100 kHz wide band in the frequency range $200 \div 350$ kHz (Fig. 7). The spectra are probably connected with perturbations of the solution surface caused by the gas emission.
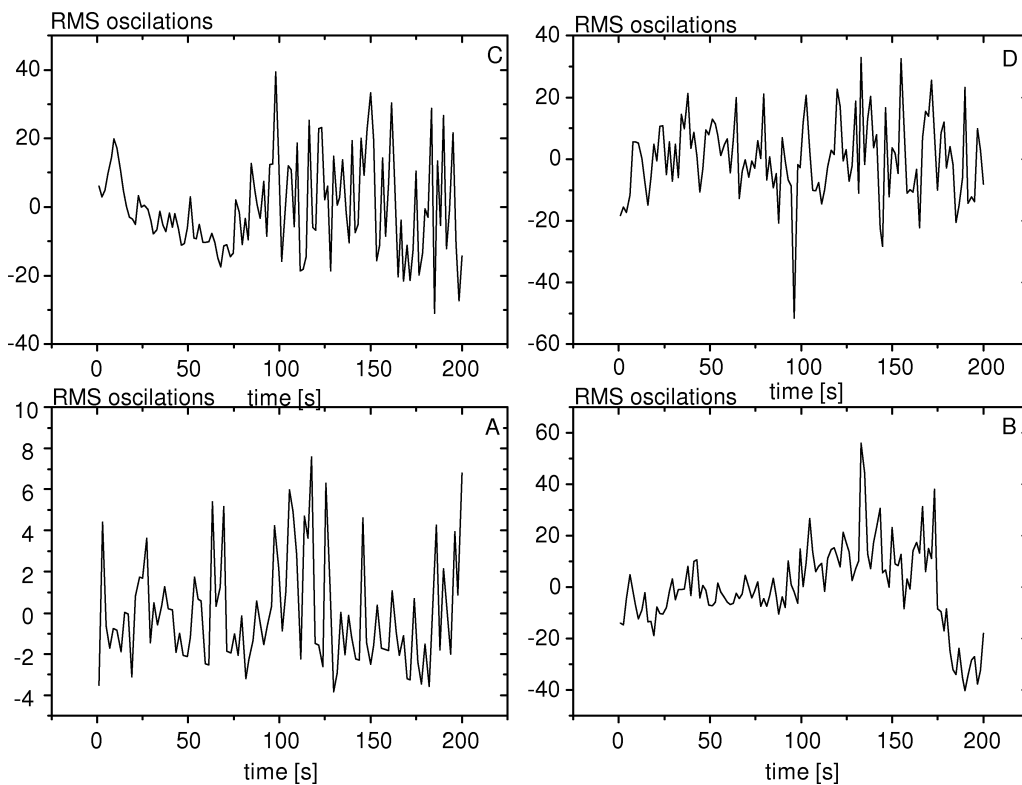
Fig. 6. Dynamics of the BR reaction during the $[I_2]/[I^-]$ oscillations (details are given in the text).
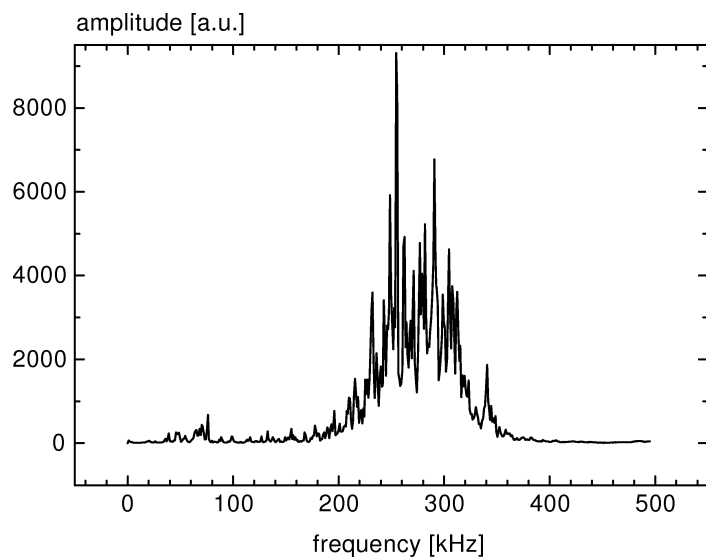
Fig. 7. Averaged spectra of 30 AE signals from the second maximum of the fountain effect (Fig. 4).

4. Conclusions

• In the BR reaction, the stirring affects the dynamics of oxygen release significantly in both the qualitative and quantitative senses. The dependencies of the RMS oscillations and AE counting rates increase with time and achieve maximum values the sooner the more intensive is the stirring (Fig. 3C and 3D). Stirring rates up to 50 r.p.m. cause a very intensive fountain effect in the oxygen emission.

• During the oscillations of the iodine concentration, the AE energy increases monotonically with time. It should be stressed that at this reaction stage, beside oxygen, also iodine is educed and the mixing rate does not affect the quantity of the observed $[I_2]/[I^-]$ oscillations. However, the analysis of the RMS courses after the subtraction of the monotonic component of the increase, shows a dependence of the RMS amplitude on the stirring rate (Fig. 6).

• The investigations of the effect of stirring on the reaction dynamics seem to be helpful in the determination of the mechanism of the BR reaction and in the modelling of the influence of hydrodynamic effects on the kinetics of complex chemical reactions. The attempts at the connection of the hydrodynamic and chemical models in non-linear chemical reaction systems were initiated by DUTTA and MENZINGER [15]; they observed an effect of the manner and rate of stirring on the bistability of the hysteresis of the $BrO_3^-/Br^-/Ce^{+3}$ system. According to Epstein, if the stirring in autocatalytic biological and chemical systems is non-ideal in time and space, the consequence are extreme variations in the dynamics of those systems [16].

• The authors of this paper have for the first time observed that gas evolution oscillators involve nucleation, growth and escape of bubbles from the supersaturated solution in the Briggs-Rauscher reaction.

References

[1] W.C. BRAY, *A periodic reaction in homogeneous solution and its relation to catalysis*, J. Am. Chem. Soc., **43**, 1262–1267 (1921).

[2] T.S. BRIGGS and W.C. RAUSCHER, *An oscillating iodine clock*, J. Chem. Educ., **50**, 496 (1973).

[3] D.A. FRANZ, F. FEURGUSON and E. BOSCHMANN, *Superoxide dismutase and the Briggs-Rauscher reaction*, J. Chem. Educ., **68**, 57 (1991).

[4] A.L. KAWCZYNSKI, *Reakcje chemiczne — od rŭwnowagi przez struktury dyssypatywne do chaosu*, WNT, Warszawa 1990.

[5] M. ORLIK, *Reakcje oscylacyjne — porzadek i chaos*, WNT, Warszawa 1996.

[6] O. GUREL and D. GUREL, *Types of oscillations in chemical reactions*, Academic Vlg., Berlin 1984.

[7] A.K. DUTT and S.C. MÜLLER, *Effect of stirring and temperature on the Belousov-Zhabotinsky reaction in a CSTR*, J. Phys. Chem., **97**, 10059–10063 (1993).

[8] P. STRIZHAK and M. MENZINGER, *Stirring effect on the bistability of the Belousov-Zhabotinsky reaction in a CSTR*, J. Phys. Chem., **100**, 19182–19186 (1996).

[9] R.M. NOYES, M.B. RUBIN and P.G. BOWERS, *An alternative model for transport of molecules between gas and solution*, J. Phys. Chem., **96**, 1000–1005 (1992).

[10] E.H. WHITE, *An efficient chemiluminescent system and chemiluminescent clock reaction*, J. Chem. Educ., **34**, 275–276 (1957).

[11] J. RZESZOTARSKA, *Application of acoustic emission as a method of quantitative chemical analysis*, Acoustics Letters, **17**, 151–155 (1994).

[12] J. RZESZOTARSKA, F. REJMUND and P. RANACHOWSKI, *Acoustic emission probes of foam drainage processes in* H_2O-C_2H_5OH-*air systems with content of detergent triton X-100*, Proc. Int. Symp. on Hydroacoustics, Jurata, 12-16 maj 1997.

[13] D. BETTERIDGE, M.T. JOSLIN and T. LILLEY, *Acoustic emissions from chemical reactions*, Anal. Chem., **53**, 1064–1073 (1981).

[14] S.D. FURROW and R.M. NOYES, *The oscillatory Briggs-Rauscher reaction*, J. Am. Chem. Soc., **104**, 38–42 (1982).

[15] A.K. DUTT and M. MENZINGER, *Effect of mixing mode and stirring rate on the bistability of the* BrO_3^-/Br^-/Ce^{3+} *system*, J. Phys. Chem., **95**, 3429–3432 (1991).

[16] I.R. EPSTEIN, *The consequences of imperfect mixing in autocatalytic chemical and biological systems*, Nature, **374**, 321–327 (1995).

SCIENTIFIC AND ENGINEERING PROBLEMS FACING POLISH ACOUSTICIANS FIFTY YEARS AGO

I. MALECKI

Polish Academy of Sciences
Institute of Fundamental Technological Research
(00-049 Warszawa, Świętokrzyska 21, Poland)

1. Introduction

After the II World War's of awful destruction of the whole country, material goods, and its population, but in the same time the common will of the nation to rebuild the ruins, to develope the home industry and to assure acceptable conditions for every-day life created the unique historical chance to undertake the huge engineering and technological tasks. The polish acousticians played a modest nevertheless significant role in the solution of the problems related with the realization of these tasks.

Polish acoustics has the tradition of the research activities since the beginning of the thirties, mainly in the field of the architectural and physiological acoustics.

During the occupation time the polish acoustics suffered the hard loss a number of acousticians did not survived or emigrated abroad, however some theoretical research was pursued. An important fact for the future was that the lectures related with acoustics and electroacoustics were continued at the electrotechnique and architecture faculties of the underground Warsaw Technical University.

In spite of everything, just after the war several young acousticians supported by the students of the newly founded or old universities were able to participate in the national efforts of rebuilding the ruins. First off all they continued to carry on the intensive efforts required of acoustics concerning the definite solutions of the key engineerings problems to be taken into account by engineers, planners, economists and the local and central authorities.

To fulfill this role of the advisers the home scientific research in the field of acoustics had to be initiated and developed, as the essential basis for the adequate treatment of the engineering problems, all the more that the west-european and american experiences e.g. in building acoustics were not fully applicable for the specific local conditions.

Four engineering problems closely related with acoustics were of crucial importance for the rebuilding of the country fifty years ago:

1) town planning,
2) dwelling houses construction,
3) public halls design,
4) noise control in industry.

2. Town planning

The cooperation of acousticians with the region and cities planners and architects was mostly related with the following objects:

1. On the global country scale — the location of newly founded large industrial centers, the foundation of new or drastic changes of the existing cities sizes and importance, the conception of the basic infrastructure principally the planning of the high-ways.

2. Inside the cities — the mutual situations of the noisy objects like the industrial plants, of heavy traffic routes and the places where relative silence is required like hospitals or universities. The protection of quiet areas e.g. parks for citizens to relax.

3. The architectural plan of the living quarters including the fixing of distances between houses and the number of its stores, the localization of streets and places of public interest.

From the point of view of acoustics, town planning is mainly related to the research of the out-doors sound waves propagation. The studies taught soon after the war included the following themes:

1) the attenuation and deflection of sound wave propagation over ground caused by strips of vegetation and screens,

2) the calculation of minimal admissible distance from the sound source as function of the source parameters and the acceptable noise level,

3) the dependence of large distance sound wave propagation from wind direction,

4) the first stage of the systematic measurements of the "acoustic atmosphere" of large cities (Warsaw) and the preparation of the "acoustic maps" of noisy streets.

To formulate the advise concerning town planning it was necessary to dispose the reference point namely, admissible noise level this general question will be discussed at the end of this paper.

The chance to influence the planners decisions depended on the scope of the projects.

It was not at all possible at global level, from the acoustical point of view, because localization of large industrial centers near the great cities like Cracow and Warsaw had an entirely political character and the directions of the principal high-ways had defined by the strategic military reasons. The position of acousticians by the detail town planning e.g. as concern the situation of the hospitals, the universities and the industrial plants of local interests was more favourable. In several cases the close cooperation of the architect and the acoustician was attached first of all in Warsaw and as its outcome the acoustic requirements were complied e.g. for the design of houses stores, number and orientation to the streets.

3. Dwelling houses construction

In consequence of the lack and vital need of flats throughout the whole country cheap and efficient technologies of house building were necessary.

The elaboration and realization of new technologies was the priority task of the civil engineers and the entire building industry. The prefabricated elements production was generally recognized as significantly advance as compared to the traditional brick construction. Later on the thermal low pressure steam technology of concrete production was typical, but after the war the prefabricated elements were first of all used for ceilings as the light hollow blocks. The brick walls were built as thin as possible. Naturally the sound insulation between flats was very poor and complaints from the inhabitants about bad acoustic conditions were common.

In theory the technical solution was very simple, by the application of flotting ceilings or floors and by the construction of thicker walls. However, such proposals were unrealistic from an economic point of view.

The polish acousticians underthought the research to find a possibly cheap and effective way to increase the insulation of the prefabricated elements to air-born sound and impact noise.

Several original theoretical works was done on the vibrations of the plates with different types of perforation and boundary conditions. The fulfillment of block hollows by the sound absorptive material, the vibration damping between the plates and the new construction of ceiling blocks were experimentally investigated.

The efforts of the acousticians to ameliorate noise insulation in dwelling houses gave in general only restricted results, nevertheless in a number of flats, the additional means for noise abatement were applied partly from private founds.

4. Design and construction of halls

During the II World War the majority of theaters, concert halls and cinemas were destroyed. In Warsaw after the uprising in 1944 all the buildings of public interest were completely in ruin.

Just a few months after the end of the war Warsaw was again confirmed as the capital and the restoration of the places important for national culture was generally approved as a priority.

The design of large halls like theaters, concert halls and broadcasting studios the advise and cooperation of the acousticians was indispensable. It was not accidental, that the acoustics of halls or more general architectural acoustics had in this time rather favourable conditions for development.

Part of the research in this field was the continuation and the experimental verification of previous theoretical works.

The scientific research was divided into two main issues

1) the analysis of sound field distribution in an enclosure,

2) the condition for the optimal subjective perception of music and speech.

As usual the three methods of sound field analysis: geometrical, statistical and waves propagation were applied.

In the range of the geometrical method the polish research concerned:

— The interaction of several waves fronts generated by the given spatial distribution of the "virtual" point sound sources.

— The graphical three dimensions sound rays presentation.

— The application of three dimensional light beams models. This last method appeared very efficient for the design of the reflective surfaces in the ceilings of the large halls.

The research in the field of the statistical method were interesting

— The calculation of the sound field inhomogeneities due to the distribution of the sound absorptive area.

— The correction of the usual reverberation time formula by taking into account the difference of absorption capability due to the local sound field intensity.

The wave method improvement was at this time one of the leading subjects of interests in several research units in Europe and the USA and of discussion at the acoustical international meetings.

Polish acousticians participated in these discussions contributing some remarks upon the more precised definitions of notions of clearness, the spatial diffusity, and limit distance.

Another field of research were the properties of sound absorptive materials. The following items were subjects of studies:

— The influence of material porosity degree and structure.

— The calculation of the materials input impedance in the function of the plane wave incidence angle.

— The designs of the bulk absorptive devices having the absorption coefficient larger than one.

For the design of the theaters, concert halls or auditoria the subjective quality of music and speech perception is a decisive factor of appraisal. The polish acousticians were fully conscious of this requirement and the psychoacoustics was one of the field of research.

Already before the war some works related to the subjective feeling of the reverberation time were done. After the war in the time of fast reconstruction of a large number of halls the well known criteria of the optimal reverberation time (e.g. Knudsen) were applied. Nevertheless some own research were undertaken, for instance it was necessary to elaborate the specific method for estimation of the intelligibility of polish speech. In research initiated in the frame of the International Broadcasting Organization (OIR) had as the aim the method for the comparative evaluation of the subjective quality of the broadcasting studies.

The measurements of the reverberation time and the estimation by the large teams of listeners the subjective acoustic quality of the newly built or reconstructed theaters and concert halls also had general value. The comparition of these data with the parameters of the halls internationally recognized as the best was interesting from the scientifical point of view. From my own experience and the relations of my friends it is underlining

the close and friendly cooperation of the architects and acousticians. The reconstruction of the large halls of great importance for the national culture should be recognized as a joint creative achievement of the architect and acoustician for this reason I would like to mention the names of Prof. M. KWIEK (Warsaw Great Theater) and dr W. STRASZEWICZ (Warsaw National Philharmonie and Great Theater in Łódź) sadly both deceased.

5. Noise control in industry

Noise control in industry is an important part of the general problem of labor protection. In principle the assurance of saver conditions of work was one of the key watchwords of the government. However, the necessity of the continuous industrial noise control were rather disregarded. Only the spread of professional diseases (deafness) caused by the long-period of work in noisy conditions has been taken into account by decision-makers.

Nevertheless acousticians tried to act in the two directions: reduction of noise and vibrations at the source and the decrease of average noise level in industrial plants. The first task was related mainly with some proposals of changes of details of machineries, the technological processes or transportation means. For instance the changes of the types of the transmission gears or other design of the transportation pipes for high pressure gas or chemical liquids were elaborated. Some research works were initiated concerning the vibration of moving parts of machines and the generation and reduction of flow-induced noise.

However, the acousticians had few occasions for direct cooperation with design institutions. The proposals for the means of noise and vibrations were often rejected, because its overcomed the obligatory rigid rules and methods of the construction of the industrial equipment and systems.

The position concerning the average noise level control in large production halls was more favourable. Some proposals concerning the placement of sound absorptive materials inside the halls, the elimination of reflecting area on the hall ceilings and the screening of very noisy machines were accepted by the managements of the several (however not numerous) industrial plants. The research related with the properties of sound absorptive materials and sound propagation in the enclosures were useful also for these projects.

6. General problems

To attain the ambitions aims of the polish acoustics fifty years ago some preconditions were indispensable.

To execute or even to formulate the requirements related with noise control, the value of admissible noise level should be defined for several most important cases, namely for trafic noise, out-door of buildings noise, noise inside houses and at the working places. The research into this matter was carried on only in the very restrain range, chiefly directed to the support of some complains e.g. related with the loss of hearing or unpleasant living conditions. For general purposes the ISO standards and experiences of well known

laboratories were admitted as references. However for efficient activity legal confirmation of this requirements was necessary. For this reasons already few years after the war the Polish State Committee for Standards accepted several polish standards for admissible noise levels. Unfortunately the law or by-law on noise abatement at the parlamentary or governmental level was not considered in these years.

Another important condition for the success of acoustics was the capability of acoustic measurements. Here the significant contribution gave the industry connected with the electroacoustic devices production and the universities and research institutes which elaborated the prototypes of the polish sound level-meter.

It is also necessary to stress the role of the international cooperation for the young polish acoustical community. The political situation at this time was of course unfavorable for the official East-West scientific agreements. However, some scientific contacts with the West of Europe based partly on previous personal links were retained. The most important acoustical journals were available, also the participation of polish acousticians in international scientific meetings gradually increased for instance since the second ICA (International Commission onAcoustics) congress in 1953 (Stuttgart) polish acoustians were represented at these congresses and even in the ICA board. To be quite objective it is necessary to underline the significant role of the close cooperation with the acoustical organizations mostly the committees on acoustics of the Academies of Sciences of the countries of the parts communistic blocks.

Finally it is worth stateing that at this time after all the prime duties of the polish acousticians was the teaching of students and the cooperation with engineers, architects, physicians and last but not least with the decision-makers at different levels. We were obliged to accept this priority in spite of pure cognitive scientific research.

In consequence the major part of publications were addressed to the home specialists and practitioners, edited in polish as the books or the papers in professional journals. Of course, the contents of these publications are now obviously out-of-date. But in spite of all this was the significant attainments of the polish acoustical community and it seems just to indicate as references the books publish in polish a few years after the war, a few later editions which include some valuable information about the past are also indicated.

This paper was a different character than the scientific papers usually published in this journal. However, it seems that the position of the polish acoustics interests as being part of world history of the development of acoustics as scientific discipline and as a modest participant in changes in social and cultural conditions after wartime disasters.

References

[1] B. BUKOWSKI, *Sound and building*, Institute of Building Research, Warsaw 1947.

[2] Z. ENGEL, *Environmental protection against vibrations and noise*, Scientific Publishers, Warsaw 1993.

[3] J. KACPROWSKI, *Outline of electroacoustics*, Transports Publisher, Warsaw 1956.

[4] M. KWIEK, *Laboratory acoustics*, Scientific Publisher, Poznań 1968.

[5] I. MALECKI, *Building acoustics*, Technical Publishers, Warsaw 1948.

[6] I. Malecki, *Propagation of sound waves in halls*, Technical University, Gdańsk 1949.

[7] I. Malecki, *Radio and film acoustics*, Technical Publishers, Warsaw 1950.

[8] I. Malecki, W. Straszewicz and W. Kołtoński, *Noise control*, Technical Publishers, Warsaw 1952.

[9] J. Sadowski and L. Wodziński, *Rooms acoustics*, Transports Publisher, Warsaw 1959.

[10] W. Żenczykowski, *Buildings constructions*, Architecture (1952).

[11] Z. Żyszkowski, *Fundations of electroacoustics*, Technical Publishers, Wrocław 1953.

CURRENT TRENDS OF THE WORKS ON ACOUSTICS PRESENTED AT THE XLVI OPEN SEMINAR ON ACOUSTICS OSA'99

R. PANUSZKA and M. IWANIEC

Technical University of Mining and Metallurgy,
Structural Acoustics and Intelligent Materials Group
(30-059 Cracow, al. Mickiewicza 30, Poland)

The XLVI Open Seminar on Acoustics was held in Zakopane from the 14th to the 17th of September 1999. It was organized by Cracow's Section of the Polish Acoustic Society, the Laboratory of Structural Acoustics and Intelligent Materials, the Faculty of Mechanical Engineering and Robotics of the Academy of Mining in Cracow and the Committee on Acoustics of the Polish Academy of Sciences. The number of participants was 175. 118 papers were presented. The honorary president was Prof. Ignacy Malecki. Prof. Zbigniew Engel was chairman of the Scientific Committee and the Organizing Committee was chaired by Prof. Ryszard Panuszka.

The Seminar was opened by the plenary lecture of Prof. Ignacy Malecki devoted to the application of acoustic emission in engineering materials. The examples of new applications presented in his lecture concerned the monitoring of the technology of ceramics, the investigation of variations in the structure and microstructure of those materials caused by thermal shocks and the monitoring of the behaviour of constructions under conditions close to those prevailing during their long term exploitation as well as the analysis of mechanical and thermo-mechanical parameters in that plasticity and pseudoplasticity effects have been considered.

At the beginning of the proceedings in each section a plenary lecture was given. All in all, seven lectures were delivered. Prof. Antoni Jaroszewski discussed the perception effects of an acoustic injury caused by exposure to music sounds with reference to loudness, height discrimination and the frequency and time resolution. Musicians are particularly subject to those injuries. Significant lasting, selective and high-frequency losses in their hearing were found. They indicate that the hearing protection of this group of people is insufficient.

Prof. Eugeniusz Kozaczka focused his lecture on some problems of the non-linear effects connected with the generation and propagation of elastic waves in water, on non-linear properties of a medium as well as on making use of those properties in parametric sources of acoustic waves. Prof. Adam Lipowczan characterized the usefulness of modern

GIS and GPS techniques in the solution of problems connected with the dangers of vibroacoustic effects to the environment. Those techniques, linking computer maps with data bases, offer new research methods and applications to the study of the propagation of noise and mechanical vibrations in the environment.

Dr Henryk Łopacz presented the possibility of the simulation of audio monitoring in physical as well as in virtual rooms. The simulation of audio monitoring conditions is realized by a convolution of pulse response for a given transmission way and the test signal. In the algorithms presented, the influence of room dimensions, the locations of transmitting and receiving points and the attenuating properties of the room can be taken into account. Profesor Stefan Weyna discussed the analysis of measurements of the vector effects of an acoustic wave represented as sound intensity in the acoustic field of real sources. The results presented concerned measurements of acoustic phenomena occurring in the near field and in small limited areas. The application of a broad-band three-way system to the identification and classification of sea fish shoals was presented by Professor Manell Zakharia. The main construction problems of this device concern the transducers, the levels of the transmitted and received signals, the directivity and impedance variations in the whole frequency region. For a correct working of the device, the algorithm of identification of the fish species is also essential. It was shown that neuron nets can be applied to this end. The device discussed is characterized by a high linearity and a better estimation of the fish size. The identification of the fish species is based only on the characteristic frequencies of the received echo.

The plenary lectures presented

Ignacy Malecki, Jerzy Ranachowski, Przemysław Ranachowski: New applications of the acoustic emission (AE) in materials engineering; Antoni Jaroszewski: Perception effects of the acoustic injury caused by the exposure to music sounds; Eugeniusz Kozaczka: Non-linear waves in water; Adam Lipowczan: The perspectives of the application of the GIS and GPS techniques in vibro-acoustic investigations of the environment; Henryk Łopacz: Models of pulse responses of rooms; Stefan Weyna: Application of the intensity method to the vector analysis of the acoustic field of real sources; Manell E. Zakharia: Wideband systems for fisheries, from individual echoes to fish classification at sea.

The acoustics of speech

The focal points of these papers were the problems of determination of speech transmission quality, elimination of disturbances and echoes in loud-speaking devices, the identification of voices masked by the speaker, the perception of amplitude and frequency modulated signals, the creation of an acoustic data base for the Polish language and the analysis of speech of stammering persons. Also, papers pertaining to the analysis of the vowel quotient were presented. Investigations performed on a group of 24 persons have indicated that the vowel quotient is the most important acoustic feature for the determination of the phrase limit. In the Polish language, the lengthening of the terminal part of the phrase concerns mainly the last or the penultimate vowels regardless of whether

they are accented or not; the lengthening effect becomes however more pronounced when those vowels are accented. The problem of the classification of stop consonants analysing the features of segments of variable length. The identification of voiceless implosive consonants, /p/, /t/, /k/, was discussed as well. The classification of sounds was done by neuron networks on the basis of cepstral coefficients obtained from the complete course of a sound; the results have been compared with those calculated on the basis of the short-period Fourier transform at the starting point of the implosion. The investigations performed have shown that there is a small decrease (3.5%) in the recognition of stop consonants when the characteristics of their complete course are used by a simultaneous simplification in the obtaining of those characteristics. The recognition of speakers on the basis of their speech has different applications. Masking of the speech results in a deterioration of the recognition results. There have been discussed experiments aimed at the determination which one of the commonly used speech signal parametration techniques is most resistant to voice masking. The problem of the non-fluent speech was discussed in terms of the variation in the concentration of the breathed out CO_2 by both stammering and fluently speaking persons during different sorts of speaking like reading, talking and talking with echo. For the recognition of consonants in the speech of stammering speakers, a computer visual echo was presented. An echo basing on the recognition of Polish syllabic vowels was shown. Also, the effect of the echo on the duration of sounds in the fluent fragments of speeches of stammering speakers was determined. A significant increase of the duration of vowels as well as consonants is observed. The automatic recognition of sound and speech requires the preparation of a proper base. The progress in the preparation of such a base for the Polish language was reported. The recording platform and elements of the basis was discussed. A measuring set for the objective evaluation of the speech transmission quality in telecommunication channels using loudness indices was presented. A review of subjective methods of such an evaluation was given as well. The Polish normalizations concerning the requirements and measuring methods of the logatomic clarity were discussed. The echo and interference control in terms of psychoacoustics was applied to the quality improvement of loud-speaking devices, particularly to that of cell phones. For the amplitude and frequency modulation of signals, the binaural perception was investigated for modulations of different deepness and frequency deviations.

The following papers were presented:

Krzysztof Bielawski: Psychoacoustics aspects of systems eliminating echoes and interferences in loud-speaking devices; Stefan Brachmański: An objective measurement of the speech transmission quality by the method of loudness indices; Stefan Brachmański: A subjective measurements of the speech transmission quality in telecommunication channels; Grażyna Demenko, Stefan Grocholewski: The acoustic analysis of the consonant quantity; Ewa Łukasik: Classification of stop consonants on the basis of the features of segments of varying length; Wojciech Majewski, Grażyna Mazur Majewska: Speech signal parameters of a voice masked by the speaker; Edward Ozimek, Jacek Konieczny: Binaural deepness of modulation for an AM signal evaluated theoretically and determined exper-

imentally; B. Raczek, B. Adamczyk: Variations of the anoumt of CO_2 exhaled during a fluent and influent speech; Elżbieta Smolka, Beata Fornal: The recognition of vowels in the speech of stammering persons; Piotr Staroniewicz: The detection of interform transitions for the needs of ARM; Piotr Staroniewicz, Jerzy Sadowski: The acoustic data base SpeechDat for the Polish language; Waldemar Suszyński, Wiesława Kuniszyk-Józkowiak, Jolanta Dalczyńska: The impact of the echo on the duration of vowels in the speech of stammering persons; A. Wicher, E. Ozimek: Dichotomic perception of signals of modulated frequency.

Acoustics of music

A statistic method of the evaluation of results of psychoacoustic investigations performed by the method of tuning. The methodology presented allows the proper preparation of a measuring experiment, i.e. the determination of the number of an audio monitoring groups, the number of the repetitions of the measuring task and the verification of the statistical reliability of the results. From the analysis of the acoustic pressure levels generated when playing percussion instruments, a hypothesis was formulated that short increasing times at relatively high peak levels cause specific unpleasant impressions of "ear clogging" by the drummers and can results in their specific hearing losses in a broad frequency range. Also, the sound levels and pulse characteristics of discotheque expositions was investigated from the point of view of the hearing loss hazard to the musicians and the audience.

The following papers were presented:

Elżbieta Aramowska, Piotr Rogowski: The problem of the trial number in psychoacoustic experiments by the tuning method; Antoni Jaroszewski, Anna Jaroszewska: Pulse characteristics of discotheque expositions; Antoni Jaroszewski, Piotr Rogowski, Andrzej Rakowski: Statistical analysis of the acoustic pressure levels when playing percussion instruments during training sessions; Lubomir Rotko: The sound levels of pop music.

Sounds in the environment

The research devoted to the propagation of sounds in the environment include the problems of determination of the sound propagation conditions, the common sound sources and the noises of typical objects, such as buildings, highways, power lines etc. The results of studies on the occurrence frequency of meteorological conditions being conducive to the propagation of the acoustic wave in the environment. Analyzing the data of meteorological stations, the frequency of conditions conducive to the propagation according to ISO, CONCAWE, and the wind component from the source to the receiver, were considered. The general relationships for the total acoustic power radiated by a system of harmonic point sources in a free space and in the presence of reflecting surfaces were given. Methods of forecasting the traffic noise applying numeric techniques

to the estimation of and decreasing of bothersome noise generated by communication routs. The noise of power lines was analysed in order to find relationships to radio and television interference. The analysis of spectra of noise generated by a railway bridge enabled the determination of the contribution arising from the rolling and that arising from the bridge structure. For the evaluation of the acoustic pressure level increase caused by the oscillation of building partitions, a measuring and calculation method, based on two-channel simultaneous measurements of the acoustic pressure level and the speed of the partition oscillations, was proposed. The Method of the Statistic Analysis of Energy was applied to the calculation of the side acoustic insulating power in houses made by the "Thermomur" technology.

The following papers were presented:

Henryk Idczak, Anna Snakowska: The symmetry of the sound sources in relation to the reflecting surface; Gabriel Kubinyi, Jerzy Wiciak: Analysis of the side acoustic insulating power of the "Thermomur" system by the Method of the Statistic Analysis of Energy; Robert Łopusiak: Forecasting of the traffic noise; Marek Niemas: The calculating and measuring method for the determination of the acoustic pressure level increase caused by oscillations of rooms arising from heavy traffic; Edyta Pilat: Acoustic insulation made of the Gullfiber Polska wool; Krzysztof Rudno-Rudziński: Distribution of the frequency of conditions conducive to the sound propagation in different regions of Poland; Krzysztof Rudno-Rudziński: Spectra of sounds generated by a railway bridge; Jerzy Wiciak, Ryszard Panuszka, Gabriel Kubinyi: The choice of a model for the analysis of the side acoustic insulating power of the "Thermomur" system by the application of the Method of the Statistic Analysis of Energy; Tadeusz Wszołek: Vibroacoustic studies of corona effects of wires supplied by a high voltage.

Acoustic Emission

The papers concentrated on the ultrasonic determination of mechanical properties and the thermal resistance of thin layers as well as on the ultrasound absorption in magnetic liquids and the Brillouin scattering in liquids and crystals. Also the influence of technological conditions on the properties of piezoceramics and the modelling of those materials by the method of finite elements were discussed. An acoustic emission method of determining the initial temperature of casting moulds was proposed for alloys that a phase deforms by slip. A method of determination of the total mineralization of water by ultrasonic velocity measurements was presented. Results measurements of ultrasound speed anisotropy and the mechanical properties of piezoelectric materials was presented as well. The results make it possible to determine the distributions of the wave velocities and heterogeneities as well as the static Young's modulus. A modification of technological conditions of the production of ceramics by the method of hot sintering and polarization by an electrostatic field leads to maximum values of the piezoelectric modulus and of the electromechanical coupling coefficients. The application of the acoustic emission for the investigation of small variations in the strength of ceramic materials caused by small

thermal shocks was presented; also, the dependence of the acoustic emission level during bending on a previous thermal shock was discussed. The application of photoacoustic and photothermic impulse methods for the determination of thermal and transport parameters of semiconductors was analysed. The successful tests of designing and optimisation of the properties of ultrasonic transducers by the method of finite elements enables us to avoid the constant constructing and measuring of new physical models of transducers which are expensive and time-consuming. Experimental studies of structural changes of magnetic liquids, due to the formation of clusters, and the variation of the absorption coefficient, depending on the rate of the magnetic filed and temperature variations, were presented. The determination of the thermal resistance of thin layers deposited on a thick basis is possible by an analysis of the crossing of a thermal wave through the sample-base interface. The highest sensitivity is achieved by a thermal fitting of the base to the liquid above the sample. Favourably is also the deposition of the layers under test on possibly thin bases. The application of the matrix calculus was suggested for the description of thermal waves generated by a modulated energy stream. The matrix formulae obtained are a convenient starting point in further calculations of the influence of the particular layers on the distribution of the temperature field in the sample and its environment.

In many papers concerning the acoustic dust removal the problem of electrification of the dust is omitted or its effect on the occurrence of the phenomena is not taken into account. The analysis of electric interactions during the acoustic agglomeration leads to the conclusion that the coagulation time is shortened when the aerosol particles are electrified by opposite charges; in this way the effectiveness of the coagulation process increases.

The following papers were presented:

Małgorzata Bebek, Krzysztof Mitko, Krzysztof Bebek: Determination of the salinity of surface and abyssal waters by acoustic methods; Tomasz Błachowicz, Zygmunt Kleszczewski, Tadeusz Łukasiewicz: Brillouing scattering in the $SrLaGaO_4$ (SLG) and $SrLaAlO_4$ (SLA) single crystals; Jerzy Bodzenta, Jacek Mazur, Bogusław Burak: An analysis of the possibilities of determination of the thermal resistance of thin layers deposited on thick bases by the photothermic method; Henryka Czyż: Electrified particles in the acoustic field; Tomasz Dębowski, Zbigniew Ranachowski: Measurements of the acoustic emission in construction materials exposed to thermal shocks; Julian Dudek, Dariusz Bochenek, Włodzimierz Rogulski, Zygmunt Surowiak: The effect of technological conditions on the properties of the S-1 piezoceramics; A. Józefczak, Mikołaj Łabowski, Andrzej Skumiel: The influence of the rate of magnetic field variations on the coefficient of ultrasonic absorption in a magnetic liquid; Michał Kępiński: Application of neuron networks and analysis of the main components (PCA) to the visualization of multidimensional information exemplified by a pathological speech signal; Leszek Książek, Mikołaj Baszun: Application of the ANSYS package to the analysis of structure oscillations including piezoelectric materials; Waldemar Lis, Roman Salamon, Józef Zielenkiewicz: Statistic investigations of the parameters of acoustic signals emitted by the temple jaw joint; Dariusz Madej, Tomasz Hornowski: Ultrasonic investigations of the

critical benzonitrile-isooctane mixture; Justyna Matachowska, Jan Ilczuk: Determination of the velocity and mechanical anisotropy of the PZT piezoceramics by the ultrasound method; Jacek Mazur, Jerzy Bodzenta: Application of the matrix calculus to the analysis of varying temperature fields in photothermic and photoacoustic experiments; Barbara Pustelny, Zygmunt Kleszczewski, Jerzy Bodzenta: The photoacoustic effect in semiconductors; Leszek Radziszewski: Analysis of laser generated interferences in plastics and the acoustic emission; Zygmunt Surowiak: Piezoelectric electroacoustic transducers of different ferroelectric hardness.

Hydroacoustics

The papers dealing with hydroacoustics concentrate on the influence of meteorological conditions on the propagation of acoustic waves, underwater disturbances caused by swimming objects, determination of geographic positions and detection of targets, identification of the sea beds, construction of hydrolocation aerials and sonars and so on. A hybrid neuro-fuzzy classifier of a multistage structure for the recognition of the sea bottom by acoustic echoes was presented. The results are better than those obtained by a parallel ANFIZ system and it needs a smaller calculation power. A multifrequency classifier with diffuse neuron webs was constructed for the identification of pelagic fish species and the type of sea bed. The classifier is a three-layer artificial neuron web, with a reverse error propagation, in that the knots of the first layer represent the input parameters, the second layer represents diffuse rules and the third one represents the classes. The method of reverse filtration, that makes use of the window decomposition, makes it possible to get a dependence of the coefficient of dispersion from the bottom on the angle of incidence or on the deepness in the sediment.

The precision of the localization of small underwater objects in opaque reservoirs is significant for a quick finding of such objects by scuba divers. The detection of targets by a side sonar with a towed carrier of hydroacoutsic aerials, in relation to the position of ship towing the carrier obtained by the GPS system, was discussed in papers concerning the sources of errors, their minimization by additional systems measuring the deepness of draught and the height of the carrier above the bottom, the linearization of the sonar range and the compensation of the effect of bending of the sound propagation route in the reservoir. For increasing the accuracy of positioning of targets, the methods of formation of multielement hydroacoustic aerials have been applied. The method of electric joining of equal transducers and selection of the surface of those transducers was presented. Both the methods eliminate the construction of multi-channel sending and receiving systems that are necessary in the commonly used method of electronic or numeric weighing. The architecture of the perceptron affects the quality of filtration of the navigation parameters that can be used in the system of detection of underwater objects by the acoustic method. The effect of the number of layers and of neurons in the hidden layers of the Kalman's neuron filter was investigated. A front sonar of a high angle and penetration resolution with a linear sending-receiving transducer of moderate size and a limited number of receiving paths was presented. Another construction presented was a sonar with an arc

cylindrical transducer shaped by the linear method of delaying signals from the particular elements. The immediate obtaining of a complex cylindrical snapshot for the beamformer FFT was presented as well.

The following papers were presented:

Jerzy Dobrzyniecki, Ignacy Gloza: Underwater disturbances caused by the main ship motor; Tran Van Dung, Joanna Maciołowska, Andrzej Stepnowski: Sea bottom recognition using mufti stage neuro-fuzzy classifier operating on multi-frequency data; Andrzej Elminowicz: Front sonar of a high angle and penetration resolution; Grażyna Grelowska, Ignacy Gloza: The effect of variations of the hydrological conditions on the propagation of acoustic waves in the South Baltic Sea; Lech Kilian, Jacek Marszał, Aleksandra Raganowicz: Determination of geographic position of targets by a side sonar; Zbigniew Łubniewski, Marek Moszyński: The inverse filtering methods to the seabed identification problem; Joanna Maciołowska, Andrzej Stepnowski, Tran Van Dung: Neurofuzzy classifier for fish species identification and bottom typing operating in multi- frequency data; Artur Makar: The effect of the preceptron architecture on the filtration quality of the motion parameters of an underwater object; Władyslaw Męciński: Investigations of the properties of echoes from underwater objects from the point of view of increasing the detection ability of a hydrolocation station; Marek Moszyński, Zbigniew Łubniewski: Modelling of scattering using a combined (surface-volume) impulse response; Roman Salamon, A. Eliminowicz, Z. Wojan, W. Lis: Non-electronic methods of shaping the direction characteristics of mufti-element hydroacoustic aerials.

Sound engineering

The papers concerning sound engineering were devoted to the problems of shaping the characteristics of sound sources, to the construction of corrective filters and power amplifiers and their cooperation with switches and loudspeaker sets. The investigations performed enabled the verification of the cepstrum function to the study of the degree of stochasticity of the sound reverberation energy in a room and to the evaluation of the acoustic properties of already existing rooms or those being just designed. A system of active sound reduction in a closed space was presented and the conditions affecting their efficiency were given. A mean reduction level of the acoustic level of 10 to 20 dB was achieved in the frequency range 50 to 250 Hz. The problems of diminishing linear deformations by corrective systems mounted in the signal path in front of the loudspeaker system were presented. In the case of digital switches, the compensation of linear deformations including the individual correction of each of the transducer includes also phase deformations so that the total compensation of the impulse responses of the transducers was closest to the proceeding of the Kronecker's delta. Results of measurements of the directional properties of loudspeaker sets with analogue and digital switches working in both the steady and transition states were presented as well. The results of some investigations proved that an intended change of the directional properties of the sound source can be achieved by controlling the velocity amplitude of the source.

Many papers were devoted to the construction of high-power amplifiers and their cooperation with loudspeaker sets. An example of a computer supported designing of a power bridge amplifier consisting of integrated circuits and discrete power transistors. The application of a computer facilitates the selection of the tolerance and the optimization of the resistor values, the calculation of the power losses of the integrated circuits; it enables also to minimize the coefficient of the content of the harmonics. The effects of the loading of a high-power amplifier by the loudspeaker device, connected with the mechanic resonance of the membrane, was evaluated on the basis of a computer simulation. The danger of a secondary breakdown of power transistors was determined.

The following papers were presented:

Wojciech Ciesielka: The sound synthesis by digital correctors; Paweł Dziechciński: A comparison of the designing of corrective filters; Andrzej Gołas, Ireneusz Czajka: The concept of a source of a controlled directional characteristic; Henryk Łopacz, Marek Niewiarowicz: Digital switches of loudspeaker sets; Marek Niewiarowicz, Henryk Łopacz: Directional properties of loudspeaker sets with analogue and digital switches; Zygmunt Musiałkowski, Józef Stanclik: A computer supported designing of an electroacoustic high-power amplifier with an increased output current; Józef Stanclik: A computer supported analysis of the conditions of cooperation of a high-power amplifier with a loudspeaker device; Józef Stanclik: Cooperation of a high-power amplifier with loudspeaker device; Józef Stanclik, Zygmunt Musiałkowski: The designing of electroacoustic highpower amplifiers with an increased output current; Krzysztof Środecki: Application of the cepstrum function for the evaluation of the tone quality in rooms.

Active Methods, Vibroacoustics

Beside acoustic emission, this branch of acoustics was the most represented one. Eighteen papers significant for the recognition, theory and applications were presented. The Green's function method, used in the study of propagation of acoustic waves in randomly heterogeneous media, was applied to the description of the behaviour of electrons in the energy band with a random distribution of impurities. A relationship between the energy and momentum of the electrons was derived for the Orstein-Zernike form. From a theoretical analysis of the acoustic radiation of annular plates integral formulae were derived that describe the acoustic radiation of a fixed circular plate. Asymptotic formulae of an elementary form were obtained that facilitate numeric calculations. In these formulae, the non-oscillating part was separated from ten oscillating one. For a circular plate, also the determination of an optimal controlling force was considered, i.e. the determination of a force that reduces the oscillation and the acoustic pressure radiation in active systems. Beside the desirable amplifying vector for the vector of state, the optimal control found contains also a correction resulting from the consideration of the acoustic pressure in the quality indicator. The simulation studies performed indicate a 40 percent reduction of the acoustic pressure radiation. For the method of finite elements, a circular element in polar coordinates was worked out. An algorithm for an analytical description of the

shape function was proposed. Pictures of some particular cases of those functions were presented. Using the energy analysis of a ribbed plate, relationships were derived that determine the amount and distribution of the energy dissipated and accumulated by the plate and the system of ribs.

The investigation of mutual phenomena made it possible to determine the acoustic transition functions. In the measuring stand presented, a satisfying agreement between the real, measured acoustic pressure and that predicted was achieved.

Circular saws are the main source of vibroacoustic danger in the manufacturing process of cutting. The vibroacoustic analysis indicates that the knowledge of the particular forms of the free vibrations allows to reduce effectively the vibrations of the saw-blade disc by gland rings, additional stiffing discs, bearing pad discs and by by a proper choice of the number of teeth, their geometry and the number of revolutions. A lot of work was devoted to problems of the noise of strokes and of hydraulic presses. A stand for the investigations of striking noise was presented as well as material and constructing solutions decreasing the noise of this type during mechanical work. Impulse noise was investigated in order to determine the statistical value of some parameters characterizing isolated impulse noise obtained from measurements in three industrial plants. The possibility of active noise decreasing was demonstrated by an example of the low frequency noise reduction in a ventilation system. The results of preliminary studies, including measurements of the effectiveness and stability of active noise decreasing systems, were presented. A new system of the acoustic analysis, based on the application of the edge elements method, was demonstrated. The systems allows the user to identify the influence of the structural elements on the sound level in chosen areas of the structure. Using the method of the Statistical Analysis of Energy, an algorithm was suggested and a corresponding computer program for the calculation of the energy spreading in mechanical-acoustic systems was worked out. An example of the application of this program was the optimization of the acoustic energy radiation by a ribbed plate placed in three dimensional acoustic volume. The method of the Statistical Analysis of Energy was also applied for a procedure of determination of the coefficient of energy losses in stochastically vibrating structures; in the procedure the interaction between the structure and the acoustic field is taken into account. In sound-isolated cabins used in the industry, their effectiveness in the low frequency range is essential. This effectiveness can be markedly improved by the application of resonance structures. In several papers, a conception of the application of individual characteristics of vibroacoustic sets and sub-sets in the production and utilization of motor vehicles was presented. Attention was paid to the possibility of drawing up a consulting system assisting the diagnosis of the technical state of both new and used vehicles. A similar system can be used to aid the designing of means of passive reduction of the machine noise.

The following papers were presented:

Wojciech Batko, Pawel Litwa, Ryszard Olszewski: Analysis of the acoustic field around a friction saw; Adam Brański: The idea of an circle element in the method of finite elements; Zbigniew Engel, Jan Sikora, Jadwiga Turkiewicz: Noise in mechanical work;

Zbigniew Engel, Jan Sikora, Jadwiga Turkiewicz: Experimental studies of striking noise; Zbigniew Engel, Aleksander Gawlik, Mirosław Gawlik: Experimental studies of vibroa-coustic mutual phenomena; Andrzej Gołaś, Robert Łopusiak, Piotr Malcharek: Vibroa-coustic diagnosis — application of the method of edge elements; Marek Iwaniec: Anal-ysis of the effect of the parameters of ribbing of a rectangular plate on the free vibra-tion frequency; Marek Iwaniec, Ryszard Panuszka: Analysis of the energy spreading in a mechanical-acoustic system; Anna Kaczmarska, Danuta Augustyńska: Methods of reduc-ing the low-frequency noise in industrial cabins; Jan Kazimierczak, Wojciech Moczulski, Arkadiusz Boczkowski: The conception of the application of individual characteristics of vibroacoustic sets and sub-sets in the production and operation of motor vehicles; Marek Komoniewski: An integrated assistance of the designing of means for the passive reduction of noise — the construction of a tool; Lucyna Leniowska: Active attenuation of vibrations and the acoustic pressure radiated by a circular plate; Lucyna Leniowska: Simulation of the active attenuation of vibrations and the acoustic field radiated by a circular plate; Lucyna Leniowska, Andrzej Szumidło: Active attenuation of the vibra-tions of a circular plate — experimental investigations I; Grzegorz Makarewicz, Grzegorz Matuszewski, Leszek Morzyński, Wiktor Zawieska: A stand for the study of the active reduction of noise in ventilation systems; W.P. Rdzanek: Theoretical analysis of the acoustic radiation of fixed circular plates; Eugeniusz Soczkiewicz: The Green function method of the study of propagation of acoustic waves in randomly heterogeneous media — electrical analogs; Jan Ąera: Some parameters of impulse noise at working positions in the industry.

Acoustic methods in biomedical engineering

The applications of acoustic methods in biomedical engineering were presented in the context of measurements of blood pressure, the investigation of bones, the propagation of blood pressure waves, the effect of infrasound of bioelectrical potentials in the brain, and its effect on the variation of the EEG signal. The results of the studies of the bioelectric courses in the human brain indicate a high sensibility of the central nervous system, even at a low acoustic pressure of the infrasounds. This can be manifested by an increase of the alpha rhythm, by the appearance of a slowly changing activity theta and by and by the appearance of the leading phenomenon. This shows a lack of concentration and a disturbance in the psycho-motoric efficiency. It was shown by the ultrasound trans-mission tomography that the application of stochastic filters enables the minimization of image deformations. The reconstruction of an image is performed by a convolution algorithm and a reverse projection. The acoustic non-invading method of measurement of the running and reflected blood pressure wave in the human neck artery makes it possible to evaluate of the degree of narrowing of the inner neck artery basing on the reflection coefficient and the delay of the reflected wave in relation to the running one.

The measurements of the propagation of ultrasonic waves in three perpendicular directions in anisotropic samples of the spongy and bark bone tissues indicate a strong correlation between the density of the a bone and the ultrasound velocity. An acoustic

microscope, operating at 100 MHz, has been used for the determination of the impedance and speed of propagation of a longitudinal ultrasonic wave in separate beams of a spongy bone. It was found that in the case of osteo-optic beams, the density and velocity of propagation of longitudinal waves are close to those obtained for a packed bone. The diminishing of the mineral phase in the collagen structure of the beam, or its complete absence, results in a decrease of density and ultrasound velocity.

The following papers were presented:

Zbigniew Damijan, Ryszard Panuszka: The effect of infraacoustic noise on the bioelectric potentials of the brain; Zbigniew Damijan, Ryszard Panuszka: The influence of infraacoustic noise on some parameters of an EEG signal; Andrzej B. Dobrucki, Krzysztof J. Opieliński: The application of a stochastic filter to an image reconstruction by the UTT method using a convolution algorithm and reverse projection; Jerzy Litniewski, Andrzej Nowicki, Andrzej Sawicki: Micro-measurements of the properties of spongy bones by an acoustic microscope; Tomasz Majchrzak, Marek Iwaniec: An acoustic method of quantitative investigations of bones; Tadeusz Powałowski: The study of running and reflected blood pressure waves in the human common neck artery by a non-invading ultrasonic method; Hanna Trębacz, Helena Gawda: Anisotropy of the speed and attenuation of ultrasounds in the bone tissue.

Normalization in the field of vibrations and sounds

An energetic method of the evaluation of local vibrations transmitted to the main — operator has been suggested. New criterion quantities have been proposed; they consist in the energy dose in [J] and in the mean energy measured in [W] that is directed to the operator in a single work shift. This method renders the unambiguous evaluation of local vibrations and designing of safe work positions possible. New proposals of acceptable levels of the exposition to infra- and ultrasound noise were given. Studies concerning the effect of mechanical vibrations in systems consisting of the operator's hand and the toll's handle make it possible to work out an indicator method of the evaluation of the influence of mechanical vibrations. Indices related to the effect of the tightening force and that exerted on the tool's handle by the operator were determined. A unique stand for the investigation of acoustic anti-noise ear-flaps, with a controlled attenuation, which meet the European norm pr EN 352-4. The stand allows to perform investigations of fundamental hearing savers and certificate investigations. An automatic audiometer allows to test the hearing of persons subject to noise by applying a scanning method in that three measurement procedures are used. The test results can be archived and the trend of the decease changes observed. The application of the intensity method for the determination of acoustic pressure levels of the emission enables an accurate determination of the latters at the utilization conditions according to the demands of the series of EN ISO 11200 norms. Also, the results of measurements of the acoustic pressure of 32 woodworking machines, performed according to the Pr PN EN ISO 3746 norm, were demonstrated.

The following papers were presented:

Bolesław Bogusz: Procedures and accuracy classes of the determination of the acoustic power of noise sources in the light of the ISO 9614-1 and ISO 9614-2 norms; Marian W. Dobry: An energetic method of determination of local vibrations; Maria Kameduła, Małgorzata Pawlaczyk-Łuczyńska: Proposals of new acceptable levels of ultrasonic noise for the work medium; Ewa Kotarbińska, Dariusz Puto: A stand for the investigation of anti-noise ear-flaps with controlled attenuation; Piotr Kowalski: Investigations of the vibration transmission in the system: operator's hand-handle; Witold Mikulski: Corrected acoustic power level A of woodworking machines determined by the method described in Pr PN-EN ISO 3746; Małgorzata Pawlaczyk-Łuczyńska: Proposals of new acceptable quantities in relation to the professional exposition to infrasounds; Dariusz Pleban, Danuta Augustyńska: A method of determination of the acoustic pressure of emission at working places for the acoustic evaluation of machines; Tadeusz Rabsztyn, Adam Lipowczan: A device for the examination of the hearing of persons subject to noise at the working place in the light of the PN-EN 26189 project; Janusz Kompała: Analysis of the risk in town and country planning in the light of the demands of the national law; an example of the evaluation of the acoustic arduousness of a chosen industrial plant.